DEVELOPMENT OF SUNSCREEN CREAM CONTAINING MANGOSTEEN PERICARP EXTRACT ENCAPSULATED IN SOLID LIPID NANOPARTICLES

Miss Siti Nur Diniyanti

A Thesis Submitted in Partial Fulfillment of the Requirements
for the Degree of Master of Science Program in Pharmaceutical Technology
Department of Pharmaceutics and Industrial Pharmacy
Faculty of Pharmaceutical Sciences
Chulalongkorn University
Academic Year 2017

การพัฒนาครีมกันแดดที่มีส่วนผสมของสารสกัดเปลือกมังคุดห่อหุ้มในอนุภาคนาโนไขมันแข็ง

นางสาวสิติ นอร์ ดินิยันติ

วิทยานิพนธ์นี้เป็นส่วนหนึ่งของการศึกษาตามหลักสูตรปริญญาวิทยาศาสตรมหาบัณฑิต
สาขาวิชาเทคโนโลยีเภสัชกรรม ภาควิชาวิทยาการเภสัชกรรมและเภสัชอุตสาหกรรม
คณะเภสัชศาสตร์ จุฬาลงกรณ์มหาวิทยาลัย
ปีการศึกษา 2560

Thesis Title	DEVELOPMENT OF SUNSCREEN CREAM CONTAINING MANGOSTEEN PERICARP EXTRACT ENCAPSULATED IN SOLID LIPID NANOPARTICLES
By	Miss Siti Nur Diniyanti
Field of Study	Pharmaceutical Technology
Thesis Advisor	Assistant Professor Walaisiri Muangsiri, Ph.D.
Thesis Co-Advisor	Associate Professor Pornpen Werawatganone, Ph.D.

Accepted by the Faculty of Pharmaceutical Sciences, Chulalongkorn University in Partial Fulfillment of the Requirements for the Master's Degree

.....Dean of the Faculty of Pharmaceutical Sciences
(Assistant Professor Rungpetch Sakulbumrungsil, Ph.D.)

THESIS COMMITTEE

.....Chairman
(Assistant Professor Nontima Vardhanabhuti, Ph.D.)

.....Thesis Advisor
(Assistant Professor Walaisiri Muangsiri, Ph.D.)

.....Thesis Co-Advisor
(Associate Professor Pornpen Werawatganone, Ph.D.)

.....Examiner
(Assistant Professor Vorasit Vongsutilers, Ph.D.)

.....External Examiner
(Associate Professor Suchada Chutimaworapan, Ph.D.)

สิติ นอร์ ดินิยันติ : การพัฒนาครีมกันแดดที่มีส่วนผสมของสารสกัดเปลือกมังคุดห่อหุ้มในอนุภาคนาโนไขมันแข็ง (DEVELOPMENT OF SUNSCREEN CREAM CONTAINING MANGOSTEEN PERICARP EXTRACT ENCAPSULATED IN SOLID LIPID NANOPARTICLES) อ.ที่ปรึกษาวิทยานิพนธ์หลัก: ผศ. ภญ. ดร. ร.ต.ท. หญิง วลัยศิริ ม่วงศิริ, อ.ที่ปรึกษาวิทยานิพนธ์ร่วม: รศ. ภญ. ดร. พรเพ็ญ วีระวัฒกานนท์, 138 หน้า.

การศึกษานี้มีจุดมุ่งหมายเพื่อ พัฒนาครีมที่มีส่วนผสมของสารสกัดเปลือกมังคุดห่อหุ้มในอนุภาคนาโนไขมันแข็ง เพื่อเพิ่มการป้องกันแสงแดด และเป็นทางเลือกแทนการใช้ครีมกันแดดที่ผสมสารกันแดดสังเคราะห์ในตลาด สกัดเปลือกมังคุดถูกเตรียมโดยวิธีการหมักและประเมินค่าเอสพีเอฟด้วยเครื่องวิเคราะห์การดูดกลืนแสงในช่วงรังสียูวีและช่วงแสงขาว อนุภาคนาโนไขมันแข็งถูกเตรียมโดยการใช้คลื่นเสียงความถี่สูง อนุภาคนาโนไขมันแข็งเปล่าถูกเตรียมขึ้น โดยใช้กรดสเตียริกหรือกรดปาล์มิติกเป็นไขมันแข็งที่ความเข้มข้น 3% ทวีน80 หรือ โพลีไวนีล แอลกอฮอล์ถูกใช้เป็นสารลดแรงตึงผิวในช่วงความเข้มข้น 1 ถึง 2% อนุภาคนาโนไขมันแข็งเปล่าที่เตรียมได้ ถูกตรวจสอบเพื่อหาลักษณะทางกายภาพ ได้แก่ รูปร่างสัณฐานวิทยา ขนาดอนุภาค ดัชนีการกระจายตัว และศักย์ซีตา อนุภาคนาโนไขมันแข็งเปล่าที่มีคุณสมบัติทางกายภาพที่เหมาะสมได้รับเลือกให้ห่อหุ้มสารสกัดเปลือกมังคุดและถูกประเมินลักษณะทางกายภาพ ความคงตัวทางเคมี และค่าเอสพีเอฟ ระหว่างเก็บรักษาที่อุณหภูมิ 4-8 องศาเซลเซียสเป็นเวลา 3 เดือน สารสกัดเปลือกมังคุดที่ได้เป็นสารหนืดสีน้ำตาลที่มีค่าเอสพีเอฟ ระหว่าง 3.09 ± 0.01 ถึง 27.20 ± 0.05 ที่ความเข้มข้นตั้งแต่ 0.02 ถึง 0.1 มิลลิกรัมต่อมิลลิลิตร จากการศึกษาลักษณะทางกายภาพเลือกใช้อนุภาคนาโนไขมันแข็งเปล่าที่เตรียมจากกรดสเตียริกหรือกรดปาล์มิติก กับโพลีไวนีล แอลกอฮอล์ 1 % สารสกัดเปลือกมังคุดห่อหุ้มในอนุภาคนาโนไขมันแข็งถูกผสมลงในครีมให้มีความเข้มข้นของสารสกัดเปลือกมังคุด 3% อนุภาคนาโนไขมันแข็งช่วยเพิ่มค่าเอสพีเอฟของครีมที่มีสารสกัดเปลือกมังคุดห่อหุ้มในอนุภาคนาโนไขมันแข็งได้ถึงสองเท่าเมื่อเทียบกับครีมที่เติมสารสกัดเปลือกมังคุด 3% ครีมที่ประกอบด้วยสารสกัดเปลือกมังคุดห่อหุ้มในอนุภาคนาโนไขมันแข็งของกรดปาล์มิติก และสารสกัดเปลือกมังคุดห่อหุ้มในอนุภาคนาโนไขมันแข็งของกรดสเตียริกมีลักษณะทางกายภาพที่ดี มีความคงตัวทางเคมี และมีค่าเอสพีเอฟที่ไม่แตกต่างกันอย่างมีนัยสำคัญหลังจากเก็บรักษาที่อุณหภูมิ 4-8 องศาเซลเซียสเป็นเวลา 3 เดือน ผลการทดลองแสดงให้เห็นว่าครีมที่ประกอบด้วยสารสกัดเปลือกมังคุดห่อหุ้มในอนุภาคนาโนไขมันแข็ง เป็นทางเลือกที่มีศักยภาพในการพัฒนาเป็นสารป้องกันรังสียูวีบีในครีมกันแดด

ภาควิชา	วิทยาการเภสัชกรรมและเภสัชอุตสาหกรรม	ลายมือชื่อนิสิต .....
		ลายมือชื่อ อ.ที่ปรึกษาหลัก .....
สาขาวิชา	เทคโนโลยีเภสัชกรรม	ลายมือชื่อ อ.ที่ปรึกษาร่วม .....
ปีการศึกษา	2560	

5976354033 : MAJOR PHARMACEUTICAL TECHNOLOGY
KEYWORDS: MANGOSTEEN PERICARP EXTRACT (MPE) / SOLID LIPID NANOPARTICLES / SUNSCREEN / CREAM

SITI NUR DINIYANTI: DEVELOPMENT OF SUNSCREEN CREAM CONTAINING MANGOSTEEN PERICARP EXTRACT ENCAPSULATED IN SOLID LIPID NANOPARTICLES. ADVISOR: ASST. PROF. WALAISIRI MUANGSIRI, Ph.D., CO-ADVISOR: ASSOC. PROF. PORNPEN WERAWATGANONE, Ph.D., 138 pp.

The aim of this study was to develop cream containing mangosteen pericarp extract (MPE) encapsulated in solid lipid nanoparticles (SLNs) in order to achieve enhanced photoprotection and to be an alternative for synthetic sunscreens in the market. The MPE was prepared by maceration method and evaluated for SPF value by UV-Vis spectrophotometer. SLNs were prepared by ultrasonication method. Blank SLNs were formulated using stearic acid (SA) or palmitic acid (PA) as a solid lipid at a concentration of 3%. Tween® 80 or PVA was employed as a surfactant with concentrations ranging from 1 to 2%. The obtained blank-SLNs were investigated for its physical characteristics, i.e., morphology, particle size, polydispersity index (PDI), and zeta potential value. The blank SLNs with suitable physical characteristics were selected to encapsulate MPE and evaluated for the physical characteristics. Finally, the cream containing MPE encapsulated in SLNs (MPE-SLNs) were formulated and evaluated for their physical properties, chemical stabilities, and SPF values during storage at 4-8^{o}C for 3 months. The obtained MPE was a dark brown powder with an SPF value ranged from 3.09±0.01 to 27.20±0.05 at concentrations ranging from 0.02 to 0.1 mg/ml. Based on the physical characteristics, the blank SLNs employing PA or SA with 1% of PVA were selected. MPE-SLNs were successfully loaded into cream at the MPE concentration of 3%. The SLNs enhanced the SPF values of cream containing MPE-SLNs by two-fold compared with cream containing 3% MPE. The cream containing MPE-PA-SLNs and MPE-SA-SLNs displayed good physical appearances, and was chemically stable, without any significant difference of SPF values after storage at 4-8 ^{o}C for 3 months. The results indicated that the cream containing MPE-SLNs had a promising potential to be used as an alternative UVB photoprotector to the synthetic sunscreens.

Department:	Pharmaceutics and Industrial Pharmacy	Student's Signature	.....
		Advisor's Signature	.....
Field of Study:	Pharmaceutical Technology	Co-Advisor's Signature	.....
Academic Year:	2017		

ACKNOWLEDGEMENTS

First of all, in the name of Allah SWT, the most beneficent and the most merciful. All praises are to Allah SWT for all blesses so that the writer can accomplish this thesis. In addition, may peace and salutation is given to the prophet Muhammad who has taken all human being from the darkness to the lightness.

I would like to express my gratitude to my advisor Assistant Professor Walaisiri Muangsiri, Ph.D. for her scientific guidance as well as for her advice, constant enthusiasm, and encouragement, all of which made the completion of this study possible.

I would like to address my appreciation and grateful thanks to my co-advisor, Associate Pornpen Werawatganone, Ph.D. for her valuable suggestion and kindness during the completion of this study.

I thank most sincerely to the reviewers of this thesis, Associate Professor Suchada Chutimaworapon, Ph.D. and Assistant Professor Vorasit Vongsutilers, Ph.D., as well as the chairwoman of my thesis examination committee, Assistant Professor Nontima Vardhanabuti, Ph.D. for their constructive criticism and for giving me a valuable suggestion for thesis improvement.

I would like to express the special gratitude towards Indonesia endowment fund for education (LPDP) scholarship for their support and encouragement which help me in the completion of this study.

Sincere thanks are also given to all staff members of Pharmaceutical Technolgy International Program, Department of Pharmaceutics, Faculty of Pharmaceutical Sciences, Chulalongkorn University for their assistance and great help.

Finally, special thanks are given to my beloved family and friends for their great love, prayers, motivation, support, spirit, and everything that they have given to me during the process of completing this thesis and other people whose names have not been mention here.

CONTENTS

Page

Page

LIST OF TABLES

LIST OF FIGURES

CHAPTER I
INTRODUCTION

1.1. Background

Sunlight is an electromagnetic radiation which is divided into ultraviolet (UV) (200-400 nm), visible (400-780 nm), and infrared light (> 780 nm). UV light (UV radiation) is the most harmful sunlight wavelength and its intensity has increased in recent years (Afaq & Mukhtar, 2002; Balogh et al., 2011; Madronich et al., 1998). The UV radiation (UVR) is classified into three categories based on the wavelengths: UVC (200-280 nm), UVB (280-320 nm), and UVA (320-400 nm). The harmful effects of UVR to the skin can be divided into chronic effects (photoaging, DNA damage, and skin cancer) and acute effects (photoallergy and sunburn or erythema) (Bennet et al., 2014; Narayanan et al., 2010; Saewan & Jimtaisong, 2013). UVC is very hazardous to the human skin, even at a very short exposure time. Fortunately, the ozone layer in the earth's atmosphere completely screens out UVC radiation (Afaq & Mukhtar, 2002). UVB is shown as a leading cause of skin cancer (basal and squamous cell carcinoma) and immunosuppressive diseases (Afaq & Mukhtar, 2002). UVA produces a tanning effect by increasing melanin production in the epidermis layer of the skin (Svobodova et al., 2006).

Using the photoprotective clothes, sunglasses and hats complemented with the use of sunscreens during the highest UVR hours are principles of photoprotection (González et al., 2008). Sunscreen products contain sunscreen agents that absorb or scatter UV light. Sunscreen agents can be divided into two categories based on their mechanisms of action: chemical and physical sunscreens. The chemical sunscreens are also known as organic sunscreens. The physical sunscreens are referred to inorganic sunscreens (Gasparro et al., 1998). Generally, chemical sunscreens have aromatic structures that allow the molecule to absorb high energy UVR and release the rays with lower energy; thus the harmful effects of UVR to the skin are reduced (Rai et al., 2012). Physical sunscreens or inorganic sunscreens reflect or scatter UVR. They consist of minerals such as titanium dioxide or zinc oxide (Rai et al., 2012). Physical blockers offer greater protective action, but their opacity, viscosity, and greasiness have limited their usage (Shannon et al., 2008). Chemical sunscreens are synthetic agents which

possess potential toxicity to human; thus, they have limited usage. Some of chemical sunscreens, such as oxybenzone and cinnamate, have an estrogenic effect and increase the uterine weight in rats (Klammer et al., 2005; Suzuki et al., 2005) whereas aminobenzoic acid and avobenzone induce photoallergy (Dromgoole & Maibach, 1990; Karlsson et al., 2009; Kimura & Katoh, 1995; Schmidt et al., 1998).

Natural extracts have recently been considered as alternative sunscreen agents due to their potency to absorb UV light. The previous findings showed that 2 mg/ml of *Dracocephalum moldavica* L. or *Viola tricolor* L. leave extracts containing polyphenolic compounds such as rutin, apigenin, luteolin, violanthin possess sun protection factor (SPF) values of 24.79 and 25.69, respectively (Khazaeli & Mehrabani, 2010). Another study reported that 0.1 mg/ml of Sri Lankan mangosteen extract containing flavonoids and polyphenols has an SPF value of 15.96 (Pathirana et al., 2016). In other words, plant extracts show a promising potential as an alternative to synthetic sunscreens.

Mangosteen is one of the tropical fruits that can be easily found in rainforests of Thailand, Malaysia, and Indonesia. Mangosteen fruit pericarp contains α-mangostin as the major compound and more than 40 other xanthones (Duthie et al., 1999; Yodhnu et al., 2009). α-Mangostin, a polyphenolic xanthone, contains a chromophore that absorbs light in a UVB region and shows the maximum absorption peaks at 244 and 317 nm. The absorption wavelength of 244 nm represents the $\pi \rightarrow \pi^*$ transition of the aromatic structure while the peak at 317 nm relates to $n \rightarrow \pi^*$ transition of carbonyl structure (Yodhnu et al., 2009).

Solid Lipid Nanoparticles (SLNs) have been shown as a promising carrier system for sunscreen preparations. Smaller particle size of SLNs scatters the light and results in higher sunscreen activity when compared to the conventional formulation (Wissing & Müller, 2002b). In addition, SLNs possess a slower release rate of organic sunscreens than nanosuspension and conventional o/w emulsion (Sanad et al., 2010; Wissing & Müller, 2002b). Thus, the sunscreens retain on the skin for a longer period of time and provide longer protective ability against UVR (Severino et al., 2012; Wissing & Müller, 2002b). Additionally, SLNs may protect labile active compounds from degradation caused by the external environment (e.g. water). SLNs are physically

stable. Moreover, SLNs preparation may avoid the use of organic solvents and are easy to scale up (Lacatusu et al., 2010; Wissing & Müller, 2002b).

The efficacy of sunscreen is determined by the SPF value. SPF is defined as the ratio of the minimal erythema dose (MED) of UVB radiation in the presence of sunscreen to the MED in the absence of sunscreen (FDA, 2015). FDA and COLIPA provide a recommended *in vivo* testing protocol to measure the SPF value of the products on human volunteers (Gaikwad & Kale, 2011). Although it is an established and recommended method by FDA and COLIPA, it has several disadvantages such as time-consuming, being expensive and potentially harmful to human volunteers. On the other hand, the measurement of SPF by *in vitro* testing has advantages such as being less expensive, safe for human, and able to provide preliminary data for further development of an effective sunscreen. Based on economical, practical and ethical considerations, the *in vitro* determination of SPF is a more suitable method and used more often than the *in vivo* method (Gaikwad & Kale, 2011).

This research was designed with an objective to evaluate the *in vitro* sun protection factor value of cream containing mangosteen pericarp extract encapsulated in SLNs (MPE-SLNs).

1.2. Hypotheses

- Mangosteen pericarp extract (MPE) possesses sun protection factor (SPF)
- MPE can be formulated into solid lipid nanoparticles (SLNs)
- Cream containing MPE-SLNs possesses sun protection factor
- Cream containing MPE-SLNs has good physical and chemical stability

1.3. Objectives

- To determine the SPF value of MPE
- To formulate solid lipid nanoparticles containing MPE
- To determine the SPF value of cream containing MPE-SLNs
- To evaluate the physical and chemical stability of cream containing MPE-SLNs

1.4. Conceptual Framework

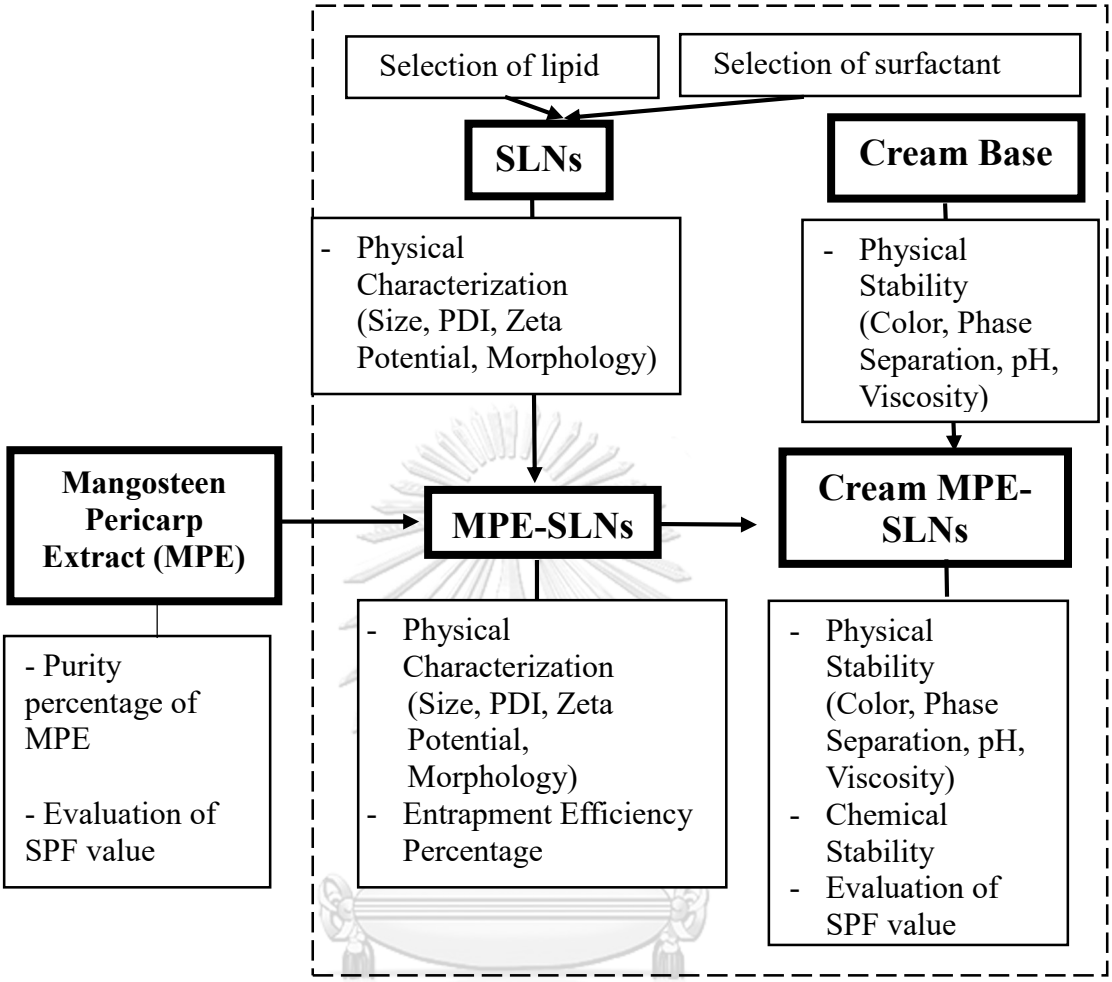

CHAPTER II
LITERATURE REVIEW

2.1. Sun Protection Factor

The sun protection factor (SPF) indicates the efficacy of sunscreen product (FDA, 2015). There are two methods for determination of SPF value; i.e. *in vivo* and *in vitro* methods. Determination of SPF value by *in vivo* method is made through an artificial source of UVR on human volunteers proposed by FDA and COLIPA. At least 10 – 20 volunteers with an appropriate skin types of I, II or III are involved in this study (COLIPA, 2005).

Table 1 The classification of skin type (Fitzpatrick, 1988)

Skin type	Skin description	Recommended SPF value
I	Burn easily, never tans	>40
II	Burn easily, tans minimally	20-40
III	Burn moderately, tans gradually	7-20
IV	Burn minimally, tans well	6-15
V	Rarely burns, tans well	5-10
VI	Never burns, always tans	4

A xenon is employed as an artificial light source. Two mg/cm^2 of test products are applied on the volunteer back between waist and scapula line. The minimum area for each product is around 30-60 cm^2**.** The tested area is exposed to maximum total UVR of 120 mW/cm^2. SPF is a value obtained from minimal dose to cause erythema in the presence of sunscreen product divided by the minimal dose to cause erythema in the absence of sunscreen product (COLIPA, 2005). Evaluation of SPF by the *in vivo* method has several drawbacks. First, this method has an ethical issue related to the damage of volunteers' skin. Moreover, it is expensive and time-consuming (Pelizzo et al., 2012). Finally, this method is not practical to be routinely used in formulation development process (Santos et al., 1999).

On the other hand, the *in vitro* method has more advantages than the *in vivo* method, such as more rapid, objective, and cost-effective screening method. Two *in vitro* methods used for determination of sun protection factor employ a UV spectrophotometer and an SPF analyzer. The UV-Vis spectrophotometry method proposed by Mansur in 1986 uses the following mathematical equation:

$$SPF = CF \times \sum_{290}^{320} EE\ (\lambda) \times I(\lambda) \times Abs\ (\lambda)$$

Where: EE : erythemal action spectrum;

I : solar intensity spectrum;

Abs : absorbance of sunscreen product;

CF : correction factor (Mansur et al., 1986).

The values of EE x I are constant and determined by Sayre et al., 1979, as shown in Table 2:

Table 2 The values of EE x I

Wavelength (nm)	EE x I value
290	0.0150
295	0.0817
300	0.2874
305	0.3278
310	0.1864
315	0.0839
320	0.0180
Total	1

Another *in vitro* method is measured by an SPF-290S analyzer. Test product (1.3 mg/cm^2) is applied on a 50 x 50 mm PMMA plate with a roughness of 5 µm (Optometrics, 2009). The SPF value is obtained by averaging results of maximum 12 scans of a sample from different locations on the PMMA plate. This method is used to determine the efficiency of lotions, creams, sprays, gels, powders, and emulsions. The measurement is obtained in the range of 290 to 400 nm (Optometrics, 2009).

$$SPF = \frac{\int_{290}^{400} E\ (\lambda) \times S(\lambda)}{\int_{290}^{400} E\ (\lambda) \times S(\lambda)\ /MPF}$$

Where: S : erythemal action spectrum (McKinlay & Diffey, 1987);

E : solar intensity spectrum;

MPF : monochromatic protection factor (1/T) (Optometrics, 2009).

2.2. Ultraviolet Radiation and Its Effect on Skin

Ultraviolet (UV) radiation is a range of electromagnetic radiation and is categorized into three types: Ultraviolet C (UVC) (200-290 nm), Ultraviolet B (UVB) (290-320 nm), and UVA (320-400 nm). Ultraviolet A (UVA) is further divided into UVA1 (340-400 nm) and UVA2 (320-340 nm). The ozone layer in the Earth's atmosphere completely absorbs UVC, absorbs 90% UVB, and absorbs 10% UVA (Rai et al., 2012). However, there is an increase in UV transmission which passes through the Earth's surface due to the depletion of the ozone layer. The understanding of UVR and its effects on the skin is important because the UVR causes aging skin, erythema, cancer and immunosuppressive disease (Rai et al., 2012). UVA associates with pigmentation and aging of the skin (Lavker, 1979). UVB exposure leads to erythema and DNA damage or skin cancer (Rai et al., 2012).

Sunburn (or erythema) is skin inflammation after UV exposure. The skin becomes redness due to an increase of blood flow and the dilatation of the superficial blood vessels in the dermis. When UVR reaches the skin, the light may be absorbed or scattered. Absorbed light by UVR-absorbing molecules (chromophores), such as DNA, triggers a photochemical process. Major chromophores in the skin, for example nucleic acids, urocanic acids, and amino acids, absorb the shorter wavelengths (less than 300 nm) while melanin absorbs the longer wavelengths in a range of 200-700 nm. In addition, the other factors including epidermal thickness, location and amount of chromophores also affect the degree to which UVR is absorbed (Hruza & Pentland, 1993).

The skin aging is a result of the damage of collagen fibres after exposure to high UVR. Tanning, the skin darkening process, results from an increase in melanin production induced by UVR (Yamaguchi et al., 2007).

The skin cancer may be promoted in two different ways. The first pathway is by damaging the DNA structure in skin cells, resulting in abnormally and excessively

growth of the skin. In addition, UVR also weakens the immune system by killing the Langerhans cells and compromises the immune system of human body against cancer cells (FDA, 2015).

The amount of UVR exposure varies with many factors including altitude, geography, season, time of day, reflection (FDA, 2015).

- Higher altitude has high intensity of UVR than lower altitude due to thin atmosphere absorbing UVR.
- The area along equator has stronger UVR because the sun is directly over the equator and ozone layer is thinner on the equator.
- Season affects the sun's angle to the Earth. The amount of UVR is higher during the summer months than the other seasons.
- Midday is the time when the UVR is the most intense. It is better to avoid going outside from 10 am to 4 pm.
- The materials such as snow, sand, grass, or water can reflect UVR. The protective clothes, sunglasses, a wide-brim hat, and sunscreen products are needed to protect your eyes and skin from reflected UV rays (FDA, 2015).

For many years, UVR has become a focus of the research strategies because it is a major cause of skin cancer (Rai et al., 2012). Currently, sun protection substances include primary protection substances, such as, sunscreens and additional protection substances such as antioxidants and DNA repair enzyme (Rai et al., 2012). Sunscreens are divided into two types based on the mechanisms of action. Chemical sunscreens generally are organic compounds. Physical sunscreens or physical blockers are inorganic substances (Rai et al., 2012). The aromatic structure of organic sunscreen allows the molecule to absorb high energy UVR and release it at lower energy state; therefore, it can prevent skin damage caused by UVR. Physical blockers or inorganic sunscreens, such as, titanium dioxide or zinc oxide reflect or scatter UVR (Rai et al., 2012). Some of chemical sunscreens; for example oxybenzone and cinnamate, have an estrogenic effect resulting in an increase of uterine weight (Klammer et al., 2005; Suzuki et al., 2005). In addition, aminobenzoic acid and avobenzone induce photoallergy (Dromgoole & Maibach, 1990; Karlsson et al., 2009; Kimura & Katoh, 1995; Schmidt et al., 1998).

2.3. *Garcinia mangostana* L.

Garcinia mangostana L. (Clusiaceae), commonly known as mangosteen, is a tropical tree found in Thailand, Myanmar, India, Sri Lanka. Mangosteen has round, red-purple to dark-purple fruits. The edible fruit has a pleasant aroma, soft, white color and sweet to slightly sour taste (Iwo et al., 2013). Mangosteen fruits pericarp contains α-mangostin (Figure 1) as a major compound and more than 40 other xanthones, approximately 20% of about 200 xanthones discovered in nature (Akao et al., 2008; Geetha et al., 2011; Yodhnu et al., 2009). The mangosteen pericarp has been utilized for wound healing, skin infections, diarrhea, inflammation, etc (Iwo et al., 2013).

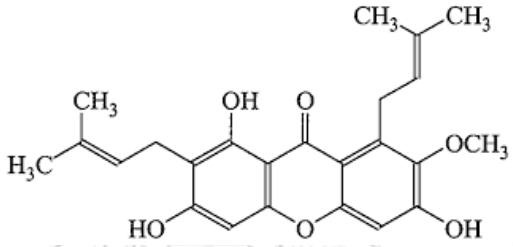

Figure 1 Molecule structure of α-mangostin (Iwo et al., 2013).

α-Mangostin is soluble in ethyl acetate and dichloromethane but it has a low solubility in the water leading to poor oral bioavailability (Iwo et al., 2013). It is stable under UV radiation with peaks at 254 and 366 nm for 6 h (irradiation dose of 32 W/m^2 per hour). It is stable under heat at 120^{o}C for 2 hours, stable in the basic hydrolytic condition in 3N NaOH solution and stable in acidic condition with pH of 2.99 (Yodhnu et al., 2009; Zhang et al., 2014). The estimated half-life of α-mangostin in the ethanolic extract is 660 days at 30°C (Jindarat, 2014). The log P of α-Mangostin is 4.64 (Chin et al., 2016). Skin permeation is generally increased with lipophilicity, but a log P value more than 4.1 is reported to give lower the skin permeability (Mälkiä et al., 2004). Highly lipophilic drugs may be retained in the lipophilic stratum corneum and resist partitioning into the more hydrophilic viable epidermis (Chin et al., 2016). However, a report showed that the ethyl acetate MPE is not toxic to human keratinocyte (HaCaT) cells at the concentration of 2,000 ppm (Rahmayanti et al., 2016). Acute toxicity of ethyl acetate MPE shows an LD_{50} at 1,000 mg/kg body weight in mice by oral administration (Kosem et al., 2013).

α-Mangostin contains chromophores that absorb at UVB wavelengths (>290 nm) with maximum absorbance at 244 and 317 nm. The excitation energy π→π* transition of the aromatic structure is related to the absorbance at 244 nm (with Ɛ= 49987.33) while the absorbance at 317 nm represents excitation energy n→π* transition of carbonyl structure (Ahmad et al., 2013; Wang & Lim, 2016).

HPLC is a common analytical method of α-mangostin. Most previous validated HPLC methods for α-mangostin analysis successfully separated α-mangostin from the other mangostins using reverse phase C18 analytical columns. The method employed isocratic mobile phase consisted of either formic acid in water–acetonitrile, acetonitrile-ortho phosphoric acid in water, methanol-water, or methanol-acetic acid (Aisha et al., 2013; Ali et al., 2012; Muchtaridi et al., 2016; Nurhidayati et al., 2014; Ruamkittham, 2005; Widowati et al., 2014; Yodhnu et al., 2009). The gradient mobile phase was also used with acetonitrile-orthophosphoric acid or formic acid in water-methanol (Ali et al., 2012; Kongkiatpaiboon et al., 2016). The UV or DAD detector were used in those studies (Aisha et al., 2013; Ali et al., 2012; Muchtaridi et al., 2016; Nurhidayati et al., 2014; Ruamkittham, 2005; Widowati et al., 2014; Yodhnu et al., 2009). Based on previous researches, the reverse phase C18 with isocratic mobile phase of methanol-water and DAD detector are employed in this study.

2.4. Herbal Medicines and Nanotechnology

Plants, animals and minerals have produced natural products used for treatment of many diseases (Verma & Singh, 2008). Currently, it is estimated that about 80% of people in developing countries still depend on herbal medicine for their primary health care. Herbal medicines gain popularity and demand by the community (Verma & Singh, 2008). It is estimated that about 1,800 species of wild plants (Thailand) and 7200 species of wild plants (Indonesia) have been used as herbal medicines (Fernquest, 2012).

Pharmacological effects of herbal medicine depend on phytochemical compounds present therein. The development of analysis method for determination of the profile and quantification of phytochemical compounds is a major challenge to the scientists (Rasheed et al., 2012). Natural products with known effects and no side effects will be a great therapeutic alternative for the human (Kumari et al., 2012).

However, natural products have several problems, such as low water solubility leading to low bioavailability in human, and instability under environmental conditions. These limitations can be overcome by encapsulation of natural product in suitable nanocarriers (Kumari et al., 2012).

Nanoparticles, one of drug delivery system can be produced from biodegradable or non-degradable materials, such as solid lipids, natural or synthetic polymers, or metals. Nanoparticles include solid lipid nanoparticles (SLNs), liposomes, microemulsions, nano lipid carriers (NLC), and polymeric nanoparticles (Yasurin, 2015). Nanoparticles have been widely applied to attach or encapsulate plant extracts. There are several advantages of nanoparticles including improvement of the activity of plant extracts, decrease of the required dose, reduction of the side effect, control of release rate (Wissing & Müller, 2002b; Yasurin, 2015). Nanoparticles also allow substances with different properties to be loaded in the same formulation, modify a substance's properties and behavior in the biological environment (Bonifácio et al., 2014; Yasurin, 2015).

Solid lipid nanoparticles (SLNs) are one of lipid-based systems which are developed in the early 1990s (Bonifácio et al., 2014; Mukherjee et al., 2009). SLNs are composed of solid lipids and surfactant (Figure 2). The lipids widely used in preparation of SLNs are fatty acids (stearic acid), triglycerides (trimyristate) partial glyceride (Imwitor®) (Lason & Ogonowski, 2011).

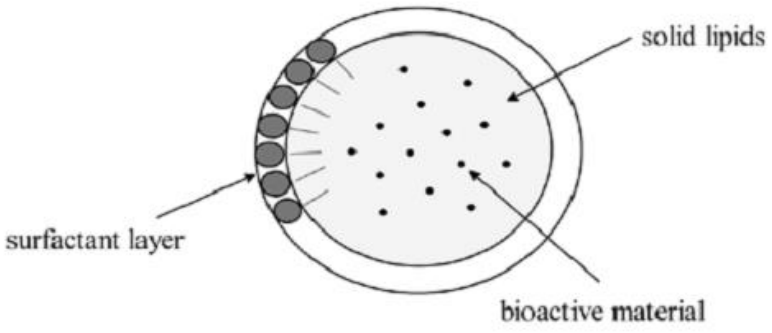

Figure 2 Solid lipid Nanoparticle's structure (Lasoń and Ogonowski, 2011).

SLNs have been applied in pharmaceutical industry because it was reported to enhance the SPF value of chemical sunscreens, protect labile compounds from

degradation, does not need organic solvent in the preparation process, and are easy to scale up. In addition SLNs offer controlled drug release, and increase the bioavailability of encapsulated active compounds (Lason & Ogonowski, 2011). The previous study reported that the smaller particle size of SLNs scatters the light and gives rise to higher sunscreen activity compared to conventional formulations. In addition, SLNs possess a slower release rate of organic sunscreens than nanosuspension and conventional o/w emulsion (Sanad et al., 2010; Wissing & Müller, 2002b). Thus, the sunscreens retain on the skin for a longer period of time and provide longer protection against UVR (Severino et al., 2012; Wissing & Müller, 2002b). Hence, SLNs have been shown as a promising carrier system for sunscreens as cosmetic formulations.

Several methods have been used for SLNs preparation. The preparation of SLNs is selected based on factors, such as, stability of active compound, the particle size of obtained SLNs, and availability of production instruments (Shah et al., 2015).

There are several methods for preparation of solid lipid nanoparticles:

- High-pressure homogenization (HPH)

In this method, a high-pressure machine pushes the hot emulsion through a narrow gap in the range of few microns. This method is widely used to produce SLNs due to its reliable and powerful technique. The dispersion accelerates on a very short distance to very high velocity (over 1000 Km/h) (Ekambaram et al., 2012). Very high cavitation and shear stress produce by the instrument break the particles down to a nano-range. This method is divided into two general approaches including hot homogenization and cold homogenization.

a. Hot homogenization uses the temperatures above the melting point of the lipid during the homogenization of pre-emulsion in order to prevent the solidification of the lipid. The oil phase consisted of drug and the molten lipid. The aqueous phase consisted of emulsifier at the same temperature. The pre-emulsion is obtained after mixing the mixture under a high-speed stirrer device (Figure 3). High temperature of pre-emulsion gives rise to the low viscosity of the inner phase and produces smaller particle sizes. The increase of the homogenization cycle and pressure often result in bigger the particle sizes caused by the collision of particles with high kinetic energy. However, heat labile drug may degrade

when they expose to a high temperature for a long time (Ekambaram et al., 2012).

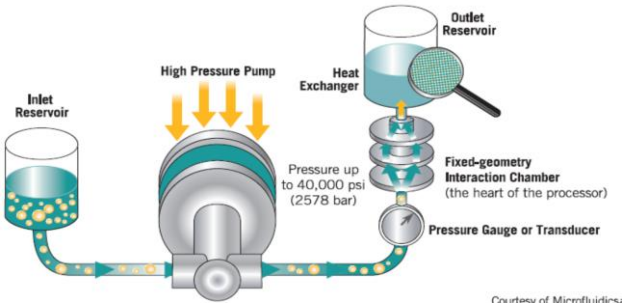

Figure 3 Hot homogenization method (Sciences, 2009).

b. Cold homogenization is a method which avoids to use high temperature in order to overcome problems associated with hot homogenization such as temperature-induced drug degradation. In this method, the drug is dissolved in molten lipid. The mixture is left to solidify. The solidified lipid is ground to form lipid microparticles then the lipid microparticles are dispersed in a surfactant solution at room temperature to form a suspension. The suspension is homogenized using a high-pressure device to break lipid microparticles into lipid nanoparticles (Ekambaram et al., 2012).

- Solvent injection technique

Solvent injection technique uses an organic solvent to dissolve the lipid. The lipid phase is injected into the aqueous phase consisted of surfactant while the aqueous phase is kept stirring. The emulsifier in the aqueous phase stabilizes lipid droplets at the site of injection until solvent injection gets completed. However, this method requires a long process time and the use of the organic solvent to dissolve drug and lipid (Das & Chaudhury, 2011).

- Solvent evaporation

Preparation of SLNs by solvent evaporation method uses an organic solvent to dissolve the lipid (Figure 4). In this method, the lipid phase including solid lipid and drug are dissolved in organic solvent (e.g cyclohexane, ether) prior to mixing with the aqueous phase. After that, the solvent is evaporated under reduced pressure of 40-60 mbar to form lipid nanoparticles in the aqueous medium (Ekambaram et al., 2012). This

method can also be combined with high-pressure homogenization method to produce smaller particle size (Ekambaram et al., 2012).

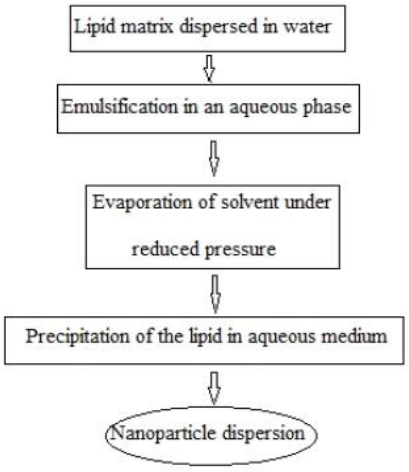

Figure 4 Solvent evaporation method (Ekambaram et al., 2012).

- Ultrasonication/high speed homogenization

SLNs are also prepared by ultrasonication method. This method usually combines the high-speed homogenization and ultrasonication to form smaller lipid nanoparticles (Ekambaram et al., 2012).

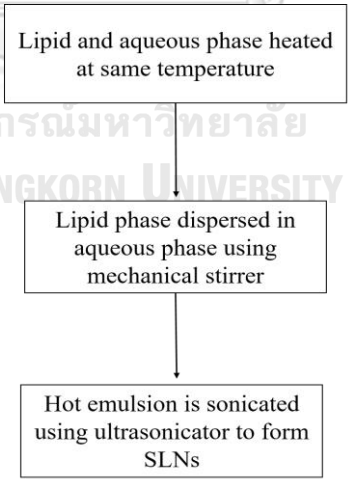

Figure 5 Ultrasonication method (Ekambaram et al., 2012).

When hot nanoemulsion is sonicated at high intensities or high amplitude, the sound waves produce high-pressure and low-pressure cycles with frequency according to the instrument specification. During these cycles, small bubbles are created in the hot nanoemulsion. When the bubbles attain a volume at which they can no longer

absorb energy, they collapse violently. This phenomenon is called cavitation. Cavitation results in intense local heat and breaks the particles down into smaller particles. Higher amplitudes result in a more effective creation of cavitation. There are several advantages of this method such as easy to do, short time of heating and handling process leading to less degradation of drug, smaller particle size and PDI (Hielscher, 2007; Xie et al., 2011).

2.4.1. Lipid

Lipid plays an important role in the preparation of SLNs. Biocompatible and biodegradable solid lipids are generally used in a concentration range of 3-10%. Previous study showed that the particle size and size distribution are increased by the increase of lipid concentration. High concentration of lipid increases the viscosity of the lipid dispersion leading to the decrease of homogenization efficiency and the acceleration of particle aggregation. Hence, the lipid content of the SLNs dispersion should not exceed 5% (Kumar & Sinha, 2016). The lipids are either triglycerides, fatty acids, fatty alcohol or mixture of mono-di-tri glycerides (Pandya et al., 2013). The lipid selection is based on the solubility of the active compound in molten lipid and type of lipid (Wissing & Müller, 2002a).

The study found that the degree of crystallinity is proportional to the occlusive effect of the lipid on the skin. Thus, non-crystalline lipid has no occlusive properties (Wissing & Müller, 2002a).

There are several types of lipid used in preparation SLNs:

- A mixture of mono-, di-, tri- glycerides have been used in the preparation of SLNs such as glyceryl behenate, glyceryl palmitostearate, and glyceryl trimyristate (Table 3) (Pandya et al., 2013).

Table 3 Lipids their chemical composition and the melting point of triglycerides (Pandya et al., 2013).

Lipids	% of Glycerides			Melting point (°C)	HLB value
	Mono	Di	Tri		
Glyceryl behenate	12	18-52	28-54	62-70	2
Glyceryl palmitostearate	-	4	95	55-58	2
Glyceryl trimyristate	8-17	54	30	52-55	5

- Stearic acid is a white, slight odor, wax-like solid lipid with a melting point of 69.3°C (Figure 6). It is a saturated fatty acid with an HLB value of 14.9. It is a stable and safe compound. Stearic is incompatible with bases, reducing agents, and oxidizing agents. Stearic acid has been used in topical pharmaceutical formulations, cosmetics and food products (Rowe et al., 2006).

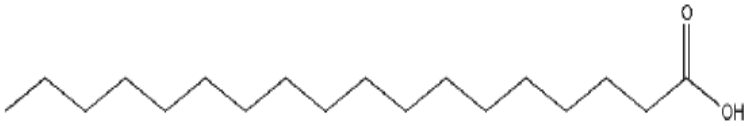

Figure 6 The structure of stearic acid (Rowe et al., 2006).

3. Palmitic acid is a white crystalline, slight odor and taste, with a with an HLB value of 15.6. It has a melting point of 63-64°C (Figure 7). Palmitic acid is used in oral and topical formulation. Palmitic acid reacts with strong oxidizing agents and bases. FDA also approves this material as a generally-recognized-as-safe (GRAS) ingredients for human use (Rowe et al., 2006).

Figure 7 The structure of palmitic acid (Rowe et al., 2006).

4. Cetyl palmitate is a white, wax-like substance with an HLB value of 10 (Abd-Elbary et al., 2013; Anarjan & Tan, 2013). It has a melting point of 47-54°C (Figure 8). Cetyl

palmitate is approved as generally-recognized-as-safe and physiologically well-tolerated lipid (Rowe et al., 2006).

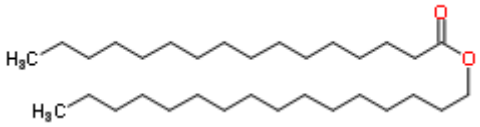

Figure 8 The structure of cetyl palmitate (Rowe et al., 2006).

2.4.2. Surfactants

Surfactants are molecules that absorbed at the interphase. The surfactants reduce interfacial tension, hence stabilize two immiscible liquids. The surfactants are categorized into cationic, anionic, amphoteric, and non-ionic surfactants. The degree of lipophilic and hydrophilic character of a surfactant decides whether it is predominantly hydrophilic or lipophilic. A polar surfactant dissolves in the polar liquid and a non-polar surfactant dissolves in non-polar phase (Martin et al., 1993).

Griffin has drawn up an arbitrary scale based on a ratio of hydrophilic-lipophilic character of the surfactants known as the HLB scale (Figure 9). The higher the HLB value the more hydrophilic surfactant, the lower the HLB value the more lipophilic surfactant (Martin et al., 1993).

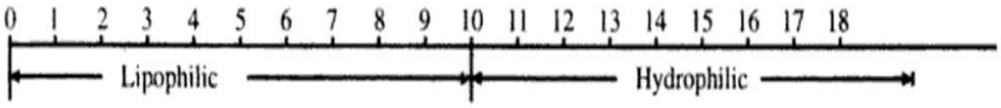

Figure 9 HLB value (Martin et al., 1993)

Surfactant selection for SLNs preparation depends on the route of administration, HLB value of surfactant, type of lipid, and particle size of SLNs (Shah et al., 2015). Poloxamer, Tween®80, and PVA are the most common surfactants used in the preparation of SLNs. Non-ionic surfactants are preferable for oral and parenteral preparations since they are less toxic and show less irritating compounds than the ionic surfactants (McClements & Rao, 2011). Cationic surfactants are most toxic compound among anionic and amphoteric surfactants. Surfactants also influence the degradation rate of lipid matrix. Ionic surfactants such as sodium cholate accelerate the degradation of lipid. On the other hand, non-ionic or polymeric surfactants such as, Tween®80 and

poloxamer, slow down the degradation of lipid due to the steric hindrance effect of poly-ethylene oxide against lipase-co-lipase complex (Olbrich & Müller, 1999).

1. Poloxamer

Polyethylene-propylene glycol copolymer or poloxamer has firstly introduced in 1950 as a non-ionic triblock copolymer. This surfactant is famously used in pharmaceutical applications (Devi et al., 2013). The polymer is divided into several types depending on the length of polymer blocks such as poloxamer 188, 407, etc. Each type has slight differences in its properties (Devi et al., 2013).

Table 4 Poloxamer their chemical composition and average molecular mass (Devi et al., 2013).

Poloxamer	Physical form	Average molecular mass	HLB value
188	Solid	7680-9510	29
407	Solid	9840-14600	22

Poloxamers are non-toxic and non-irritant; thus it can be administered by oral, parenteral, topical routes and used as a solubilizer, wetting agent in ointments emulsifier, and stabilizer (Devi et al., 2013). Poloxamer is used at a range concentration of 4-22 g/L as an emulsifier (Devi et al., 2013).

2. Tween® 80

Tween 80® is a non-ionic hydrophilic surfactant. It is also known as polysorbate 80 or sorbitan mono-9-octadecenoate poly(oxy-1.2-ethanediol). It is used as an emulsifier, stabilizer, and dispersing agent for medications. The HLB value of Tween 80® is 15. It is miscible with alcohol, water, and organic solvents such as toluene (Kopec et al., 2008). The concentration of Tween® 80 used in the SLNs preparation varies from 1-7.5%. (Ebrahimi et al., 2015; Prabhakar et al., 2013).

3. PVP

Polyvinylpyrrolidone (PVP) is a linear polymer consisting of 1-vinyl-2-pyrrolidone monomers with the molecular weight of the polymer in the range from 10,000 to 700,000 and viscosity expressed as K-value in the range from 10 to 95. PVP is a faintly yellow solid and is soluble in water, ethanol, and chloroform (Nair, 1998).

PVP is commonly used in the preparation of SLNs at the concentration of 1% (Ebrahimi et al., 2015).

4. PVA (polyvinyl alcohol)

PVA is a synthetic water-soluble polymer with an empirical formula of $(C_2H_4O)_n$ (Figure 10). The viscosity ranges from 20,000 to 200,000 as shown in Table 5.

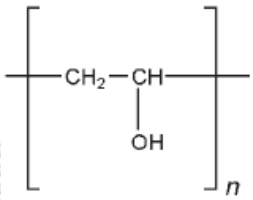

Figure 10 Structural formula of PVA (Rowe et al., 2006).

Table 5 Commercial grades of PVA (Rowe et al., 2006).

Viscosity	Molecular weight
High Viscosity	200,000
Medium Viscosity	130,000
Low Viscosity	20,000

Polyvinyl alcohol is a white to off-white granule and odorless. Polyvinyl alcohol is used in a topical pharmaceutical formulation. It is used as a stabilizing agent for emulsion preparation ranging from 0.25-3% and as a viscosity- increasing agent. PVA is also considered as a non-toxic and non-irritant material to the skin and eye at a concentration up to 7% (Rowe et al., 2006).

In the preparation of SLNs, PVA is used with the concentration ranging from 0.1 to 4%. PVA at a concentration of 2-4% gives rise to an increase of particle size and size distribution of SLNs because it increases the viscosity of the external phase resulting in a decrease of net shear stress (Mohanty et al., 2015; Sharma et al., 2016). PVA-JP18 is one of the PVA's commercial product with the degree of hydrolysis of 87 – 89 % and viscosity of 23-27 mPas at a concentration of 4% (20^{o}C). The HLB value of PVA is 18 (Anarjan & Tan, 2013).

2.4.3. Characterization

1. Particle Size and Polydispersity Index (PDI)

Solid lipid nanoparticles are often spherical and regular in shape with the dimension smaller than 1 μm. Particle size can substantially affect the properties of the nanoparticles. Particles larger than 5 μm may cause blood vessel blockades or embolism. The elimination of particles by the reticuloendothelial system (RES) also depends on the particle size (Shah et al., 2015). Based on the previous study, the particle size less than 300 nm can penetrate into the deeper layers of the skin and preferentially accumulate in hair follicles (Adib et al., 2016). Therefore, solid lipid nanoparticles with the particle size larger than 300 nm are preferable in sunscreen products in order to prevent the penetration of SLNs into a deeper layer of the skin (Wissing & Müller, 2002b).

Lipid, surfactant, other excipients and process parameters (preparation method, temperature, sonication time, homogenization pressure and cycle, centrifugation) affect the particle size. Particle size is used as a parameter to predict formulation instability (Shah et al., 2015). Determination of particle size is commonly performed by the light scattering methods, such as photon correlation spectroscopy (PCS) or laser diffraction method. PCS is also known as dynamic light scattering. This technique detects the particle size in the range of 3-10,000 nm. It is widely used because it is a simple, rapid, and non-destructive method. However, this method is not suitable for the detection of larger particle than 10 μm (Shah et al., 2015).

PCS measures the intensity fluctuation of scattered light caused by the Brownian motion of the particles in the dispersion medium. Brownian motion of particles in the dispersion medium is caused by the collision of particles with molecules of the dispersion medium. Particles are irradiated with a laser beam at the particular wavelength and angle. High intensity fluctuations indicate small particle size. On the other hand, lower fluctuation indicates the larger particle size (Shah et al., 2015).

The characterization of particle size using PCS is based on the translational diffusion coefficient (D). Stokes-Einstein equation is used to convert the translational diffusion coefficient (D) into a diameter (hydrodynamic diameter) to calculate the particle size (Shah et al., 2015).

$$d = \frac{kT}{6\pi\eta D}$$

Where,

d: Hydrodynamic diameter of particle

D: the translational diffusion coefficient

k: Boltzmann constant

T: Temperature

η*:* dispersion medium viscosity (Einstein, 1956).

The polydispersity index (PDI) characterizes the width of the size distribution. A PDI of 0.01-0.04 indicates a monodisperse system with relatively narrow distribution. A value >0.5 is indicative to the aggregation of particles with a polydisperse system. Polydisperse particles have a high tendency to aggregation than monodisperse system (Anbu et al., 2016; Müller et al., 1998).

Another method used in the determination of particle size in micrometer size range is laser diffraction (LD) which has a wider detection range between 20 nm to 2,000 μm (Keck & Müller, 2008). PCS and LD methods are often combined to detect the particle distribution from ultra-small to large particles. The principle of LD is based on the correlation between the diffraction angle and the particle diameter. The light scattered from an illuminated particle is detected by the detectors in a laser diffractometer which determines its angular distribution. The large particles scatter light at narrow angles with high intensities. On the other hand, small particles scatter light at wide angles with low intensities (Shah et al., 2015).

2. Morphology

The evaluation of particle morphology often uses electron microscope, such as SEM (scanning electron microscopy), TEM (transmission electron microscopy), and AFM (atomic force microscopy). Electron microscopes (EMs) use a focused beam of electrons instead of light to image the specimen and gain information as to its structure and composition (Stefanaki & Voutou, 2008).

In SEM, the electron source is focused in a vacuum and projected over the specimen surface. The electron beam passes through scan coils and the objective lens that deflect horizontally and vertically to scan the sample surface (Stefanaki & Voutou,

2008). As the electrons penetrate the surface, a number of interactions occur and result in the emission of electrons or photons from or through the surface which are collected by the detectors (Stefanaki & Voutou, 2008).

The SEM images are classified into 3 different types: secondary electron imaging, back-scattered electron imaging and X-rays imaging (Stefanaki & Voutou, 2008). Secondary electron imaging is the most common form of imaging which produces a high-resolution image of specimen topography. Back-scattered electron imaging is obtained because there are atomic number differences on the sample surface. The higher the atomic numbers of the atom, the brighter the image. X-rays are emitted from sub-surface of the specimen, providing information on specimen composition (Carter & Shieh, 2015). SEM is only used for conductive sample, so non-conductive materials must be coated by conductive materials, such as gold, palladium, silver, platinum, etc. Materials with atomic number lower than the carbon are not detected with SEM (Carter & Shieh, 2015). Resolution of SEM is approximately 2 nm (Carter & Shieh, 2015).

Transmission Electron Microscopy (TEM) is a powerful method with the resolution of 0.2 nm where an electron beam interacts and passes through a specimen. Some electrons are scattered and disappeared depending on the density of materials. Unscattered electrons pass the specimen and hit a fluorescent screen at the bottom of microscope, which gives rise to a “shadow image”. The darkness of the different displayed parts depends on the density of the specimen (Carter & Shieh, 2015). TEM produces 2D and black-white images and suitable for thin layer specimen (Carter & Shieh, 2015).

Atomic force microscopy (AFM) has been commonly used to determine the topography of solid lipid nanoparticles (Alex et al., 2011; Shahgaldian et al., 2003; Sitterberg et al., 2010). AFM produces a high-resolution image of the particle topography and is suitable for nanoparticles in the size range of nanometer to angstrom. The advantage of AFM is that it requires no sophisticated sample preparation. AFM produces the image by measuring the force acting between the particle surface and the probe tip. However, the interaction between sample and probe tip may distort the specimen surface (Dubes et al., 2003).

3. Zeta Potential

Zeta potential is the electric potential at the interfacial double layer of a dispersed particle. The charge on the surface of SLNs is commonly due to the presence of ionic surfactant/stabilizer, and also be an intrinsic charge from used lipids, such as free fatty acid (Shah et al., 2015). Zeta potential of +/−30 mV generally suggests that the dispersion is likely to be a stable, whereas solutions with zeta potentials between +/−10 and +/−30 mV are unstable over long storage time (McNeil, 2011). But, the previous study reported that the zeta potential of SLNs in the range of -15 to -38 mV is stable under 4ºC for 12 months (Khalil et al., 2013).

Determination of zeta potential is usually based on the principle of Doppler shift (laser Doppler anemometry). In this method, a weak electric field is applied to a diluted SLNs dispersion. The velocity of scattered light is used to estimate the electrophoretic mobility (μ, particle velocity/strength of electric field) (Deshiikan & Papadopoulos, 1998).

The zeta potential is commonly calculated from the electrophoretic mobility using the Helmholtz-Smoluchowski equation:

$$\zeta = \frac{4\eta\Pi}{\varepsilon} f(ka).\mu$$

Where,

Ɛ : permittivity

η : viscosity of the dispersion medium

μ : electrophoretic mobility

f(ka) : Debye function

ζ : zeta potential (Deshiikan & Papadopoulos, 1998).

Zeta potential measurement is conducted on diluted SLNs in order to avoid multiple scattering effects (Xu, 2008). The SLNs is dispersed in water with very low conductivity to provide the information about the surface charge of particles (Xu, 2008). The zeta potential value is increased by the addition of surfactants/co-surfactants such as phosphatidylcholine or Tween® 80 (Lim & Kim, 2002).

There are three different mechanisms that impart stability to SLN dispersions: (1) the electrostatic stabilization with either positive or negative charges on the particle

surface arising from the ionic surfactant, (2) the steric stabilization accomplishes by the addition of large molecular surfactant (polymers) that are soluble in the dispersion medium due to the adsorption of surfactant on nanoparticle surface, and (3) the electrostatic stabilization that is a combination of electrostatic and steric stabilization (Freitas & Müller, 1998).

The destabilizing of lipid nanoparticle in the dispersion is divided into several types:

a. Phase Inversion

In this phenomenon, the two phases of the system are inverted spontaneously and may occur at a critical temperature, pressure or concentration. This destabilization may occur during formulation but will not occur once the particles have cooled to form SLNs (Shah et al., 2015).

b. Flocculation

This phenomenon is caused by the Van der Waals forces between particles leading to the particle aggregation. Although the particles are close to each other, they are still separated by a finite distance with water remaining between them. This is a reversible phenomenon because the particles still maintain their integrity. The formed flocs are easily dispersed by shaking or mechanical agitation (Shah et al., 2015).

c. Creaming and Sedimentation

The lipid density relative to the density of the dispersion medium affects the sedimentation or creaming phenomenon. Creaming is the process in which dispersed particles move upwards when the dispersed particles density is lower than the density of continuous phase. Sedimentation is the process in which the dispersed particles move downwards when the dispersed particles density is higher than the density of continuous phase (Shah et al., 2015).

2.5. Sunscreen Cream

Cream is one of topical formulations which is semisolid emulsion systems with opaque appearances intended for application to the skin, hair or mucous membrane. The viscosity of cream is in the range of 20,000- 150,000 cps (Gupta et al., 2015; Lowe, 1996; A. Sharma & Prasar, 2013) with pH value in the range of 4-6.5 (Chen et al., 2016; Kumar et al., 2011).

Good characteristics of chemical sunscreen:

- The chemical should absorb the harmful UV radiation, at least in UVB region (280-320 nm).
- Sunscreen chemical should possess a high molecular extinction coefficient at the wavelength at which it absorbs the maximum UV radiation. The value of 20,000 would be desirable to be used as sunscreens.
- The chemical should be stable under the light.
- The chemical should not be toxic, skin-sensitizing, nor photo-sensitizing
- The ideal sunscreen should be inexpensive to use (Lowe, 1996).

Based on characteristics mentioned above, α-mangostin is suitable as sunscreen due to its ability to absorb UVB, its molecular extinction coefficient more than 20,000 (with Ɛ= 49987.33), its stability under light and its low price (Ahmad et al., 2013; Yodhnu et al., 2009; Zhang et al., 2014).

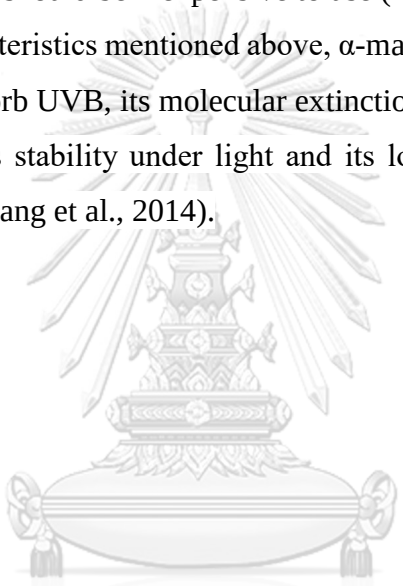

CHAPTER III
MATERIALS AND METHOD

3.1. Materials & Instruments

3.1.1. Raw Materials

Fresh fruit of *Garcinia mangostana* (purchased in June 2017, in Bangkok, Thailand)

3.1.2. Chemicals

Cetyl alcohol, cetyl palmitate (Emery Oleochemicals, Malaysia); ethanol, methanol, ethyl acetate AR grade & HPLC grade (RCI labscan, Thailand); glyceryl behenate (P.C. Intertrade Co., Ltd, Thailand); glyceryl palmitostearate (Gattefose, Germany); glyceryl trimyristate (The Sun Chemical Co., Ltd, Thailand); lanolin (NK Chemicals, Singapore); α-mangostin (Wuhan Chemfaces Biochemical Co., Ltd, China, lot no CFS201702A015); methyl paraben (UENO Fine Chemicals Industry, LTD, Japan); mineral oil (Kukdong Oil & Chemicals); palmitic acid, stearic acid (Namsiang company limited, Thailand); poloxamer 188 (Lutrol® F68) (BASF, Germany); polyvinyl alcohol, JP-18FT (Japan VAM & POVAL Co., Ltd, Japan); propylene glycol (Dow Chemical Thailand, Thailand); polyvinyl pyrollidone, potassium hydroxide, triethanolamine, Tween® 80 (East Asiatic Company, Thailand); Sorbitol Syrup (East Asiatic Company, Thailand).

3.1.3. Equipment and Instruments

Analytical balance AX105 (Mettler Toledo, Switzerland); automatic sample injector (G7129A Agilent 1260 Infinity, USA); botanical Grinder (Retsch GmbH SK 1, Germany); Brookfield viscometer RVDV (Brookfield Ametek, USA); centrifuge Z323 (Hermle, Germany); DAD detector (G7115A Agilent 1260 Infinity, USA); field emission scanning electron microscope (SEM) JSM-7800 FP (JEOL, USA); filter paper nylon membrane disc (Fortune scientific, Thailand); high performance liquid chromatography system: column (BDS Hypersil C18, 5µm, 250mm x 4.6mm, lot no.6596); high-speed stirrer (Wiggen Houser, Germany); ultracentrifuge CP100 NX (Hitachi, Japan); ultrasonicator VCX-750 (Sonics & Material, Australia); pH meter (Metler Toledo, Switzerland); photon correlation spectroscopy, Zetasizer ZS (Malvern

Instrument, UK); rotary evaporator (Buchi heating bath B-490, Switzerland); SPF analyzer 290-AS (Solar Light Company, USA); syringe filter cellulose acetate 13 mm, 0.2 µm (Chrome Tech Inc, USA); UV-Visible Spectrophotometer 600 (Thermo Fisher Scientific Inc, US).

3.2. High Performance Liquid Chromatographic (HPLC) Analytical Method

The HPLC conditions for analysis of α-mangostin (modified from Ruamkittham, 2005) were as follows:

Column	: BDS Hypersil C18, 5 µm (4.6 x 250 mm)
Mobile phase	: methanol : water (87:13)
Injection volume	: 20 µl
Flow rate	: 1 ml/min
Detector	: DAD detector at 244 nm
Run time	: 16 min
Temperature	: ambient

The mobile phase was filtered through a 0.45-µm nylon membrane filter and degassed by the sonicator for 30 min prior to use. The α-mangostin reference standard, MPE, and finished product were dissolved in ethanol prior to HPLC analysis.

3.3. Method Validation

3.3.1. Method Validation of Raw Material

3.3.1.1. Specificity

Retention time of major peaks in the MPE was compared along with the retention time of α-mangostin reference standard. Under the chromatographic conditions used, the peak of α-mangostin must be separated from and not be interfered by the peaks of other compounds. Peak purity index of α-mangostin should be higher ≥ 990.000.

3.3.1.2. Linearity

A weight about 20 mg of α-mangostin reference standard was placed into a 10 ml volumetric flask and diluted to volume with an addition of ethanol. This stock solution gave the final concentration of 2,000 µg/ml. Then 5 ml of the stock solution was transferred into a 100 ml volumetric flask and was diluted with mobile phase to give a solution of 100 µg/ml. The aliquot (1, 2, 3, 4, 5, 6 ml) of the second stock solution was added into 10 ml volumetric flasks. The obtained dilution gave 10, 20, 30, 40, 50,

60 µg/ml of α-mangostin. The standard solutions were done in triplicates. Each standard solution was analyzed under the HPLC condition stated above. The obtained peak areas were plotted against its corresponding concentration. The coefficient of determination (R^2) should be higher than 0.999.

3.3.1.3. Accuracy

The accuracy of the method was determined from the percentage of recovery. Three sets of three standard solutions at 10, 30, 50 µg/ml were prepared and analyzed. The percentage recovery was calculated from the ratio of the estimated concentration to the theoretical concentration multiplied by 100. The percentage of recovery of each concentration should be in a range of 98 - 102%.

3.3.1.4. Precision

The within run precision was determined by analyzing six sets of 30 µg/ml α-mangostin standard solution in the same day. The percent coefficient of variation or RSD was obtained from the ratio of mean peak area to standard deviation and should be lower than ± 2%.

3.3.2. Method Validation of Finished Product

3.3.2.1. Specificity

Retention time of major peaks of the MPE in the product was compared along with the retention time of α-mangostin reference standard. Under the chromatographic conditions used, the peak of α-mangostin must be separated from and not be interfered by the peaks of other compounds and excipients in the sample. Peak purity index of α-mangostin should be higher ≥ 990.000.

3.3.2.2. Linearity

A weight about 20 mg of α-mangostin reference standard was placed into a 10 ml volumetric flask and diluted to volume with an addition of ethanol. This stock solution gave the final concentration of 2,000 µg/ml. Then 5 ml of this solution was transferred into a 100 ml volumetric flask and was diluted with mobile phase to give solution of 100 µg/ml. The aliquot (1, 2, 3, 4, 5, 6 ml) of the second stock solution was spiked in about 500 mg of cream containing blank SLNs (PA-SLN or SA-SLNs). The mixture was dissolved with ethanol and adjusted to 10 ml in volumetric flask. The obtained dilution gave 10, 20, 30, 40, 50, 60 µg/ml of α-mangostin. Each process was done three times. As a result, linear regression analysis of the peak areas versus their

concentrations was performed. The coefficient of determination (R^2) should be higher than 0.999.

3.4. Preparation and Characterization of Mangosteen Pericarp Extract (MPE)

3.4.1. Preparation of MPE

The mangosteen fruit pericarps were cut into small pieces about 1 x 1 inch and dried at the temperature of 45 ± 0.5 °C in a hot air oven. The dried fruit pericarps were ground into powder by using a botanical grinder (Modified from Hiranras, 2001; Pothitirat et al., 2010).

Mangosteen pericarp powder was macerated with ethyl acetate at room temperature for 48 h. The extract was concentrated using a rotary evaporator (Rotavap-or Buchi R-200, Switzerland). The mangosteen pericarp extract (MPE) was kept in a desiccator for further studies (Modified from Aisha et al., 2013; Hiranras, 2001; Siriphan, 2008).

3.4.2. Characterization of MPE

Presence of α-mangostin in the MPE, purity percentage of the MPE and SPF value were investigated. The presence of α-mangostin in the MPE was identified by comparing the HPLC retention time and spectral match factor of the MPE with that of the α-mangostin reference standard. Spectral match factor was obtained by overlaying the spectra of major peak of MPE with that of the α-mangostin reference standard and calculating the numerical value that defines the closeness of the match. The spectral match factor should be more than 999.

Purity percentage of the MPE was calculated as the percentage of α-mangostin in the MPE. The MPE stock solution was prepared by weighing 100 mg of MPE into a 100 ml of volumetric flask adjusted to the volume by an addition of ethanol. This stock solution had a concentration of 1 mg/ml. Then, 4 ml of stock solution were transferred into a 50 ml volumetric flask. The solution was adjusted to volume using ethanol to give the MPE solution of 80 µg/ml and subjected to HPLC analysis.

Purity percentage was calculated as:

$$\text{Purity percentage} = \frac{\text{α-mangostin concentration}}{\text{MPE concentration}} \text{X100}$$

The SPF value of the MPE was measured using a UV-Vis spectrophotometer. The MPE ethanolic solution was prepared by weighing 100 mg of MPE into 100 ml of volumetric flask and adjusted using ethanol to volume. The concentration of this solution was 1 mg/ml. Then 5 ml of this solution was transferred into 50 ml to obtain the concentration of MPE solution of 100 µg/ml. Then 2, 4, 5, 6, 8, 10 ml of this solution were pipetted into 10 ml volumetric flask to obtain the concentration of MPE solution at a concentration of 20, 40, 50, 60, 80, 100 µg/ml. The absorption spectra of samples in solution using 1 cm quartz cell was measured in the range of 290 to 320 nm using ethanol as a blank. The absorbance was taken at every 5 nm in the specified range and calculated for SPF value using Mansur equation (Dutra et al., 2004; Mansur et al., 1986).

$$SPF = CF \times \sum_{290}^{320} EE\ (\lambda) \times I(\lambda) \times Abs\ (\lambda)$$

EE : action spectrum of erythema (see Table 2, page 14);

I : spectrum of solar intensity (see Table 2);

Abs : sunscreen product absorbance;

CF : correction factor (=9.37). The calculation used a standard sunscreen formulation containing 1% octyl methoxycinnamate presented an SPF value of 1.5 (Dutra et al., 2004; Mansur et al., 1986).

3.5. Selection of Solid Lipids

Glyceryl palmitostearate, glyceryl behenate, glyceryl trimyristate, stearic acid, palmitic acid and cetyl palmitate were screened for their potential to solubilize MPE. Briefly, 3 g of solid lipid was taken in screw capped test tubes and heated above its melting point. The MPE (1.5 g) was gradually added into molten solid lipid. The lipid selection criteria were the lipids that gave homogeneous mixture both in molten and solidified stages (Baek et al., 2018; Siriphan, 2008).

3.6. Preparation and Characterization of Solid Lipid Nanoparticles (SLNs)

3.6.1. Preparation and Characterization of Blank SLNs

Ultrasonication method was used for the preparation of aqueous SLNs dispersions (Xie et al., 2011). The oil and aqueous phases were prepared separately. The oil phase consisted of molten solid lipid and aqueous phase consisted of hydrophilic surfactant dispersed in water. The solid lipid was melted at 5 ^{o}C above its melting point. Using a high-speed stirrer (Wiggen Houser, Germany), the oil phase was dispersed in a hot aqueous phase at same temperature for 5 minutes. The obtained hot pre-mixed emulsion was sonicated using an ultrasonicator (Sonics & Material, Australia) at the amplitude of 80% for 15 minutes to form hot nanoemulsion. The hot nanoemulsion was poured into cold water (3-5 ^{o}C) to form SLNs dispersion with a 1:2 ratio of nanoemulsion to cold water. The nanoparticles were collected by centrifugation (Hitachi, Japan) at 18,000 rpm for 15 minutes at 25^{o}C.

The concentration of chosen lipids was kept constant at 3%. The type of surfactant was varied, i.e., Tween® 80, poloxamer 188, PVP and polyvinyl alcohol (PVA) and their concentration were in a range of 1 - 2%. The effect of types of solid lipid and types and amount of surfactant were evaluated on the characteristic of SLNs (Modified Siriphan, 2008; Xie et al., 2011).

Characterization of blank SLNs included physical appearances, morphology, particle size, PDI, and zeta potential value.

- Physical appearances of the formulations such as color and phase separation were visually observed.
- Morphology analysis was performed by a scanning electron microscopy (SEM) (JEOL, USA). The 100 mg of SLNs dispersion was diluted using 50 ml of distilled water to obtain the concentration of 2 mg/ml. The 200 µl of this dilution was pipetted on the petri dish and dried in a desiccator for 72 hours. The dried sample was placed on a stage using double-sided adhesive carbon tape and coated with gold prior to measurement. The accelerating voltage was set at 5 kV with a working distance of 6 mm using secondary electron image.
- The particle size, size distribution (PDI), and zeta potential were investigated by photon correlation spectroscopy (PCS) using a Zetasizer Nano ZS90 (Malvern Instrument, UK). The 40 mg of blank SLNs dispersion was diluted into 100 ml of

volumetric flask and adjusted to the volume by the addition of distilled water to obtain the concentration of 0.4 mg/ml. The samples were placed into disposable sizing cuvettes DT50012 and measured at 25 ^{o}C with dispersant refractive index of 1.33 and dispersant viscosity of 0.8872 cP using 173^{o} backscattered angle for size and PDI measurement. The zeta potential measurement used disposable folded capillary cells following the same dispersant setting of size measurement with dielectric constant of 78.5. Zeta potential calculation was based on Smoluchowski approximation.

3.6.2. Preparation and Characterization of MPE-SLNs

The concentration of MPE exhibiting the SPF value approximately 15 was selected as loading concentration in SLNs. 1.5 g of MPE was added to the molten lipids. The MPE-SLNs were prepared according to the procedure as described in 3.6.1. (Modified from Siriphan, 2008).

The characterization of the formulations such as color, phase separation, morphology, size, PDI, and zeta potential value was performed before and after centrifugation at 18,000 rpm for 15 minutes 25^{o}C as described in 3.6.1. Yield percentage of MPE-SLNs was investigated by the centrifugation of 1 g of MPE-SLNs dispersion. The MPE-SLNs pellet was dried at desiccator for 72 hours.

Yield percentage (%): $\frac{\text{mass of the dried MPE-SLNs pellet}}{\text{theoretical mass of MPE-SLNs}} \times 100$

Entrapment efficiency percentage was measured by HPLC. To investigate the entrapment efficiency, 1 g of MPE-SLNs dispersion was weighed into the ultracentrifuge (Hitachi, Japan) assembly and was separated by ultracentrifugation at 25,000 rpm for 15 minutes at 25^{o}C. The precipitated pellet containing MPE was dissolved into 50 ml of volumetric flask by an addition of ethanol to volume. The solution was filtered using Whatmann no 1 to separate the insoluble PVA. The clear solution was analyzed for entrapped α-mangostin content by HPLC. All analyses were determined in triplicates (Modified from Tan, 2004). Freshly prepare standard curve was constructed from peak areas of α-mangostin standard solution in ethanol in a concentration range of 10 – 60 μg/mL. The concentration of α-mangostin in the formulation was calculated from the corresponding standard curve.

The entrapment efficiency was calculated by the following equation.

$$\text{EE (\%)}: \frac{\text{mass of the MPE in nanoparticle}}{\text{theoretical mass of MPE used in nanoparticle preparation}} \times 100$$

(Xie et al., 2011).

3.7. Preparation and Characterization Cream

3.7.1. Preparation and Characterization of Blank Cream

In this study, vanishing cream base was prepared using a beaker method. Two cream base formulations were prepared in order to select the most stable cream to be used (Table 6).

Table 6 Cream base formulation

Ingredients	C1 (g) (Young, 1972)	C2 (g) (USP 31)
Oil phase		
Stearic acid	12	10
Cetyl alcohol	0.5	1
Mineral oil	-	5
Lanolin	-	2
Aqueous phase		
TEA	1.0	-
Methyl paraben	0.1	0.1
Sorbitol syrup	5	-
Propylene glycol	3.0	5
Potassium hydroxide	-	0.5
Distilled water	q.s. 100	q.s. 100

To prepare the cream base, the oil phase was heated up to 75 ± 1 ^{o}C. At the same time, the aqueous phase was heated to the same temperature. After heating, the oil phase was gradually added to the aqueous phase. The mixture was kept stirring using a mechanical stirrer at 4,000 rpm until it was congealed. Finally, cream base was characterized for its physical stability (Modified from Waqas et al., 2010).

Physical stabilities of the prepared cream including color, phase separation, pH and viscosity were recorded before and after 6 heating-cooling cycles (1 cycle= 4-8^{o} C for 24 hours and 40^{o} C for 24 hours) or centrifugation test at 6,000 rpm for 30 minutes according to Thai Industrial Standard (152-2539). Color and phase separation were

investigated by visual observation. pH of cream base was investigated using pH meter (Orion model 420A, Orion Research Inc., USA). In this measurement, the 100 mg of cream base was weighed and dissolved in 10 ml of deionized water to prepare the samples. The pH probes were calibrated using buffered pH standards of pH 4, 7, and 10. The measurement of pH of each formulation was done in triplicate and average values are calculated (Waqas et al., 2010).

Viscosity was measured using Brookfield viscometer RVDV (Brookfield Ametek, USA). The samples were prepared by weighing 0.5 gram of cream base and placing on specimen cup. The spindle no. 52 was rotated at speed of 2.5 rpm with factor as shown in Table 7. Samples were measured triplicates at room temperature. The reading was noted and calculated using following equation:

$$\text{Viscosity} = \frac{\text{Display range}}{100} \text{X Factor}$$

Table 7 Factor of cone 52 of viscometer Brookfield

Speed (rpm)	Shear rate (/sec)	Factor of cone 52
2.5	5	39,320
1	2	98,300
0.5	1	196,600

3.7.2. Preparation and Characterization of Cream Containing MPE-SLNs

In this study, the preparation of cream containing MPE-SLNs was prepared by an addition of MPE-SLNs into cream base to get the concentration of 0.06 mg MPE/ 2 mg cream (3%) (Modified from Waqas et al., 2010). Morphologies of cream containing MPE-SLNs were evaluated at the initial time following the same procedure as 3.6.1 at cream containing MPE-SLNs concentration of 0.125 mg/ml. Other physical stabilities of cream containing MPE-SLNs such as color, phase separation, pH and viscosity were evaluated during storage at 4-8 ^{o}C for 3 months following the same procedure as 3.7.1. Samples were evaluated at 0, 1, 2, and 3 months.

The chemical stability (the α-mangostin content) during storage at 4-8 ^{o}C was analyzed using HPLC at 0, 1, 2, and 3 months. The degradation percentage should less

than 5%. The 100 mg of cream containing MPE-SLNs was weighed into 50 ml of volumetric flask and dissolved by an addition of ethanol to volume and filtered through syringe filter prior to inject into HPLC.

The evaluation of SPF value of cream base, cream containing blank SLNs, 3% MPE cream, standard sunscreen (8% homosalate cream) and cream containing MPE-SLNs was performed using an SPF analyzer at 0 and 3 months and was evaluated by applying about 1.3 mg/cm^2 on PMMA plate (5 x 5 cm). The sample was deposited on the plate using a syringe in order to aid the uniform coverage and spread on the plate with a very light pressure for 30 seconds followed by greater pressure for approximately 30 seconds using a finger cot. A finger cot should be saturated using glycerin prior to use. The sample was dried in dark place for 15 minutes before measurement. UV light should be avoided during this period. The SPF value was obtained by averaging results of 9 scans of the sample at different locations on the PMMA plate (Optometrics, 2009).

The measurement was obtained in the range of 290-400 nm using the following equation.

$$SPF = \frac{\int_{290}^{400} E\ (\lambda) \times S(\lambda)}{\int_{290}^{400} E\ (\lambda) \times S(\lambda)\ /MPF}$$

Where: S : erythemal action spectrum (McKinlay & Diffey, 1987);

E : solar intensity spectrum;

MPF : monochromatic protection factor (1/T) (Optometrics, 2009).

3.8. Statistical Analysis

The data of particle size, size distribution, zeta potential, entrapment efficiency percentage, viscosity, pH and SPF value were analyzed by statistically using ANOVA and a significant difference (p<0.05) be indicated, the data was subjected to multiple comparisons by Tukey test to compare the difference.

CHAPTER IV
RESULTS AND DISCUSSION

4.1. Analytical Method Validation

The validation of analytical method is the process in which the method is established to meet the specific parameters for its intended application (ICH, 2005). The performance characteristics are expressed in terms of analytical parameters. The parameters for HPLC assay are specificity, linearity, accuracy, and precision.

The preliminary study of α-mangostin absorbance using a spectrophotometer UV-Vis showed that the spectra of α-mangostin in 87% v/v methanol has the maximum absorbance at 244 nm (Figure 11), thus, the detection wavelength of α-mangostin was performed at this wavelength.

Different mobile phase composition such as 70% acetonitrile, 95% acetonitrile, or methanol - 0.4% formic acid, did not affect the maximum absorbance at 244 nm which indicated that there was no solvent effect on the maximum wavelength of α-mangostin (Ahmad et al., 2013; Aisha et al., 2013; Rasyid et al., 2016; Tatiya et al., 2016; Widowati et al., 2014). The maximum absorption at 244 nm is related to the excitation energy π→π* transition by aromatic structure (with Ɛ= 49987.33) (Ahmad et al., 2013).

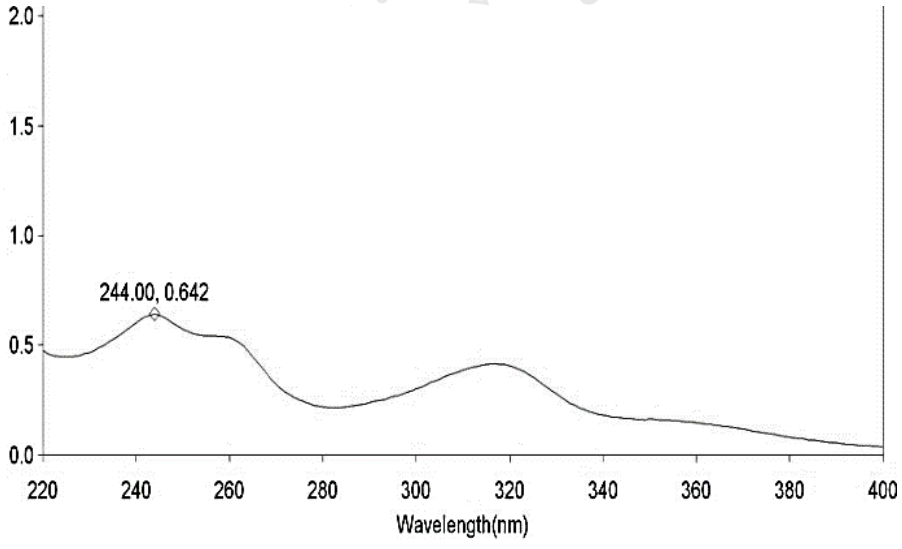

Figure 11 Absorption spectra of α-mangostin in 87% methanol in water

4.1.1. Analytical Method Validation of Raw Material

4.1.1.1. Specificity

The specificity of an analytical method is the ability to specifically detect the analyte in the presence of other components (ICH, 2005). Peak purity index is calculated based on the collected spectra during the separation process. The same UV spectra shape across the peak indicates that there is no co-elution of other compounds with the compound of interest.

The separation was obtained using methanol 87% in water (v/v) as the mobile phase. The typical chromatograms of ethanol, α-mangostin reference standard and MPE solution are shown in Figures 12, 13, and 14, respectively. Chromatogram of MPE showed similar retention time to that of the standard α-mangostin with the retention time of 8.8 minutes. Peak purity index of the major peak of MPE and α-mangostin reference standard was higher than 990.000 (Figure 15).

In other words, there was no interference from coeluting analytes. This result confirms that the HPLC method has the ability to determine the α-mangostin even in the presence of other compounds (Abiramasundari et al., 2014).

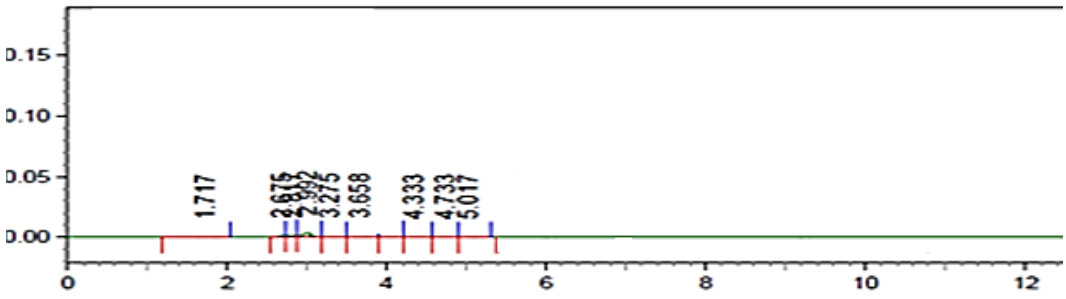

Figure 12 Chromatogram of ethanol

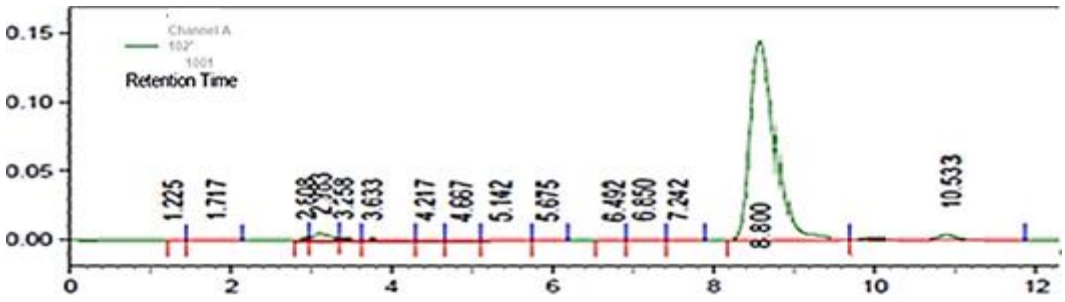

Figure 13 Chromatogram of α- mangostin reference standard

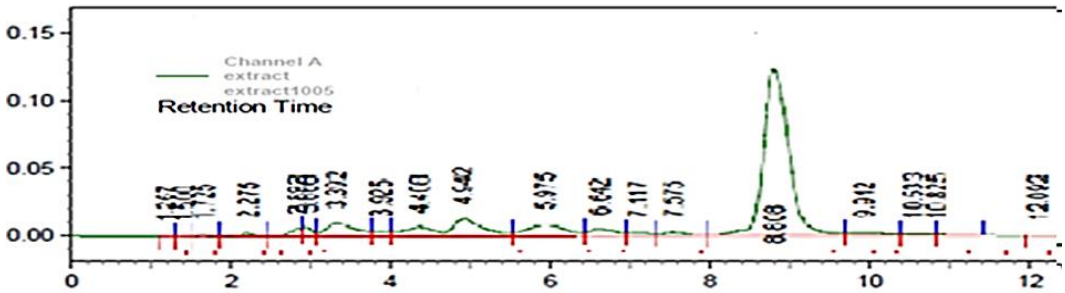

Figure 14 Chromatogram of MPE

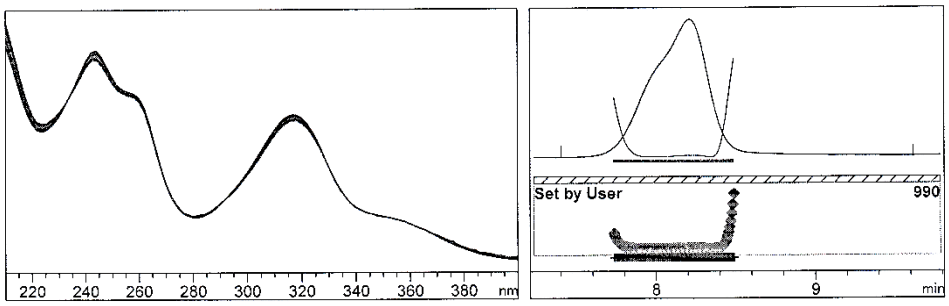


```
-> The purity factor is within the threshold limit. <-

Purity factor : 999.555 (114 of 114 spectra are within the threshold limit.)
Threshold     : 990.000  (Set by user)
```

Figure 15 Peak purity index of α-mangostin in MPE

4.1.1.2. Linearity

Linearity is the ability of a method to show the proportional relationship between the concentration of the analyte in the sample and the response of the instrument. Linearity is calculated from an established mathematical test results obtained with varying analyte concentrations. The calibration curve of α-mangostin reference standard in the range of 10-60 µg/ml is shown in Table 8. The plot between peak area and α-mangostin reference standard concentration showed the linear

correlation in the studied concentration range of 10-60 µg/ml. The coefficient of determination (R^2) of this line was higher than 0.9998.

All coefficient determination result met the specified coefficient of determination of 0.999 which indicated that this method showed a proportional relationship between α-mangostin reference standard concentration in the range of 10-60 µg/ml and the instrument response in the terms of peak area. This method was acceptable for analysis of α-mangostin in the specified concentration range.

Table 8 Data for calibration curve of α-mangostin by HPLC method

Concentration (µg/ml)	Peak area		
	Set 1	Set 2	Set 3
10.09	898533	902208	905943
20.18	1781719	1781339	1741665
30.27	2681982	2680990	2683064
40.36	3580108	3579853	3579367
50.45	4515235	4515197	4517472
60.54	5389682	5391872	5394257
R^2	0.9999	0.9999	0.9998

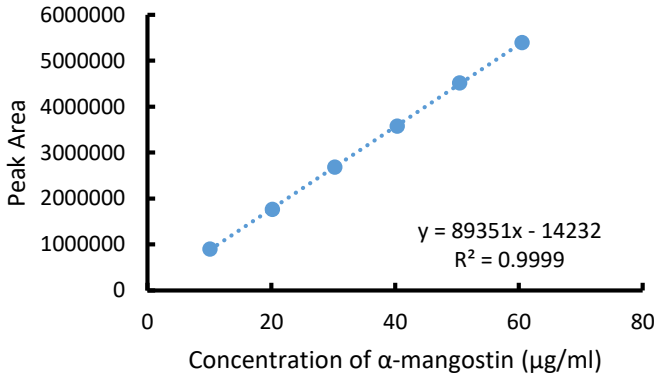

Figure 16 Calibration curve of α-mangostin reference standard (Set 1)

4.1.1.3. Accuracy

The accuracy of the analytical method refers to the closeness of theoretical value or true value with the found value from the instrument measurement. The determination of accuracy is performed by analyzing three sets of three known concentrations of α-

mangostin standard solution (10.09, 30.27, 50.45 μg/ml). The estimated concentration and analytical recovery percentages of α-mangostin standard concentration are shown in Tables 9 and 10, respectively.

The results showed that all analytical recovery percentages are in the range of 99.73±0.005 to 100.55±0.003, which indicates that this method meets the criteria (98-102%) and could be used for the α-mangostin analysis.

Table 9 The estimated concentration of α-mangostin by HPLC method

Concentration (μg/ml)	Estimated concentration (μg/ml)			Mean ± SD
	Set 1	Set 2	Set 3	
10.09	10.10	10.07	10.09	10.09±0.01
30.27	30.19	30.18	30.18	30.19±0.01
50.45	50.73	50.73	50.72	50.73±0.01

Table 10 The analytical recovery percentages of α-mangostin by HPLC method

Concentration (μg/ml)	Analytical recovery percentage (%)			Mean ± SD
	Set 1	Set 2	Set 3	
10.09	100.12	99.86	100.01	99.99±0.13
30.27	99.74	99.73	99.73	99.73±0.01
50.45	100.56	100.55	100.55	100.55±0.01

4.1.1.4. Precision

Precision is commonly expressed as a coefficient of variation from a series of measurements. Precision can be obtained by analyzing either nine examinations of three sets of three known concentrations of standard solution or six determinations at 100% of the test concentration (ICH, 2005). Six determinations at 100% of the test concentration were done in this study because the allowed degradation percentage was less than 5%.

Table 11 shows the data of precision. Coefficient of variation value was less than 2% which indicated this method was acceptable to be used in α-mangostin analysis.

Table 11 Data of precision by HPLC method

Conc (µg/ml)	Peak area		Mean	SD	%CV
30.27	Set 1	2677554	2669660.33	12749.14	0.01
	Set 2	2677540			
	Set 3	2647457			
	Set 4	2677384			
	Set 5	2660803			
	Set 6	2677224			

4.1.2. Analytical Method Validation of Finished Product

4.1.2.1. Specificity

The typical chromatograms of the finished product including MPE-PA-SLNs, MPE-SA-SLNs, cream containing MPE-PA-SLNs, and cream containing MPE-SA-SLNs were shown in Figures 17, 18, 19, 20. All finished products showed the peak with retention time of 8.8 minutes corresponding to α-mangostin. Peak purity index of the major peak of MPE in all finished products is shown in Table 12 and was higher than 990.000.

The results indicated that this HPLC method could separate α-mangostin from the other compounds and pharmaceutical excipients proved by peak purity index of MPE-PA-SLNs and MPE-SA-SLNs which were higher than 990.00.

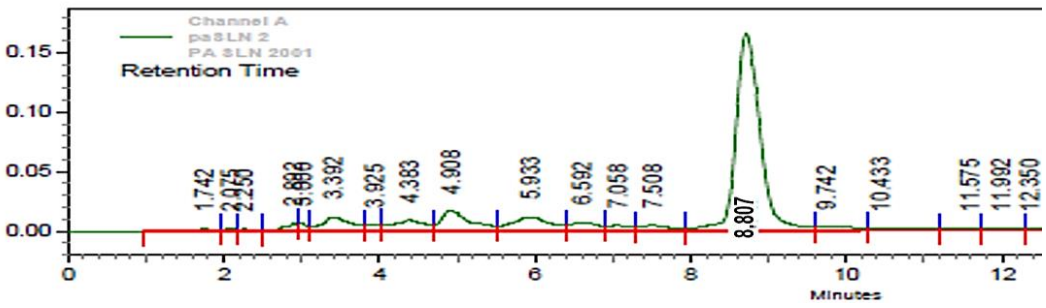

Figure 17 Chromatogram of MPE-PA-SLNs

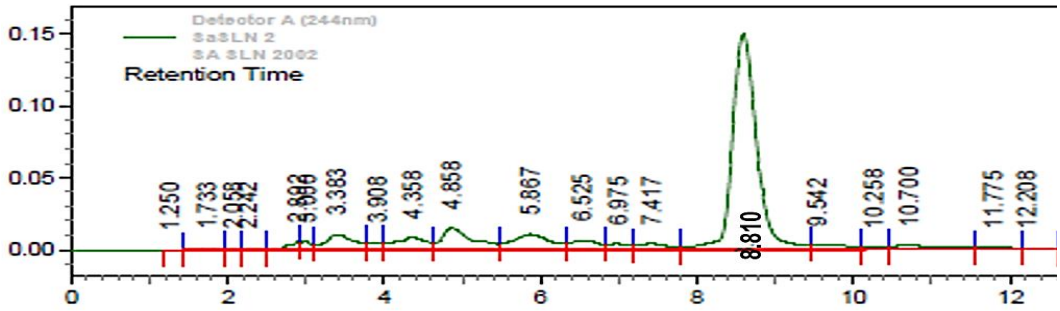

Figure 18 Chromatogram of MPE-SA-SLNs

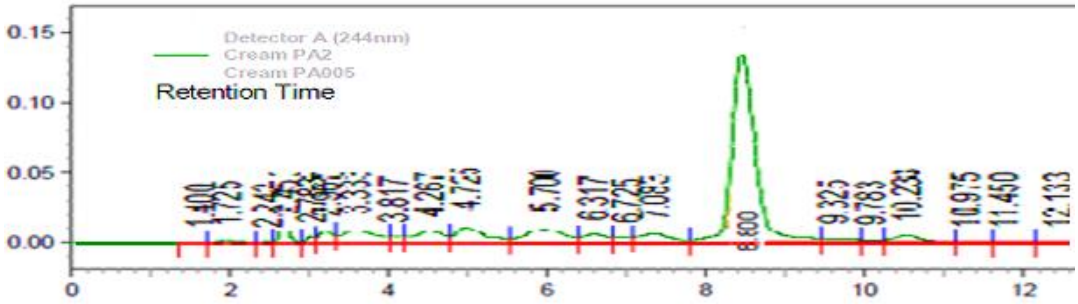

Figure 19 Chromatogram of cream containing MPE-PA-SLNs

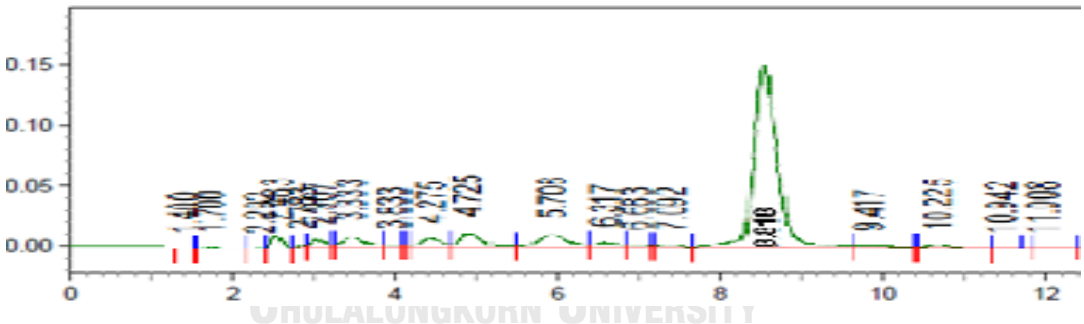

Figure 20 Chromatogram of cream containing MPE-SA-SLNs

Table 12 Peak purity index of MPE major peak in the finished products

Formulations	Peak purity index
α-mangostin + cream containing PA-SLNs	999.78
α-mangostin + cream containing SA-SLNs	999.55
MPE-PA-SLNs	999.22
MPE-SA-SLNs	999.22
Cream containing MPE-PA-SLNs	999.38
Cream containing MPE-SA-SLNs	999.48

4.1.2.2. Linearity

The calibration curve of α-mangostin reference standard in the presence of blank cream-PA-SLN or blank cream-SA-SLNs was compared with that of α-mangostin reference standard in order to examine matrix effect on the α-mangostin analysis. All standard curves were prepared in a concentration range of 10-60 µg/ml as shown in Figure 21.

All coefficient of determination results met the criteria (more than 0.99). The slope of calibration curves of α-mangostin reference standard spiked in that of blank cream-PA-SLNs or blank cream-SA-SLNs were superimposed on one another. In addition, the slopes of those three calibration curves were not significant difference (p>0.05).

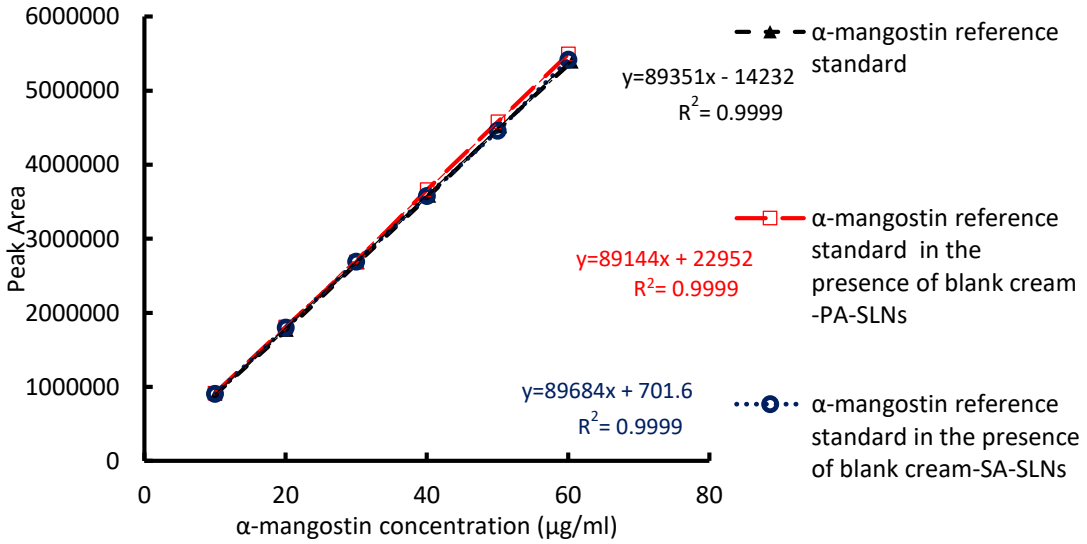

Figure 21 Overlaid calibration curve of α-mangostin reference standard in the presence of blank cream-PA-SLNs, α-mangostin reference standard in the presence of blank cream-SA-SLNs and α-mangostin reference standard

This method was acceptable for analysis of α-mangostin in the specified concentration range and showed that there was no matrix effect from the pharmaceutical excipients used in this study.

4.2. Preparation and Characterization of Mangosteen Pericarp Extract (MPE)

4.2.1. Preparation of MPE

The MPE was obtained via maceration of 450 grams of the dried pericarp powder using ethyl acetate. The extract was dark brown powder after drying with a rotary evaporator and keeping in a desiccator. The weight of final yield was about 45 grams with yield percentage of 9.85% ± 0.5%, n = 3. The yield percentage in this study was higher than that reported by Ruamkittham, with a yield percentage of 7.47%, which might be due to different environmental factors such as provenance, soil condition, time of harvest, etc (Medina-Holguín et al., 2007).

4.2.2. Characterization of MPE

The retention times between major peak of MPE (Figure 14) and that of α-mangostin reference standard (Figure 13) were similar. Spectral match factor of 999.987 showed that the major peak of MPE is α- mangostin (Figure 22).

The validated HPLC method was used to calculate the percentage of α-mangostin in MPE. The percentage of α-mangostin present in the MPE was 44.30 ± 3.45 %, n=3 from three maceration batches (Table 13). Hiranras, 2001, used the same extraction procedure but obtained the α-mangostin percentage in the MPE of 55.86%. The lower α-mangostin percentage present in the MPE found in this study might be a result from several factors such as provenance, soil condition, time of harvest, etc (Medina-Holguín et al., 2007).

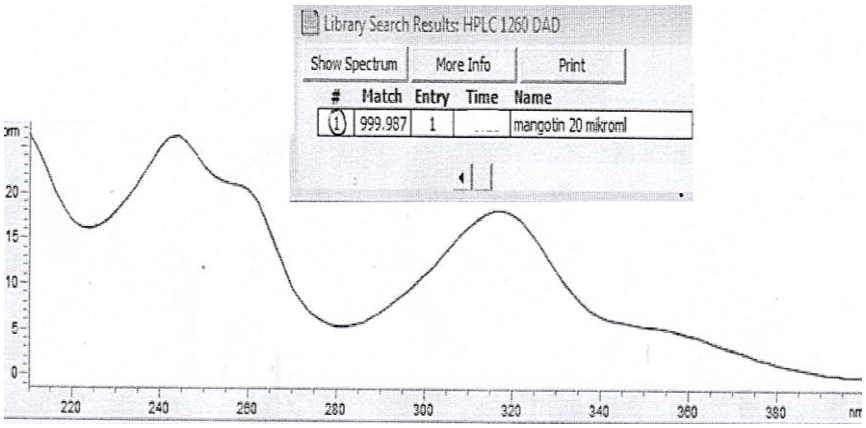

Figure 22 Spectral match factor of MPE and α-mangostin

Table 13 Purity percentage of MPE

Extract weight (mg)	α-Mangostin percentage (%)	Mean	STD
100.40	48.28	44.31	3.45
100.00	42.31		
100.01	42.32		

The SPF is a quantitative measurement of the UVB protective ability of sunscreen. The SPF value was determined using UV-Vis spectrophotometer in the range of 290-320 nm to show the ability of MPE in absorbing UVB range. The UV-Vis spectrophotometer was employed in SPF estimation of MPE because it was suitable for a liquid sample while SPF analyzer was suitable for semisolid sample (Optometrics, 2009). The ability of MPE as sunscreen came from the chromophores present in α-mangostin which could absorb UVB with maximum absorbance at 244 and 317 nm (Ahmad et al., 2013).

Figure 23 shows that MPE in the range concentration of 0.02-0.1 mg/ml gave the SPF value ranging from 3.09 to 27.2. The previous study reported that the methanolic mangosteen pericarp extract has an SPF value of 15.96 at the concentration at 0.1 mg/ml (Pathirana et al., 2016) which is lower than the SPF value of ethyl acetate mangosteen pericarp extract used in this study. The methanolic mangosteen pericarp extract had lower α-mangostin content (36.18 %) than ethyl acetate mangosteen pericarp extract (44.30 %) (Pathirana et al., 2016; Raghavendra et al., 2011).

In this study, the final concentration of MPE in the product was targeted at 0.06 mg/ml in order to obtain an SPF value around 15 (Fitzpatrick, 1988) which was recommended by FDA USA for Asian people (FDA, 2015).

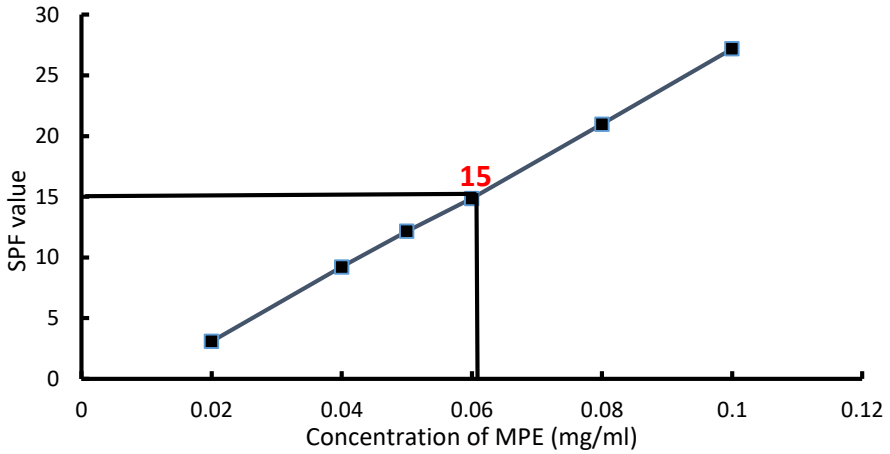

Figure 23 *In vitro* assessment of the SPF of the mangosteen pericarp extract (MPE)

4.3. Selection of Solid Lipids

Solubility of lipid is an important factor that affects the entrapment efficiency of MPE (Kumar & Sinha, 2016). In this study, different lipid types with different HLB value were used. Glyceryl palmitostearate, glyceryl behenate, glyceryl myristate are the mixture of mono-, di-, and triglycerides, whereas cetyl palmitate is wax, and stearic and palmitic acid are fatty acids. These lipids were screened for their ability to solubilize MPE. The characteristics of MPE in different lipids at molten state (75°C) and solidified state (room temperature) are displayed in Figure 24.

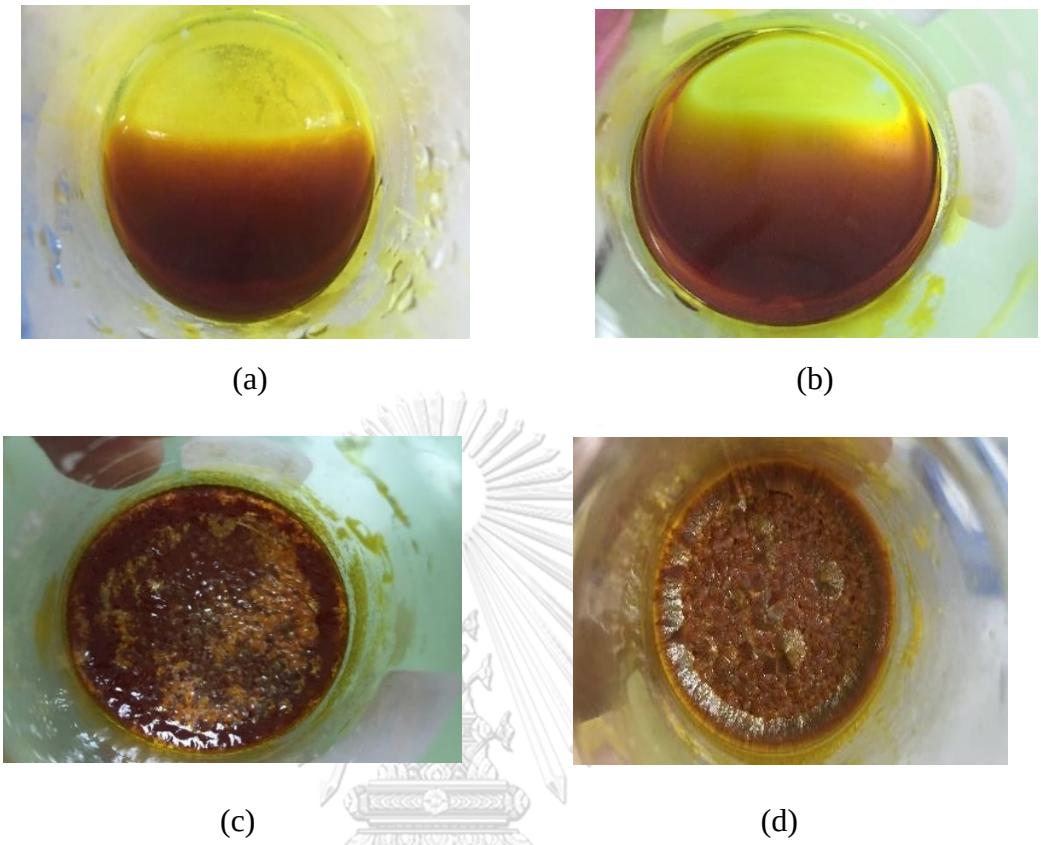

(a) (b)

(c) (d)

Figure 24 Photographs of MPE in different lipids at molten state at 75 °C and solidified state at room temperature (RT);
(a) Palmitic acid (75°C) (b) Stearic Acid (75°C)
(c) Palmitic acid (RT) (d) Stearic Acid (RT)

Selection of lipids was performed in order to dissolve 1.5 g of MPE in 3 g of solid lipids. Amongst the investigated solid lipids, stearic acid and palmitic acid demonstrated the effective solubilizing potential of MPE and yielded a brown transparent mixture at both molten and solidified stages. No separation was found after molten lipids were solidified. However, MPE was not dissolved in wax (cetyl palmitate) or triglycerides (glyceryl palmitostearate, glyceryl behenate, glyceryl trimyristate).

As regulated by the US FDA, all six lipids under this investigation are generally recognized as safe lipids. The MPE was dissolved in palmitic acid (HLB=15.6) and stearic acid (HLB=14.9) which are saturated fatty acids but was not dissolved in wax and triglycerides (HLB in the range of 2-10) due to the less lipophilic nature of the ethyl

acetate extract (Abd-Elbary et al., 2013; Anarjan & Tan, 2013). Based on the above result, the obtained MPE was appeared to have hydrophilic nature.

4.4. Preparation and Characterization of Solid Lipid Nanoparticles (SLNs)

4.4.1. Preparation and Characterization of Blank SLNs

The physical appearances of blank SLNs were white milky dispersion. The blank-SLNs containing PVA were more viscous than the blank SLNs containing Tween® 80 as shown in Figures 25 and 26. The physical characteristics of blank SLNs are shown in Table 14.

(a) (b) (c) (d) (e) (f)

Figure 25 Photograph of blank SLNs, (a) PA-Tween®80 1%, (b) PA-Tween®80 1.5%, (c) PA-Tween®80 2%, (d) SA-Tween®80 1%, (e) SA-Tween®80 1.5%, (f) SA- Tween®80 2%

(a) (b) (c) (d) (e) (f)

Figure 26 Photograph of blank SLNs, (a) PA-PVA 1%, (b) PA-PVA 1.5%, (c) PA-PVA 2%, (d) SA-PVA 1%, (e) SA-PVA 1.5%, (f) SA-PVA 2%

Table 14 Formulations of blank SLNs (mean ±SD, n=3)

Code	Lipid 3% (w/w)	Surfactant (% w/w)		Particle size (nm)	PDI	Zeta potential
F1	Stearic acid (SA)	Tween® 80	1	584.3±8.39	0.53±0.02	-28.5±1.18
F2			1.5	818.9±0.04	0.69±0.04	-27.9±0.48
F3			2	Physical properties can not be measured (size >1000 nm)		
F4		PVA	1	382.6±5.82	0.15±0.01	-15.76±0.79
F5			1.5	341.5±3.46	0.07± 0.01	-16.55±0.21
F6			2	336.1±1.94	0.05±0.01	-16.65±0.53
F7	Palmitic acid (PA)	Tween® 80	1	553.4±10.02	0.48±0.01	-30.1±1.83
F8			1.5	765.3±0.02	0.59±0.02	-31.01±1.48
F9			2	985.7±15.28	0.85±0.08	-29.33±2.06
F10		PVA	1	306.5±0.01	0.09±0.01	-15.75±0.37
F11			1.5	304.8±1.55	0.06±0.01	-14.92±0.50
F12			2	301.6±1.99	0.04±0.01	-15.21±0.19

The morphology of blank SLNs was investigated using scanning electron microscopy (SEM). Figure 27 shows the spherical shape and non-smooth surface.

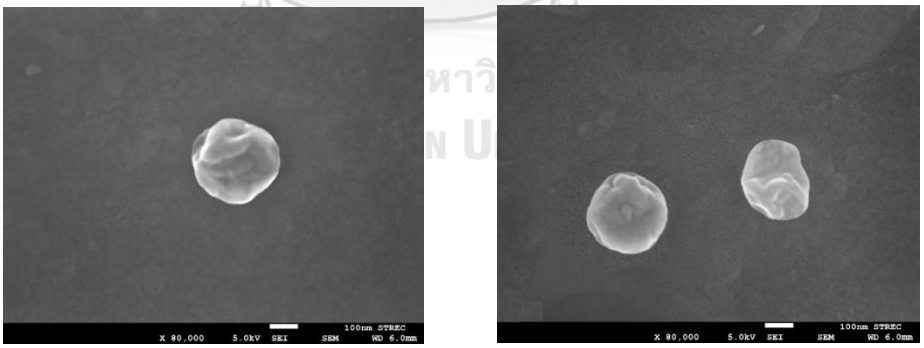

(a) (b)

Figure 27 The SEM of blank SLNs, (a) SA-PVA 1%, (b) PA-PVA 1%

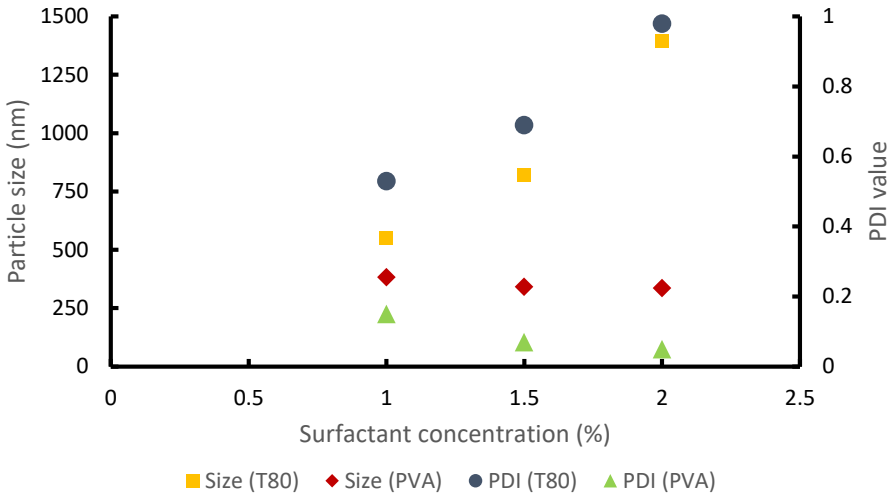

Figure 28 Plots between particle size, surfactant type and concentration of SA-SLNs

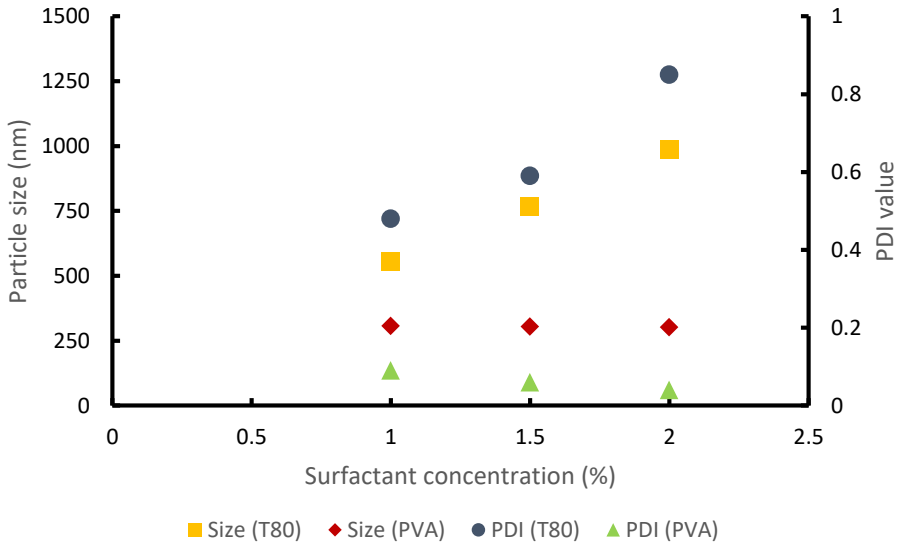

Figure 29 Plots between particle size, surfactant type and concentration of PA-SLNs

Blank SLNs were prepared via ultrasonication method using 3% stearic acid or palmitic acid. The type of surfactant was varied, i.e., Tween® 80, poloxamer 188, PVP and polyvinyl alcohol (PVA). Their concentrations were varied in a range of 1 - 2%. From the preliminary study, it was found that PVA and Tween® 80 at a concentration of 1 to 2% as surfactants are suitable for the preparation of blank SLNs and produce SLNs with good physical characteristics, whereas the employment of poloxamer 188 and PVP as surfactant results in gel formation.

The reason of those phenomena may be due to the HLB value of surfactant. Tween® 80 and PVA have similar HLB values as that of chosen lipids which are in the range of 14.9-15.6 (Hayakawa et al., 1994; Park et al., 1992). On the other hand, the other surfactants have higher HLB values than the required HLB values of solid lipids; i.e. poloxamer 188 (HLB value = 29) (Anarjan & Tan, 2013). Therefore, PVA and Tween® 80 were used as the surfactant for further studies as shown in Table 14.

Other studies reported that the ultrasonication method results in smaller particle size and PDI than the solvent injection method or high-pressure homogenization method due to the difficulty to control the hot temperature and pressure during homogenization process (Rawat et al., 2010). Thus, ultrasonication was selected in this study. The ultrasonication amplitude of 80% was chosen based on the finding reported by Xie et al, 2011, since the employment of high amplitude produced small particle size (Hielscher, 2007; Xie et al., 2011). The preliminary study also showed that the employment of 80% amplitude results in smaller particle size and PDI in compared with 30% and 70% amplitude for 15 minutes.

Different lipid types affect the particle size and PDI of blank SLNs. When the same type and concentration of surfactant were employed, SA-SLNs had bigger particle size than PA-SLNs ($p<0.05$). The particle size and PDI of blank SLNs for both lipids using Tween® 80 were larger than those produced by PVA ($p<0.05$). The particle size and PDI of both lipids using PVA decreased by increasing surfactant concentration. On the other hand, an increase of particle size and PDI was obtained by increasing surfactant concentration from 1 to 2% using Tween® 80. The zeta potential value of blank SLNs for both lipids using Tween® 80 was lower ($p<0.05$) than those SLNs containing PVA.

The shorter hydrocarbon chain length of PA leads to smaller particle size in comparison with the longer hydrocarbon chain length of SA (Mohanty et al., 2015). In addition, the higher melting point of stearic acid (69.6^{o}C) compared to that of palmitic acid (62.9^{o}C) (Rowe et al., 2006), results in the higher viscosity of the dispersed phase and leads to larger particle size (Mohanty et al., 2015).

Surfactant plays an important role in emulsion formation. It helps to stabilize the system and control the particle size. High surfactant concentration decreases the surface tension of the lipid droplet, stabilizes the droplet surface during

homogenization, and results in smaller particle size and lower PDI (Weiss et al., 2008). Likewise, low surfactant concentration may be insufficient to stabilize the system and results in aggregation and larger droplet size (Weiss et al., 2008).

High surfactant concentration may give rise to bigger particle size. This phenomenon may be related to the depletion-flocculation mechanism of surfactant. It happens due to the formation of micelles at high concentration of surfactant in the continuous phase. The micelle increases the local osmotic pressure. The depletion of surfactant at droplet interphases leads to coalescence of oil droplets. Ultimately, the aggregation takes place and the particle size is increased (Wulff-Pérez et al., 2009). Another possibility is the long tail chain of Tween® 80 that forms the inter-particle bridge leading to gelatinization of Tween® 80 at the oil/water interface during nanoparticle formation process and increasing the particle size (Sharma et al., 2016).

Zeta potential indicates a repulsive force between nanoparticles to prevent the aggregation. All blank SLNs were found to be negatively charged due to fatty acid residues of PA and SA (Mohanty et al., 2015). Blank SLNs using Tween® 80 had lower zeta potential value than those SLNs using PVA due to the existence of oleic acid traces in Tween® 80 (Al-Qushawi et al., 2016).

The blank SLNs that had good physical stability were chosen to load MPE. The blank SLNs (F4-F6 and F10-F12) as shown in Table 14 with particle sizes in the range of 300-500 nm were selected to encapsulate the MPE in order to prevent the penetration of nanoparticles into the deeper layer of the skin. Based on the previous study, the particle size less than 300 nm are able to penetrate into the deeper layers of the skin and preferentially accumulate in hair follicles (Adib et al., 2016) .

Based on the preliminary study, the high concentration of PVA formed a thicker film when it was applied on the skin resulted in unpleasant feeling during application. Therefore, the blank SLNs with 1% PVA, the lowest concentration, were selected (F4 and F10).

4.4.2. Preparation and Characterization of MPE-SLNs

After incorporation of MPE, the physicochemical properties of solid lipid nanoparticles were reexamined including determination of entrapment efficiency percentage.

The physical appearances of MPE-SA-SLNs and MPE-PA-SLNs were yellow fluid dispersion as shown in Figure 30. The morphological features of PA-SLNs and SA-SLNs were investigated using scanning electron microscope (SEM) which were shown in Figure 31. The particle topography of both formulations showed regular, spherical and uniform nanospheres (PDI 0.4-0.6). The particle sizes measured by SEM were approximately around 440-550 nm. The SEM result supported the obtained result measured by PCS that particle sizes of the dispersion were about 440-550 nm (Table 15).

(a) (b)

Figure 30 Photographs of MPE-SLNs, (a) MPE-PA-SLNs, (b) MPE-SA-SLNs

(a) (b)

Figure 31 The SEM results of MPE-SLNs, (a) MPE-PA-SLNs, (b) MPE-SA-SLNs

MPE-SLNs had the larger particle size and higher PDI when compared with blank SLNs ($p < 0.05$). The particle sizes of all formulations were in the order of MPE-SA-SLNs > MPE-PA-SLNs > blank SA-SLNs > blank PA-SLNs ($p < 0.05$). The PDI values of all formulations were also in the same order ($p < 0.05$). Zeta potential and entrapment efficiency percentage between MPE-PA-SLNs and MPE-SA-SLNs were not significant differences ($p > 0.05$). Yield percentage of MPE-PA-SLNs and MPE-SA-SLNs obtained from this study were 98.05% and 98.24%. After centrifugation, the

particle size and PDI were larger when compared with that of before centrifugation ($p < 0.05$) but zeta potential did not change when compared with that of before centrifugation ($p > 0.05$).

Table 15 The physical properties of MPE-SLNs

Code	MPE	Before Centrifugation		After Centrifugation		Zeta potential[a]	EE %[a]
		Particle Size[a] (nm)	PDI [a]	Particle Size[a] (nm)	PDI[a]		
MPE-SA-SLNs	1.5 g	533.52±16.15	0.459±0.02	612.74±7.02	0.63±0.01	-18.9±0.50	83.24±1.11
MPE-PA-SLNs		443.51±6.50	0.35±0.01	568.15±6.68	0.44±0.03	-18.61±0.19	84.17±0.21

[a]mean ±SD, n=3

The previous finding reported the same result in which particle size and PDI are increased after extract encapsulation (Kim et al., 2017). The incorporation of MPE into molten lipids probably increased the viscosity and lipophilicity of the dispersed phase, led to less emulsification capability of the system and homogenization efficiency. Therefore, it resulted in larger particle size of MPE-SLNs. The particle size and PDI of MPE-SA-SLNs were larger than that of MPE-PA-SLNs because the hydrocarbon chain length of SA (C18) was longer than that of PA (C16) (Mohanty et al., 2015).

Centrifugation was evaluated in order to evaluate the alteration of the physical properties of MPE-SLNs prior to the addition of MPE-SLNs into cream. Centrifugation causes the collision of the particles under high velocity leading to particle agglomeration and larger particle size (Mohanty et al., 2015). The obtained physical characteristics and entrapment efficiencies of MPE-SA-SLNs and MPE-PA-SLNs indicated that these two formulations were suitable to be formulated into cream.

4.5. Preparation and Characterization of Cream

4.5.1. Preparation and Characterization Blank Cream

Vanishing cream (o/w emulsion) was formulated using 2 different formulations according to Young, 1972 (C1) and USP 31 (C2), respectively. Cream of the o/w type, most widely used for sunscreen is due to its ability to retain longer on the skin, its slower release rate compound when compared to gels, and its favorable sensory attributes compared to w/o formulations (Fahr, 2018; Hafeez & Kazmi, 2017; Maru et al., 2012).

According to formulation (Table 6), all formulations were prepared using a beaker method in which the oil phase and the water phase were heated prior to an

addition of oil phase to the water phase. These two formulations produced a semisolid white cream without observable separation. C1 was more creamy and softer than C2 as shown in Figure 32.

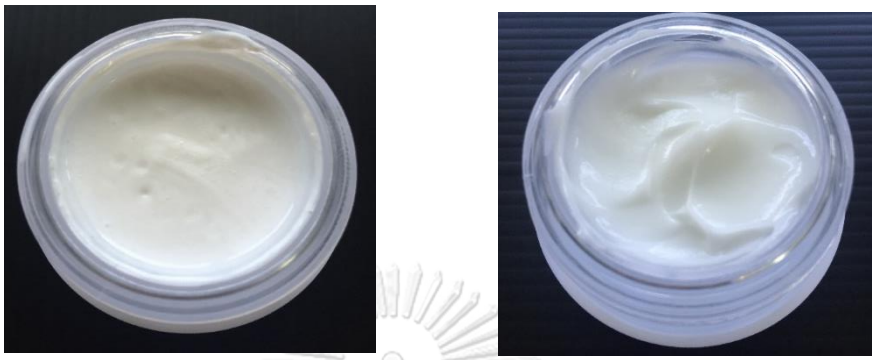

(a) (b)

Figure 32 Photographs of cream formulations, (a) C1, (b) C2

Physical stabilities of the prepared cream including color and phase separation after centrifugation test at 6,000 rpm for 30 minutes were recorded. There was no change in color and no observable phase separation of CI and C2 after centrifugation test at 6,000 rpm for 30 minutes as shown in Figure 33.

(a) (b) (c) (d)

Figure 33 Photographs of formulation after centrifugation test at 6,000 rpm, (a) C1 before centrifugation, (b) C1 after centrifugation, (c) C2 before centrifugation, (d) C2 after centrifugation

There was also no change in color and phase separation after 6 heating-cooling cycles for C1 and C2. The pH and viscosity data are shown in Figure 34 and Figure 35. The pH of both formulations met the recommended pH for skin in the range of 4-6.5 and was constant during heating-cooling cycles test (Chen et al., 2016; Kumar et al., 2011). The viscosity of C1 and C2 were stable during heating-cooling cycles. C1 had lower viscosity than C2 and did not meet the required cream viscosity. On the other hand, C2 viscosity met the required cream viscosity in the range of 20,000- 150,000 cps (Gupta et al., 2015; Lowe, 1996; A. Sharma & Prasar, 2013).

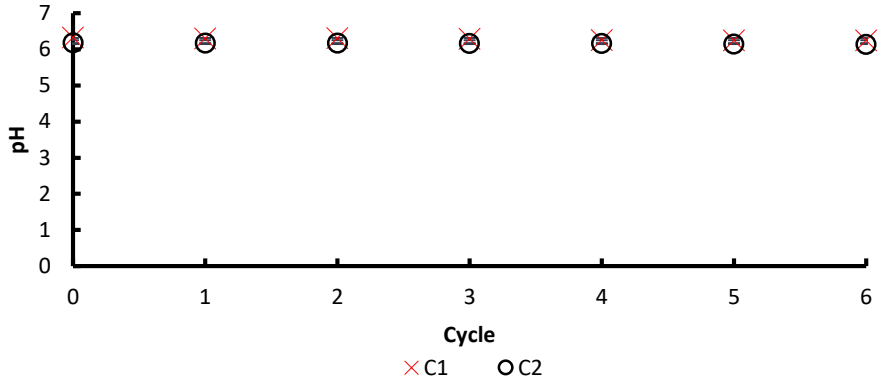

Figure 34 Data plots of blank cream between cycles and pH

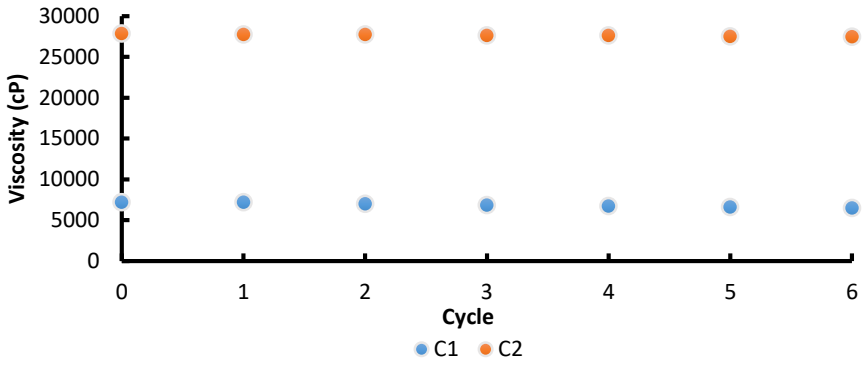

Figure 35 Data plots of blank cream between cycles and viscosity

Lower viscosity of C1 may be caused by the use of TEA as the base to produce soap tends to form a foamy cream resulting to lower viscosity. In addition, the employment of higher concentration of stiffening agents in C2 than C1 also led to higher viscosity (Baki & Alexander, 2015). Based on the obtained results of blank

cream evaluation, C2 showed better physical characteristics and was stable when compared with C1. Therefore, C2 was chosen for further studies.

4.5.2. Preparation and Characterization Cream Containing MPE-SLNs

Cream containing MPE-SLNs was prepared by an addition of MPE-SLNs into cream base (Modified from Waqas et al., 2010). The physical stabilities of cream containing MPE-SLNs such as color, phase separation, pH and viscosity were evaluated during storage at 4-8 ^{o}C for 3 months.

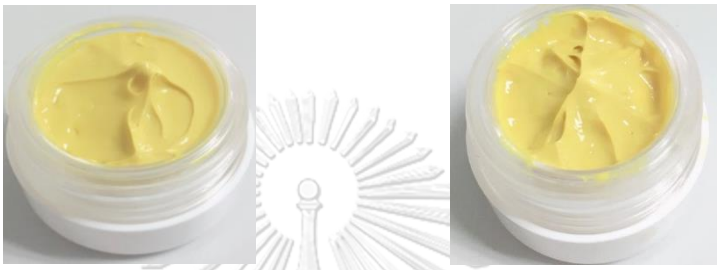

(a) (b)

Figure 36 Photographs of cream containing MPE-SLNs, (a) cream containing MPE-PA-SLNs, (b) cream containing MPE-SA-SLNs

The physical appearances of cream containing MPE-SA-SLNs and MPE-PA-SLNs were yellowish semisolid cream as shown in Figure 36. The SEM results of cream containing MPE-PA-SLNs and cream containing MPE-SA-SLNs confirmed the presence of SLNs in the cream base (Figure 37). In addition, the morphology of MPE-SLNs did not change after incorporation of MPE-SLNs into cream base.

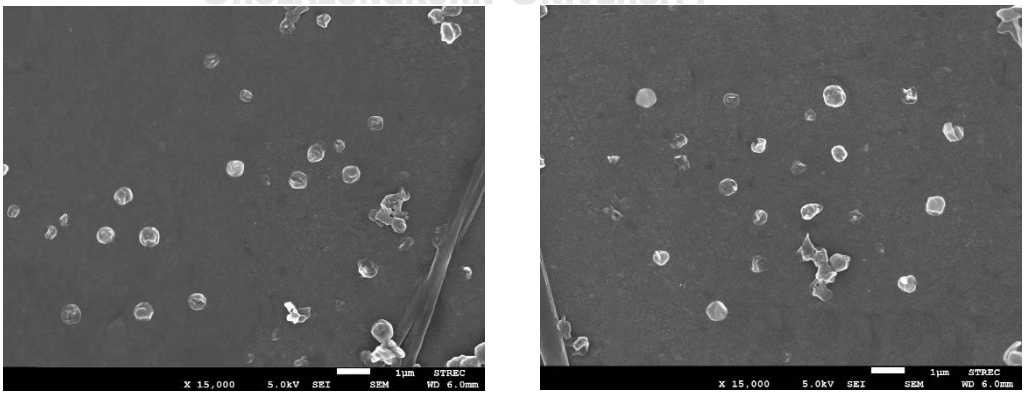

(a) (b)

Figure 37 SEM results of cream containing MPE-SLNs with magnification (15,000 X), (a) cream containing MPE-PA-SLNs, (b) cream containing MPE-SA-SLNs

Cream containing MPE-SA-SLNs or MPE-PA-SLNs, were more viscous than cream base due to the presence of the SLNs. There was no phase separation. Figure 38 shows cream containing MPE-PA-SLNs had a lower viscosity than the cream containing MPE-SA-SLNs (p<0.05). The pH of cream containing MPE-SA-SLNs and cream containing MPE-PA-SLNs decreased after the addition of MPE-SLNs into the bases from 6.18 to 5.9 (p<0.05). However, the viscosity of these two creams did not change over the period of 3 months. The pH between these two formulations were stable during stability test (p>0.05).

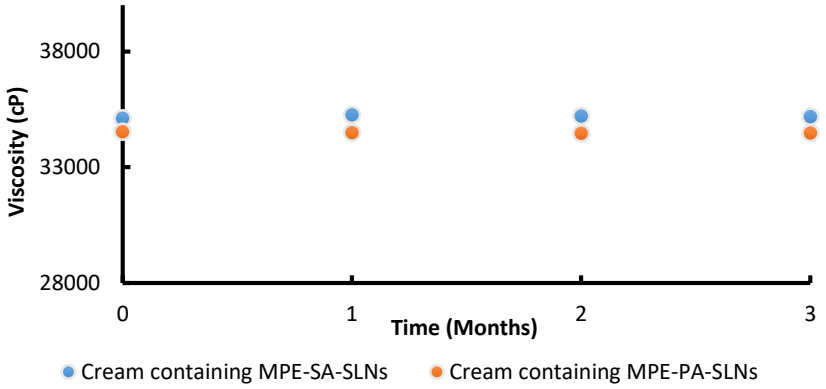

Figure 38 Viscosities of cream containing MPE-SLNs under storage

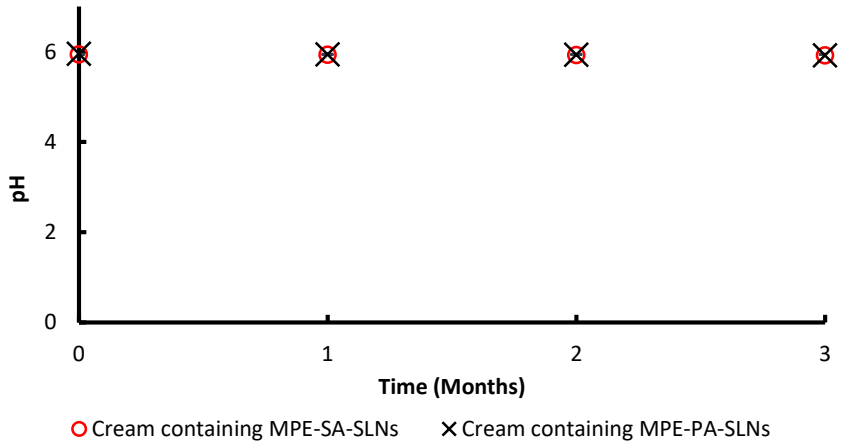

Figure 39 pH of cream containing MPE-SLNs under storage

The remaining α-mangostin percentage in cream containing MPE-SA-SLNs and that of containing MPE-PA-SLNs after 3 month storage were 98.69% and 98.89%, respectively. Both cream formulations had the estimated shelf-life about 8.5 months.

Shelf-life is estimated as the time corresponding to the intersection point of 95% confidence limit for the mean (blue line) and the proposed acceptance criterion or 95 (black line) as shown in Figure 41 and 42. SPF values of cream base, cream containing PA-SLNs, cream containing SA-SLNs about 1 and they were not significant differences from one another (p>0.05) (Table 16). 3% MPE cream had the SPF value around 4 which was not significantly different from 8% homosalate cream (p>0.05). Cream containing MPE-SA-SLNs and cream containing MPE-PA-SLNs had SPF values about 8-10. The SPF values of both creams were significantly higher than the SPF value of 3% MPE cream and 8% homosalate cream (p<0.05).

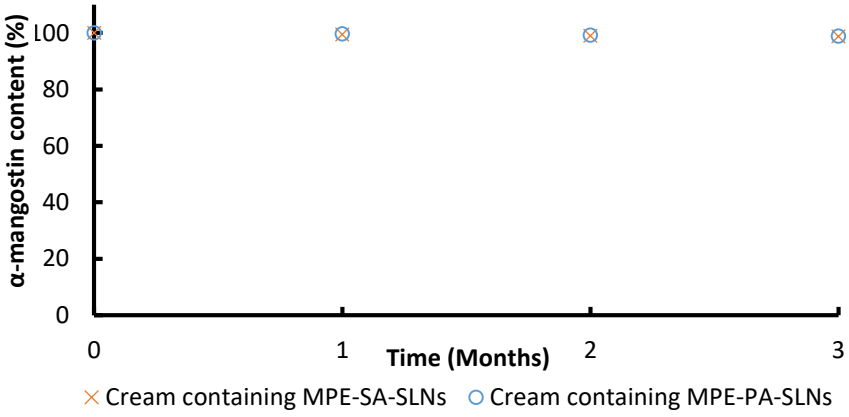

Figure 40 α-Mangostin content of cream containing MPE-SLNs under storage

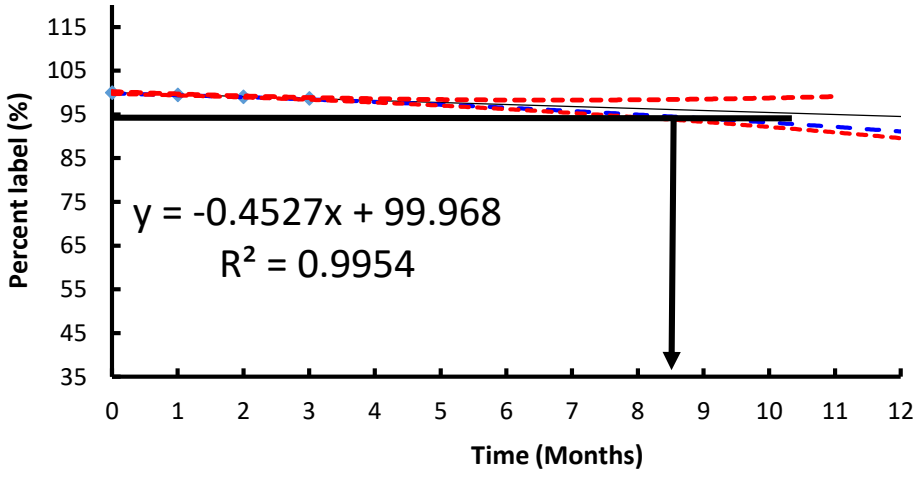

Figure 41 The estimated shelf-life of cream containing MPE-PA-SLNs

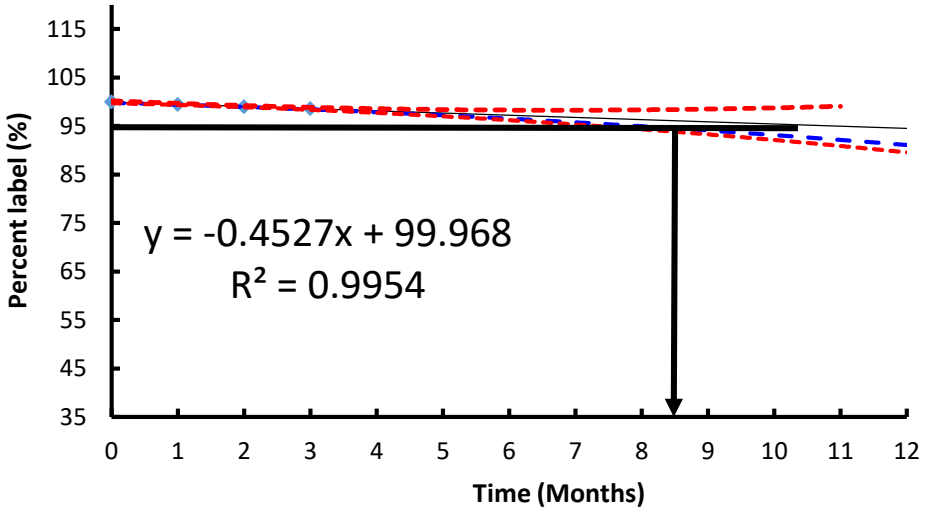

Figure 42 The estimated shelf-life of cream containing MPE-SA-SLNs

Table 16 The SPF value of cream formulations

Formulations	SPF value	
	0 month	3 months
Cream base	1.03±0.01	1.02±0.01
3% MPE cream	4.24±0.67	4.13±0.44
Cream-PA-SLNs	1.15±0.01	1.13±0.01
Cream-SA-SLNs	1.06±0.01	1.08±0.01
Cream-MPE-PA-SLNs (3%)	9.94±1.42	9.57±1.96
Cream-MPE-SA-SLNs (3%)	8.75±0.87	8.53±1.19
8% Homosalate Cream	4.47±1.28	

The products were designed to store at 4-8 ºC in order to prevent the melting of solid lipids. Therefore, the stability study was done at 4-8 ºC instead of at 40 ºC. Viscosity is an important attribute associated with physical characteristics and sensory effects. The previous findings suggested a correlation between physical characteristics assessment and individual consumer preference (Inoue et al., 2014). The cream containing MPE-SA-SLNs was more viscous than the cream containing MPE-PA-SLNs. It was possibly due to the fact that MPE-SA-SLNs had lower entrapment

efficiency percentage of α-mangostin. Therefore, in order to obtain the same MPE loading concentration in both creams, the amount of MPE-SA-SLNs loaded in the cream base were more than that of MPE-PA-SLNs.

pH is a key parameter related to its stability and efficacy. The normal range of skin pH is 4-6.5, therefore the creams intended to be applied on the skin should have pH closer to this range (Chen et al., 2016; Kumar et al., 2011). If the alkaline cream is applied on the skin, the stratum corneum will be disrupted leading to skin dryness or leading to bacterial infection. However, if the cream is acidic, it can cause skin irritation and sensitivity. Thus, pH is an important physical characteristic to be concerned (Tarun et al., 2014). The fact that cream containing MPE-SA-SLNs and cream containing MPE-PA-SLNs have lower pH values than the pH value of cream base is possibly due to non-esterified fatty acids (Damiyanti et al., 2014). These two creams had constant pH values over a 3-month storage and were in the range of 4.5-6. Therefore, they were acceptable to be used on the skin (Smaoui et al., 2017).

The percentage α-mangostin content should be between 95-105%. The α-mangostin content of cream containing MPE-SA-SLNs and MPE-PA-SLNs were stable during stability test indicates these two creams could maintain the efficacies of cream in terms of SPF value the cream for 3 months. The short estimated shelf-life about 8.5 month was likely due to the oxidation of hydroxyl groups of α-mangostin (Nishihama et al., 2006). This phenomenon could be prevented by the addition of lipid soluble antioxidant such as butylated hydroxytoluene (BHT) or tocopherols (Choe & Min, 2009).

The sun protection factor (SPF) indicates the efficacy of sunscreen product. The *in vitro* determination of SPF value was done using SPF analyzer due to the good correlation of SPF analyzer with that of *in vivo* efficacy test (Lin & Lin, 2011). The obtained SPF value of cream containing MPE-SLNs (0.06 mg MPE/2 mg cream) lower than the expected SPF value (SPF value=15). It was due to the standard protocol of SPF analyzer which only 1.3 mg/cm^2, about half of the application amount using by *in vivo* test (2 mg/cm), was applied on the PMMA sample holder. Therefore, the obtained SPF value was lower than the expected SPF value. The SPF value of 3% MPE cream was not different with 8% homosalate cream indicating the MPE have an ability to act as a UVB protector. The SPF values of cream containing MPE-SA-SLNs and cream

containing MPE-PA-SLNs were two times higher than 3% MPE cream and 8% homosalate cream. This suggests that the smaller particle size may contribute to an improved SPF value. It was likely due to better coverage and may be due to the beneficial effect of SLNs which also act as physical sunscreens (Wissing & Müller, 2002b). The SLNs can act as physical sunscreens on their own, from its particulate nature to scatter or reflect incident UV radiation (Gulbake et al., 2010).

Next study should perform the irritation test of cream containing MPE-SLNs in order to confirm the safety of these formulations. The SPF value of cream containing MPE-SLNs also could be increased by the combination with the other natural sunscreens.

CHAPTER V
CONCLUSION

This study was aimed to develop cream containing mangosteen pericarp extract encapsulated into solid lipid nanoparticles (SLNs). The investigation of sun protective ability of MPE and cream containing MPE encapsulated in SLNs were performed by spectrophotometer UV-Vis and SPF analyzer, respectively. Ultrasonication method was used in MPE-SLNs preparation. Creams containing MPE-SLNs were prepared by the addition of MPE-SLNs into o/w cream base. The physicochemical properties and stabilities of cream containing MPE-SLNs were investigated. The results of this study could be concluded as follows:

1. The dark brown powder of MPE was obtained after maceration and evaporation. The MPE showed an ability to absorbs UVB in the range of 290-320 nm at the concentration of 0.02 to 0.1 mg/ml with the SPF value in the range of 3.09 to 27.20.
2. The MPE-SLNs were successfully prepared using palmitic acid or stearic acid as solid lipid at a concentration of 3%, and PVA or Tween® 80 as the surfactant at the concentration in the range of 1-2%. The MPE-SLNs were spherical. The particle size ranged from 443.51 to 533.52 nm; PDI ranged from 0.35 to 0.459; and zeta potential value ranged from -18.61 to -18.9. The entrapment efficiencies of MPE-PA-SLNs and MPE-SA-SLNs were 83.23% and 84.17%, respectively.
3. MPE-SLNs were successfully loaded into cream at the MPE concentration of 3%. The SLNs enhanced the efficacy of UVB protection. SPF values of cream containing MPE-SA-SLNs and cream containing MPE-PA-SLNs which were two times higher (8.75 to 9.94) than that of 3% MPE cream (4.24).
4. Cream containing MPE-PA-SLNs and MPE-SA-SLNs displayed good physical stabilities, including appearances, pH, viscosities, and good chemical stabilities during a 3-month storage at 4-8 ^{o}C. The SPF values of cream containing MPE-

PA-SLNs and cream containing MPE-SA-SLNs did not significantly change during a 3-month storage as well.

REFERENCES

Abd-Elbary, A., Tadros, M., and Alaa-Eldin, A. 2013. Sucrose stearate-enriched lipid matrix tablets of etodolac: modulation of drug release, diffusional modeling and structure elucidation studies. *AAPS PharmSciTech* 14(2): 656-668.

Abiramasundari, A., Joshi, R., Jalani, H., Sharma, J., Pandya, D., Pandya, A., Sudarsanam, V., and Vasu, K. 2014. Stability-indicating assay method for determination of actarit, its process related impurities and degradation products: Insight into stability profile and degradation pathways. *Journal of Pharmaceutical Analysis* 4(6): 374-383.

Adib, Z., Ghanbarzadeh, S., Kouhsoltani, M., Khosroshahi, A., and Hamishehkar, H. 2016. The effect of particle size on the deposition of solid lipid nanoparticles in different skin layers: a histological study. *Advanced Pharmaceutical Bulletin* 6(1): 31-36.

Afaq, F., and Mukhtar, H. 2002. Photochemoprevention by botanical antioxidants. *Skin Pharmacology and Physiology* 15(5): 297-306.

Ahmad, M., Yamin, B., and Lazim, A. M. 2013. A Study on dispersion and characterisation of α-mangostin loaded pH sensitive microgel systems. *Chemistry Central Journal* 7(1): 1-6.

Aisha, A., Abu-Salah, K., Ismail, Z., and Majid, A. 2013. Determination of total xanthones in *Garcinia mangostana* fruit rind extracts by ultraviolet (UV) spectrophotometry. *Journal of Medicinal Plants Research* 7(1): 29-35.

Akao, Y., Nakagawa, Y., and Nozawa, Y. 2008. Anti-cancer effects of xanthones from pericarps of mangosteen. *International Journal of Molecular Sciences* 9(3): 355-370.

Al-Qushawi, A., Rassouli, A., Atyabi, F., Peighambari, S., Esfandyari-Manesh, M., Shams, G., and Yazdani, A. 2016. Preparation and characterization of three tilmicosin-loaded lipid nanoparticles: physicochemical properties and *in vitro* antibacterial activities. *Iranian Journal oF Pharmaceutical Research* 15(4): 663.

Alex, M., Chacko, AJ., Jose, S., and Souto, EB. 2011. Lopinavir loaded solid lipid nanoparticles (SLN) for intestinal lymphatic targeting. *European Journal of Pharmaceutical Sciences* 42(1-2): 11-18.

Ali, A., Taher, M., Helaluddin, A., and Mohamed, F. 2012. Development and validation of analytical method by RP-HPLC for quantification of alpha-mangostin encapsulated in PLGA microspheres. *Journal of Analitical Bioanalitical Techniques* 3(7): 1-5.

Anarjan, N., and Tan, C P. 2013. Effects of selected polysorbate and sucrose ester emulsifiers on the physicochemical properties of astaxanthin nanodispersions. *Molecules* 18(1): 768-777.

Anbu, S., Sahi, S., and Venkatachalam, P. 2016. Synthesis of bioactive chemicals cross-linked sodium tripolyphosphate (TPP) - chitosan nanoparticles for enhanced cytotoxic activity against human ovarian cancer cell Line (PA-1). *Journal of Nanomedicine and Nanotechnology* 7(418): 1-9.

Baek, J., Na, Young-Guk., and Cho, Cheong-Weon. 2018. Sustained cytotoxicity of wogonin on breast cancer cells by encapsulation in solid lipid nanoparticles. *Nanomaterials* 8(3): 159.

Baki, G., and Alexander, K. 2015. *Introduction to Cosmetic Formulation and Technology*. USA: John Wiley & Sons.

Balogh, T. S., Velasco, M. V., Pedriali, C. A., Kaneko, T., and Baby, A. R. 2011. Ultraviolet radiation protection: current available resources in photoprotection. *Anais Brasileiros De Dermatologia* 86(4): 732-742.

Bennet, D., Kang, S., Gang, J., and Kim, S. 2014. Photoprotective effects of apple peel nanoparticles. *International Journal of Nanomedicine* 9(2014): 93-108.

Bonifácio, B., Da Silva, P., Dos Santos Ramos, M., Negri, K., Bauab, T., and Chorilli, M. 2014. Nanotechnology-based drug delivery systems and herbal medicines: a review. *International Journal of Nanomedicine* 2014(9): 1-15.

Carter, M., and Shieh, J. 2015. *Guide to Research Techniques in Neuroscience*. Second edition. UK: Academic Press.

Chen, M., Alexander, KS., and Baki, G. 2016. Formulation and evaluation of antibacterial creams and gels containing metal ions for topical application. *Journal of Pharmaceutics* 2016(57): 1-10.

Chin, G., Todo, H., Kadhum, W., Hamid, M., and Sugibayashi, K. 2016. *In vitro* permeation and skin retention of α-Mangostin proniosome. *Chemical and Pharmaceutical Bulletin* 64(12): 1666-1673.

Choe, E., and Min, D. 2009. Mechanisms of antioxidants in the oxidation of foods. *Comprehensive Reviews in Food Science and Food Safety* 8(4): 345-358.

COLIPA. 2005. International sun protection factor (SPF) test method. https://www.perkinelmer.com/.../APP_011499_01_Sunscreen_Testing_ [Retrieved March 14, 2017]

Damiyanti, M., Soufyan, A., Kusuma, E ., and Ditta, SU. 2014. Effect of mangosteen (*Garcinia mangostana*) peel solution on human enamel surface color. *Journal of Medical Sciences* 14(6-8): 297.

Das, S., and Chaudhury, A. 2011. Recent advances in lipid nanoparticle formulations with solid matrix for oral drug delivery. *American Association of Phamrmaceutical Scientist* 12(1): 62-76.

Deshiikan, SR., and Papadopoulos, KD. 1998. Modified Booth equation for the calculation of zeta potential. *Colloid and Polymer Science* 276(2): 117-124.

Devi, D ., Sandhya, P., and Hari, B. 2013. Poloxamer: a novel functional molecule for drug delivery and gene therapy. *Journal of Pharmaceutical Sciences and Research* 5(8): 159-165.

Dromgoole, S., and Maibach, H. 1990. Sunscreening agent intolerance: contact and photocontact sensitization and contact urticaria. *Journal of the American Academy of Dermatology* 22(6): 1068-1078.

Dubes, A., Parrot-Lopez, H., Abdelwahed, W., Degobert, G., Fessi, H., Shahgaldian, P., and Coleman, A. 2003. Scanning electron microscopy and atomic force microscopy imaging of solid lipid nanoparticles derived from amphiphilic cyclodextrins. *European journal of Pharmaceutics and Biopharmaceutics* 55(3): 279-282.

Duthie, MS., Kimber, I., and Norval, M. 1999. The effects of ultraviolet radiation on the human immune system. *British Journal of Dermatology* 140(6): 995-1009.

Dutra, E., Oliveira, D., Kedor, E., and Santoro, M. 2004. Determination of sun protection factor (SPF) of sunscreens by ultraviolet spectrophotometry. *Revista Brasileira de Ciências Farmacêuticas* 40(3): 381-385.

Ebrahimi, H., Javadzadeh, Y., Hamidi, M., and Jalali, M. 2015. Repaglinide-loaded solid lipid nanoparticles: effect of using different surfactants/stabilizers on physicochemical properties of nanoparticles. *Journal of Pharmaceutical Sciences* 23(1): 46.

Einstein, A. 1956. On the theory of the brownian movement. *Koninklijke Nederlandse Akademie van Wetenschappen* 20(4): 1254-1271.

Ekambaram, P., Sathali, A ., and Priyanka, K. 2012. Solid lipid nanoparticles: a review. *Scientific Reviews and Chemical Communications* 2(1): 80-102.

Fahr, A. 2018. *Voigt's Pharmaceutical Technology*. USA: Wiley.

FDA. 2015. Sunburn protection factor (SPF). http://www.fda.gov/AboutFDA/CentersOffices/OfficeofMedicalProductsandTobacco/CDER/ucm106351.htm [Retrieved December 12, 2016]

Fernquest, J. (2012). Saving Thailand's wild medicinal plants. *Bangkok Post*. Retrieved from https://www.bangkokpost.com/learning/learning-news/292719/saving-thailand-wild-medicinal-plants [Retrieved December 24, 2016]

Fitzpatrick, T. 1988. The validity and practicality of sun-reactive skin types I through VI. *Archives of Dermatology* 124(6): 869-871.

Freitas, C., and Müller, R. 1998. Effect of light and temperature on zeta potential and physical stability in solid lipid nanoparticle (SLN™) dispersions. *International Journal of Pharmaceutics* 168(2): 221-229.

Gaikwad, M., and Kale, S. 2011. Formulation and *in vitro* evaluation for sun protection factor of *Moringa oleifera* Lam (family-moringaceae) oil sunscreen cream. *International Journal of Pharmacy and Pharmaceutical Sciences* 3(4): 371.

Gasparro, F., Mitchnick, M., and Nash, J. 1998. A review of sunscreen safety and efficacy. *Photochemistry and Photobiology* 68(3): 243-256.

Geetha, R., Roy, A., and Lakshmi, T. 2011. Evaluation of antibacterial activity of fruit rind extract of Garcinia mangostana Linn on enteric pathogens–an in vitro study. *Asian Journal of Pharmaceutical and Clinical Research* 2011(4): 115-118.

González, S., Fernández-Lorente, M., and Gilaberte-Calzada, Y. 2008. The latest on skin photoprotection. *Clinics in Dermatology* 26(6): 614-626.

Gulbake, A., Jain, A., Khare, P., and Jain, S. 2010. Solid lipid nanoparticles bearing oxybenzone: *in vitro* and *in vivo* evaluation. *Journal of Microencapsulation* 27(3): 226-233.

Gupta, N., Dubey, A., Prasad, P., and Roy, A. 2015. Formulation and evaluation of herbal fairness cream comprising hydroalcoholic extracts of *Pleurotus ostreatus*, *Glycyrrhiza glabra* and *Camellia sinensis*. *UK Journal of Pharmaceutical and Biosciences* 3(3): 40-45.

Hafeez, A., and Kazmi, I. 2017. Dacarbazine nanoparticle topical delivery system for the treatment of melanoma. *Scientific Reports* 7(1): 16517.

Hayakawa, I., Kanno, T., Yoshiyama, K., and Fujio, Y. 1994. Oscillatory compared with continuous high pressure sterilization on *Bacillus stearothermophilus* spores. *Journal of Food Science* 59(1): 164-167.

Hielscher, T. 2007. Ultrasonic production of nano-size dispersions and emulsions. https://arxiv.org/ftp/arxiv/papers/0708/0708.1831.pdf [Retrieved March 16, 2018]

Hiranras, P. 2001. *Formulation of Garcinia Mangostana Linn. Extract Buccal Muchoadhesive Film.* Master's Thesis. Pharmaceutics, Chulalongkorn University.

Hruza, L., and Pentland, A. 1993. Mechanisms of UV-induced inflammation. *Journal of Investigative Dermatology* 100(1): S35-S41.

ICH. (2005). *Validation of analytical procedures: text and methodology Q2 (R1).* Paper presented at the International Conference on Harmonization, Geneva, Switzerland, 11-12.

Inoue, Y., Suzuki, K., Maeda, R., Shimura, A., Murata, I., and Kanamoto, I. 2014. Evaluation of formulation properties and skin penetration in the same additive-containing formulation. *Results in Pharma Sciences* 4(2014): 42-49.

Iwo, M., Soemardji, A., and Hanafi, M. 2013. Sunscreen activity of α-mangostin from the pericarps of Garcinia mangostana. *Imperial Journal of Interdisciplinary Research* 3(1): 2225-2229.

Jindarat, S 2014. Xanthones from mangosteen (Garcinia mangostana): multi-targeting pharmacological properties. *Journal of Medical Association of Thailand* 97(2): 196-201.

Karlsson, I., Hillerström, L., Stenfeldt, A., Mårtensson, J., and Börje, A. 2009. Photodegradation of dibenzoylmethanes: potential cause of photocontact allergy to sunscreens. *Chemical Research in Toxicology* 22(11): 1881-1892.

Keck, CM., and Müller, RH. 2008. Size analysis of submicron particles by laser diffractometry—90% of the published measurements are false. *International Journal of Pharmaceutics* 355(1-2): 150-163.

Khalil, R., El-Bary, A., Kassem, M., Ghorab, M., and Ahmed, M. 2013. Solid lipid nanoparticles for topical delivery of meloxicam: development and in vitro characterization. *European Scientific Journal* 9(21): 779-798.

Khazaeli, P., and Mehrabani, M. 2010. Screening of sun protective activity of the ethyl acetate extracts of some medicinal plants. *Iranian Journal of Pharmaceutical Research* 7(1): 5-9.

Kim, JH., Baek, JS., Park, JK., Lee, BJ., Kim, MS., Hwang, SJ., Lee, JY., and Cho, CW. 2017. Development of *Houttuynia cordata* extract-loaded solid lipid nanoparticles for oral delivery: high drug loading efficiency and controlled release. *Molecules* 22(12): 2215-2226.

Kimura, K., and Katoh, T. 1995. Photoallergic contact dermatitis from the sunscreen ethylhexyl-p-methoxycinnamate (Parsol® MCX). *Contact Dermatitis* 32(5): 304-305.

Klammer, H., Schlecht, C., Wuttke, W., and Jarry, H. 2005. Multi-organic risk assessment of estrogenic properties of octyl-methoxycinnamate in vivo: A 5-day sub-acute pharmacodynamic study with ovariectomized rats. *Toxicology* 215(1): 90-96.

Kongkiatpaiboon, S., Vongsak, B., Machana, S., Weerakul, T., and Pattarapanich, C. 2016. Simultaneous HPLC quantitative analysis of mangostin derivatives in Tetragonula pagdeni propolis extracts. *Journal of King Saud University-Science* 28(2): 131-135.

Kopec, S., Irwin, R., DeBellis, R., Bohlke, M., and Maher, T. 2008. The effects of Tween-80 on the integrity of solutions of capsaicin: useful information for performing tussigenic challenges. *Cough* 4(1): 3.

Kosem, N., Ichikawa, K., Utsumi, H., and Moongkarndi, P. 2013. *In vivo* toxicity and antitumor activity of mangosteen extract. *Journal of Natural Medicines* 67(2): 255-263.

Kumar., Sasikanth, K., Sabareesh, M., and Dorababu, N. 2011. Formulation and evaluation of diacerein cream. *Asian Journal of Pharmeutical and Clinical Research* 4(2): 93-98.

Kumar., and Sinha, V. 2016. Solid lipid nanoparticle: an efficient carrier for improved ocular permeation of voriconazole. *Drug Development and Industrial Pharmacy* 42(12): 1956-1967.

Kumari, A., Kumar, V., and Yadav, SK. 2012. Nanotechnology: a tool to enhance therapeutic values of natural plant products. *Trends in Medical Research* 7(2): 34-42.

Lacatusu, L., Badea, N., Murariu, A., Bojin, D., and Meghea, A. 2010. Effect of UV sunscreens loaded in solid lipid nanoparticles: a combinated SPF assay and photostability. *Molecular Crystals and Liquid Crystals* 523(1): 247/[819]-259/[831].

Lason, E., and Ogonowski, J. 2011. Solid Lipid Nanoparticles–characteristics, application and obtaining. *Chemik* 65(10): 960-967.

Lavker, R. 1979. Structural alterations in exposed and unexposed aged skin. *Journal of Investigative Dermatology* 73(1): 59-66.

Lim, SJ., and Kim, CK. 2002. Formulation parameters determining the physicochemical characteristics of solid lipid nanoparticles loaded with all-trans retinoic acid. *International Journal of Pharmaceutics* 243(1-2): 135-146.

Lin, C., and Lin, W. 2011. Sun protection factor analysis of sunscreens containing titanium dioxide nanoparticles. *Journal of Food and Drug Analysis* 19(1): 1-8.

Lowe, NJ. 1996. *Sunscreens: Development: Evaluation, and Regulatory Aspects*. New York: CRC Press.

Madronich, S., McKenzie, R., Björn, Lars O., and Caldwell, M. 1998. Changes in biologically active ultraviolet radiation reaching the Earth's surface. *Journal of Photochemistry and Photobiology* 46(1): 5-19.

Mälkiä, A., Murtomäki, L., Urtti, A., and Kontturi, K. 2004. Drug permeation in biomembranes: in vitro and in silico prediction and influence of physicochemical properties. *European Journal of Pharmaceutical Sciences* 23(1): 13-47.

Mansur, J., Breder, M., Mansur, M., and Azulay, R. 1986. Determinação do fator de proteção solar por espectrofotometria. *Anais Brasileiros Dermatology* 61(1986): 121-124.

Martin, A., Swarbrick, J., and Cammarata, A. 1993. *Physical Pharmacy: Physical Chemical Principles in The Pharmaceutical Sciences*. Philadelpia: Lippincott Williams & Wilkins.

Maru, S., Gathu, L., Mathenge, A., Okaru, A., Kamau, F., and Chepkwony, H. 2012. *In vitro* drug release studies of metronidazole topical formulations through cellulose membrane. *East and Central African Journal of Pharmaceutical Sciences* 15(3): 57-62.

McClements, D., and Rao, J. 2011. Food-grade nanoemulsions: formulation, fabrication, properties, performance, biological fate, and potential toxicity. *Critical Reviews in Food Science and Nutrition* 51(4): 285-330.

McKinlay., and Diffey. 1987. Reference action spectrum for ultraviolet induced erythemal in human skin. *Computers and Industrial Engineering Journal* 6(1): 17-22.

McNeil, S. 2011. *Characterization of Nanoparticles Intended for Drug Delivery*. UK: Springer.

Medina-Holguín, A., Micheletto, S., Holguín, F., Rodriguez, J., O'Connell, M., and Martin, C. 2007. Environmental influences on essential oils in roots of *Anemopsis californica*. *HortScience* 42(7): 1578-1583.

Mohanty, B., Majumdar, D., Mishra, S., Panda, A., and Patnaik, S. 2015. Development and characterization of itraconazole-loaded solid lipid nanoparticles for ocular delivery. *Pharmaceutical Development and Technology* 20(4): 458-464.

Muchtaridi, M ., Suryani, D., Qosim, W., and Saptarini, N. 2016. Quantitative analysis of alpha mangostin in mangosteen (Garcinia mangostana L.) pericarp extract from four district of West Java by HPLC method *International Journal of Pharmacy and Pharmaceutical Sciences* 8(8): 232-236.

Mukherjee, S., Ray, S., and Thakur, R. 2009. Solid lipid nanoparticles: a modern formulation approach in drug delivery system. *Indian Journal of Pharmaceutical Sciences* 71(4): 349.

Müller, R., Benita, S., and Böhm, B. 1998. *Emulsions and Nanosuspensions for The Formulation of Poorly Soluble Drugs*. Germany: Medpharm Scientific Publisher.

Nair, B. 1998. Final report on the safety assessment of polyvinylpyrrolidone (PVP). *International Journal of Toxicology* 17(4): 95-130.

Narayanan, D., Saladi, R., and Fox, J. 2010. Review: Ultraviolet radiation and skin cancer. *International Journal of Dermatology* 49(9): 978-986.

Nishihama, Y., Amano, Y., Ogamino, T., and Nishiyama, S. 2006. Oxidation of mangostins, the naturally occurring xanthone derivatives carrying diverse biological activities. *Electrochemistry* 74(8): 609-611.

Nurhidayati, L., Sofiah, S., Sumarny, R., and Caesar, K. (2014). *HPLC method optimation of α-Mangostin assay in mangosteen (Garcinia mangostana L.) fruit rind extract formulated in oral solution.* Paper presented at the International Symposium on Medicinal Plant and Traditional Medicine, Indonesia.

Olbrich, C., and Müller, R. 1999. Enzymatic degradation of SLN—effect of surfactant and surfactant mixtures. *International Journal of Pharmaceutics* 180(1): 31-39.

Optometrics. 2009. SPF-290S Analyzer System. http://solarlight.com/spf-290as-spf-analyzer [Retrieved December 18, 2016]

Pandya., Ramesh, D ., Soniwala., and Chavda. 2013. Solid Lipid Nanoparticles: Overview on Excipients. *Asian Journal of Pharmaceutical Technology & Innovation* 1(3): 1-9.

Park, J., Takahata, Y., Kajiuchi, T., and Akehata, T. 1992. Effects of nonionic surfactant on enzymatic hydrolysis of used newspaper. *Biotechnology and Bioengineering* 39(1): 117-120.

Pathirana, R., Ratnasooriya, W., Gamage, R., Hasanthi, K., and Hettihewa, S. 2016. Sunscreen activity of pericarp of fruit of Sri Lankan *Garcinia mangostana* L.(Mangosteen) *in vitro*. *Imperial Journal of Interdisciplinary Research* 3(1): 2225-2229.

Pelizzo, M., Zattra, E., Nicolosi, P., Peserico, A., Garoli, D., and Alaibac, M. 2012. In vitro evaluation of sunscreens: an update for the clinicians. *International Scholarly Reserach Notices Dermatology* 2012(2012): 1-4.

Pothitirat, W., Chomnawang, M., Supabphol, R., and Gritsanapan, W. 2010. Free radical scavenging and anti-acne activities of mangosteen fruit rind extracts prepared by different extraction methods. *Pharmaceutical Biology* 48(2): 182-186.

Prabhakar, K., Afzal, S., Surender, G., and Kishan, V. 2013. Tween 80 containing lipid nanoemulsions for delivery of indinavir to brain. *Acta Pharmaceutica Sinica B* 3(5): 345-353.

Raghavendra, HL., Kumar, SV ., Kekuda, TR ., Ramalingappa., Ejeta, E., Mulatu, K., Khanum, F., and Anilakumar, KR. 2011. Extraction and evaluation of α-mangostin for its antioxidant and acetylcholinesterase inhibitory activity. *Journal of Biologically Active Products from Nature* 1(5-6): 314-324.

Rahmayanti, F., Suniarti, D., Mas' ud, Z., BACHTIAR, B., WIMARDHANI, Y., and SUBITA, G. 2016. Ethyl acetate fraction of *Garcinia mangostana*-Linn pericarp extract: Anti *Candida albicans* and epithelial cytotoxicity. *Asian Jounal of Pharmceutical and Clinical Research* 9(1): 335-338.

Rai, R., Shanmuga, S., and Srinivas, C. 2012. Update on photoprotection. *Indian Journal of Dermatology* 57(5): 335.

Rasheed, A., Shama, S., Mohanalakshmi, S., and Ravichandran, V. 2012. Formulation, characterization and in vitro evaluation of herbal sunscreen lotion. *Oriental Pharmacy and Experimental Medicine* 12(4): 241-246.

Rasyid, R., Meri, S., and Indah, G. 2016. Development of analytical method of α-mangostin in dichloromethane extract of green fruit latex *Garcinia mangostana* L. using high performance liquid chromatography. *De Pharma Chemics* 8(16): 52-57.

Rawat, MK., Jain, A., Mishra, A., Muthu, MS., and Singh, S. 2010. Development of repaglinide loaded solid lipid nanocarrier: selection of fabrication method. *Current Drug Delivery* 7(1): 44-50.

Rowe, R., Sheskey, P., and Weller, P. 2006. *Handbook of Pharmaceutical Excipients*. Sixth Edition. London: Pharmaceutical Press London.

Ruamkittham, N. 2005. *Formulation of fast dissolving oral strips containing Garcinia mangostana extract.* Master's Thesis. Pharmaceutics, Chulalongkorn University.

Saewan, N., and Jimtaisong, A. 2013. Photoprotection of natural flavonoids. *Journal of Applied Pharmaceutical Science* 3(9): 129-141.

Sanad, R., Abdel Malak, N., El-Bayoomy, T., and Badawi, A. 2010. Preparation and characterization of oxybenzone-loaded solid lipid nanoparticles (SLNs) with enhanced safety and sunscreening efficacy: SPF and UVA-PF. *Drug Discoveries and Therapeutics* 4(6): 472-483.

Santos, E., Freitas, Z., Souza, K., Garcia, S., and Vergnanini, A. 1999. In vitro and in vivo determinations of sun protection factors of sunscreen lotions with octylmethoxycinnamate. *International Journal of Cosmetic Science* 21(1): 1-5.

Sayre, R., Agin, P., LeVee, G., and Marlowe, E. 1979. A comparison of in vivo and in vitro testing of sunscreening formulas. *Photochemistry and Photobiology* 29(3): 559-566.

Schmidt, T., Ring, J., and Abeck, D. 1998. Photoallergic contact dermatitis due to combined UVB (4-methylbenzylidene camphor/octyl methoxycinnamate) and UVA (benzophenone-3/butyl methoxydibenzoylmethane) absorber sensitization. *Dermatology* 196(3): 354-357.

Sciences. 2009. Emulsion and emulsification. http://www.particlesciences.com/news/technical-briefs/2009/emulsions-and-emulsification.html [Retrieved March 3, 2018]

Severino, P., Moraes, L., Zanchetta, B., Souto, E., and Santana, M. 2012. Elastic liposomes containing benzophenone-3 for sun protection factor enhancement. *Pharmaceutical Development and Technology* 17(6): 661-665.

Shah, R., Eldridge, D., Palombo, E., and Harding, I. 2015. *Lipid Nanoparticles: Production, Characterization and Stability*. UK: Springer.

Shahgaldian, P., Quattrocchi, L., Gualbert, J., Coleman, A., and Goreloff, P. 2003. AFM imaging of calixarene based solid lipid nanoparticles in gel matrices. *European Journal of Pharmaceutics and Biopharmaceutics* 55(1): 107-113.

Shannon, M., Bohn, P., Elimelech, M., Georgiadis, J., Marinas, B., and Mayes, A. 2008. Science and technology for water purification in the coming decades. *Nature* 452(7185): 301-310.

Sharma., Madan, P., and Lin, S. 2016. Effect of process and formulation variables on the preparation of parenteral paclitaxel-loaded biodegradable polymeric nanoparticles: A co-surfactant study. *Asian Journal of Pharmaceutical Sciences* 11(3): 404-416.

Sharma, A., and Prasar, B. 2013. Formulation and Evaluation of herbal cosmetic cream to produce multipurpose effect on skin. *Research Journal of Topical and Cosmetic Sciences* 4(1): 1-4.

Siriphan, P. 2008. *Antioxidant evaluation and formulation development of Zingiber officinale extract loaded in solid lipid nanoparticles for skin delivery.* Master's Thesis. Pharmaceutics, Chulalongkorn University.

Sitterberg, J., Özcetin, A., Ehrhardt, C., and Bakowsky, U. 2010. Utilising atomic force microscopy for the characterisation of nanoscale drug delivery systems. *European Journal of Pharmaceutics and Biopharmaceutics* 74(1): 2-13.

Smaoui, S., Hlima, H., Chobba, I., and Kadri, A. 2017. Development and stability studies of sunscreen cream formulations containing three photo-protective filters. *Arabian Journal of Chemistry* 10(2017): S1216-S1222.

Stefanaki, E., and Voutou, B. 2008. Electron microscopy: the basics. *Physics of Advanced Materials* 8(2008): 1-11.

Suzuki, T., Kitamura, S., Khota, R., Sugihara, K., Fujimoto, N., and Ohta, S. 2005. Estrogenic and antiandrogenic activities of 17 benzophenone derivatives used as UV stabilizers and sunscreens. *Toxicology and Applied Pharmacology* 203(1): 9-17.

Svobodova, A., Walterova, D., and Vostalova, J. 2006. Ultraviolet light induced alteration to the skin. *Biomedical Papers* 150(1): 25.

Tan, Voratai. 2004. *Formulation of monoglyceride-base drug delivery system containing Garcinia mangostana extract.* Master's Thesis. Pharmaceutics, Chulalongkorn University.

Tarun, J., Susan, J., Jacob-Suria, V., and Criton, S. 2014. Evaluation of pH of bathing soaps and shampoos for skin and hair care. *Indian Journal of Dermatology* 59(5): 442.

Tatiya, N., Chatuphonprasert, W., and Jarukamjorn, K. 2016. In vivo antibacterial activity of *Garcinia mangostana* pericarp extract against methicillin-resistant

Staphylococcus aureus in a mouse superficial skin infection model. *Pharmaceutical Biology* 54(11): 2606-2615.

Verma, S., and Singh, S. 2008. Current and future status of herbal medicines. *Veterinary World* 1(11): 347-350.

Wang, S., and Lim, H. (2016). Principles and Practice of Photoprotection. UK: Springer

Waqas, M., Akhtar, N., Ahmad, M., Murtaza, G., Khan, H., Iqbal, M., Rasul, A., and Bhatti, N. 2010. Formulation and characterization of a cream containing extract of fenugreek seeds. *Acta Poloniae Pharmaceutica* 67(2): 173-178.

Weiss, J., Decker, EA., McClements, DJ., Kristbergsson, K., Helgason, T., and Awad, T. 2008. Solid lipid nanoparticles as delivery systems for bioactive food components. *Food Biophysics* 3(2): 146-154.

Widowati, W., Darsono, L., Suherman, J., Yelliantty, Y., and Maesaroh, M. 2014. High performance liquid chromatography (HPLC) analysis, antioxidant, antiaggregation of mangosteen peel extract (Garcinia mangostana L.). *International Journal of Bioscience, Biochemistry and Bioinformatics* 4(6): 458-466.

Wissing, S., and Müller, R. 2002a. The influence of the crystallinity of lipid nanoparticles on their occlusive properties. *International Journal of Pharmaceutics* 242(1-2): 377-379.

Wissing, S., and Müller, R. 2002b. Solid lipid nanoparticles as carrier for sunscreens: *in vitro* release and *in vivo* skin penetration. *Journal of Controlled Release* 81(3): 225-233.

Wulff-Pérez, M., Torcello-Gómez, A., Gálvez-Ruíz, MJ., and Martín-Rodríguez, A. 2009. Stability of emulsions for parenteral feeding: preparation and characterization of o/w nanoemulsions with natural oils and Pluronic f68 as surfactant. *Food Hydrocolloids* 23(4): 1096-1102.

Xie, S., Zhu, L., Dong, Z., Wang, X., Wang, Y., Li, X., and Zhou, W. 2011. Preparation, characterization and pharmacokinetics of enrofloxacin-loaded solid lipid nanoparticles: influences of fatty acids. *Colloids and Surfaces B: Biointerfaces* 83(2): 382-387.

Xu, R. 2008. Progress in nanoparticles characterization: sizing and zeta potential measurement. *Particuology* 6(2): 112-115.

Yamaguchi, Y., Brenner, M., and Hearing, V. 2007. The regulation of skin pigmentation. *Journal of Biological Chemistry* 282(38): 27557-27561.

Yasurin, P. 2015. The Bioavailability Activity of Centella asiatica. *International Journal of Applied Science and Technology* 9(1): 1-9.

Yodhnu, S., Sirikatitham, A., and Wattanapiromsakul, C. 2009. Validation of LC for the determination of α-mangostin in mangosteen peel extract: a tool for quality assessment of *Garcinia mangostana* L. *Journal of Chromatographic Science* 47(3): 185-189.

Young, A. 1972. *Practical Cosmetic Sciences*. London: Mills & Boon Limited.

Zhang, Q., Bailey, B., Plante, M., and Acworth, I. 2014. Fast analysis of selected xanthones in mangosteen pericarp using accelerated solvent extraction and ultra high performance liquid chromatography. http://208.89.142.230/content/dam/tfs/ATG/CMD/cmd-documents/sci-res/-Xanthones-in-Mangosteen-Pericarp [Retrieved February 8, 2018]

APPENDICES

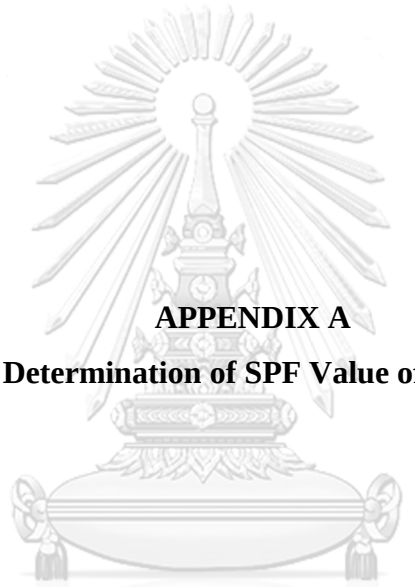

APPENDIX A
Determination of SPF Value of MPE

Table 17 Determination of SPF value of MPE solution in ethanol at a concentration of 0.02 mg/ml

Wavelength (nm)	EEXI	CF	Absorbance		
			n=1	n=2	n=3
290	0.0150	9.375	0.175	0.176	0.174
295	0.0817		0.211	0.211	0.210
300	0.2874		0.267	0.268	0.267
305	0.3278		0.338	0.338	0.337
310	0.1864		0.399	0.400	0.399
315	0.0839		0.464	0.464	0.463
320	0.0180		0.488	0.490	0.488
SPF value			3.09	3.09	3.08
Average SPF value			3.09 ±0.01		

Table 18 Determination of SPF value of MPE solution in ethanol at a concentration of 0.04 mg/ml

Wavelength (nm)	EEXI	CF	Absorbance		
			n=1	n=2	n=3
290	0.0150	9.375	0.636	0.636	0.636
295	0.0817		0.726	0.727	0.726
300	0.2874		0.854	0.852	0.852
305	0.3278		1.006	1.005	1.003
310	0.1864		1.141	1.145	1.141
315	0.0839		1.254	1.251	1.252
320	0.0180		1.262	1.258	1.260
SPF value			9.23	9.22	9.21
Average SPF value			9.22±0.01		

Table 19 Determination of SPF value of MPE solution in ethanol at a concentration of 0.05 mg/ml

Wavelength (nm)	EEXI	CF	Absorbance		
			n=1	n=2	n=3
290	0.0150	9.375	0.853	0.856	0.851
295	0.0817		0.969	0.972	0.969
300	0.2874		1.132	1.132	1.131
305	0.3278		1.321	1.326	1.322
310	0.1864		1.500	1.503	1.498
315	0.0839		1.635	1.640	1.634
320	0.0180		1.640	1.643	1.639
SPF value			12.16	12.18	12.15
Average SPF value			12.16±0.01		

Table 20 Determination of SPF value of MPE solution in ethanol at a concentration of 0.06 mg/ml

Wavelength (nm)	EEXI	CF	Absorbance		
			n=1	n=2	n=3
290	0.0150	9.375	1.050	1.052	1.050
295	0.0817		1.193	1.193	1.192
300	0.2874		1.384	1.385	1.383
305	0.3278		1.617	1.617	1.619
310	0.1864		1.834	1.830	1.828
315	0.0839		1.982	1.995	1.986
320	0.0180		1.992	1.988	1.987
SPF value			14.86	14.87	14.85
Average SPF value			14.86±0.01		

Table 21 Determination of SPF value of MPE solution in ethanol at a concentration of 0.08 mg/ml

Wavelength (nm)	EEXI	CF	Absorbance		
			n=1	n=2	n=3
290	0.0150	9.375	1.511	1.507	1.512
295	0.0817		1.706	1.706	1.710
300	0.2874		1.968	1.969	1.972
305	0.3278		2.288	2.286	2.283
310	0.1864		2.580	2.568	2.569
315	0.0839		2.742	2.772	2.784
320	0.0180		2.755	2.758	2.771
SPF value			20.98	20.98	21.00
Average SPF value			20.99±0.01		

Table 22 Determination of SPF value of MPE solution in ethanol at a concentration of 0.1 mg/ml

Wavelength (nm)	EEXI	CF	Absorbance		
			n=1	n=2	n=3
290	0.0150	9.375	1.966	1.966	1.968
295	0.0817		2.220	2.211	2.218
300	0.2874		2.557	2.559	2.547
305	0.3278		2.965	2.950	2.966
310	0.1864		3.309	3.342	3.346
315	0.0839		3.578	3.552	3.620
320	0.0180		3.545	3.547	3.633
SPF value			27.17	27.16	27.26
Average SPF value			27.20±0.05		

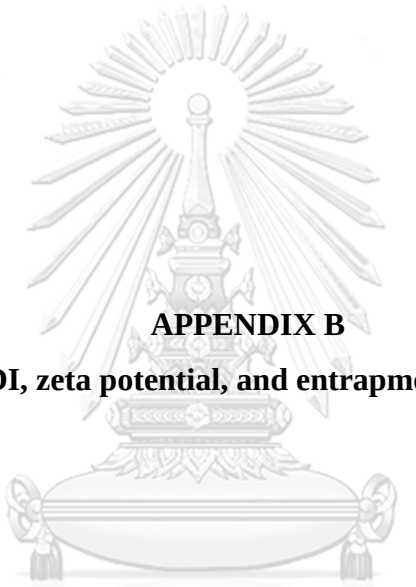

APPENDIX B

Particle size, PDI, zeta potential, and entrapment efficiency analysis

Table 23 The raw data of particle size, polydispersity index and zeta potential of F1

No	Particle Size (nm)	PDI	Zeta Potential
1	571.9	0.56	-29.1
2	579.2	0.53	-27.2
3	577.6	0.50	-27.5
4	585.3	0.55	-29.9
5	594.2	0.51	-29.2
6	598.5	0.51	-28.5
7	587.2	0.56	-28.6
8	579.1	0.53	-30.2
9	586.0	0.53	-26.8
Mean	584.3	0.53	-28.5
STD	8.39	0.02	1.18

Table 24 The raw data of particle size, polydispersity index and zeta potential of F2

No	Particle Size (nm)	PDI	Zeta Potential
1	815.8	0.77	-27.9
2	825.8	0.68	-27.7
3	818.9	0.76	-28.0
4	805.0	0.68	-27.8
5	814.1	0.62	-28.3
6	824.8	0.68	-29.0
7	815.8	0.68	-27.5
8	825.8	0.70	-27.7
9	824.8	0.66	-27.4
Mean	818.9	0.69	-27.9
STD	0.04	0.04	0.48

Table 25 The raw data of particle size, polydispersity index and zeta potential of F3

No	Particle Size (nm)	PDI	Zeta Potential
1	1085.0	1.00	-27.5
2	2351.0	0.99	-27.7
3	2611.0	0.98	-27.4
4	1139.0	0.93	-28.8
5	1014.0	0.93	-27.4
6	1189.0	1.00	-28.6
7	1108.0	1.00	-30.2
8	1025.0	1.00	-27.6
9	1054.0	1.00	-26.7
Mean	1397.3	0.98	-27.9
STD	620.2	0.02	1.04

Table 26 The raw data of particle size, polydispersity index and zeta potential of F4

No	Particle Size (nm)	PDI	Zeta Potential
1	375.8	0.15	-17.4
2	376.1	0.17	-16.2
3	375.6	0.14	-15.8
4	381.8	0.15	-16.3
5	388.8	0.16	-15.3
6	386.1	0.12	-15.6
7	381.5	0.14	-15.2
8	389.9	0.15	-15.1
9	387.9	0.15	-14.9
Mean	382.6	0.15	-15.7
STD	5.82	0.01	0.79

Table 27 The raw data of particle size, polydispersity index and zeta potential of F5

No	Particle Size (nm)	PDI	Zeta Potential
1	341.7	0.07	-16.2
2	338.0	0.08	-16.8
3	340.5	0.07	-16.7
4	339.4	0.07	-16.5
5	348.7	0.06	-16.3
6	344.5	0.07	-16.7
7	337.7	0.08	-16.5
8	342.9	0.07	-16.8
9	340.4	0.08	-16.5
Mean	341.5	0.07	-16.5
STD	3.46	0.01	0.21

Table 28 The raw data of particle size, polydispersity index and zeta potential of F6

No	Particle Size (nm)	PDI	Zeta Potential
1	333.9	0.06	-16.9
2	335.4	0.06	-16.7
3	335.1	0.05	-16.6
4	333.4	0.04	-16.8
5	338.3	0.06	-16.7
6	335.6	0.04	-16.8
7	338.9	0.04	-17.0
8	336.3	0.04	-17.1
9	338.0	0.05	-15.3
Mean	336.1	0.05	-16.6
STD	1.94	0.01	0.53

Table 29 The raw data of particle size, polydispersity index and zeta potential of F7

No	Particle Size (nm)	PDI	Zeta Potential
1	546.2	0.49	-29.3
2	543.4	0.46	-29.0
3	546.2	0.50	-32.4
4	543.4	0.49	-32.6
5	551.5	0.46	-32.4
6	552.8	0.49	-29.2
7	562.1	0.49	-29.3
8	565.2	0.48	-27.6
9	570.3	0.49	-29.9
Mean	553.4	0.48	-30.1
STD	10.05	0.01	1.81

Table 30 The raw data of particle size, polydispersity index and zeta potential of F8

No	Particle Size (nm)	PDI	Zeta Potential
1	795.0	0.62	-29.2
2	770.8	0.55	-29.3
3	789.9	0.60	-29.0
4	764.6	0.61	-32.3
5	783.8	0.60	-31.4
6	759.1	0.57	-31.0
7	712.0	0.55	-31.8
8	726.4	0.59	-32.3
9	786.3	0.61	-32.8
Mean	765.3	0.59	-31.0
STD	0.02	0.02	1.48

Table 31 The raw data of particle size, polydispersity index and zeta potential of F9

No	Particle Size (nm)	PDI	Zeta Potential
1	994.6	0.84	-28.9
2	971.8	0.81	-29.2
3	976.2	0.90	-27.9
4	963.1	0.90	-27.5
5	994.0	0.72	-32.3
6	990.2	0.73	-28.6
7	1001.0	0.86	-33.3
8	1008.0	0.95	-28.7
9	972.5	0.94	-27.6
Mean	985.7	0.85	-29.3
STD	15.28	0.08	2.06

Table 32 The raw data of particle size, polydispersity index and zeta potential of F10

No	Particle Size (nm)	PDI	Zeta Potential
1	306.4	0.09	-15.9
2	306.7	0.08	-15.6
3	304.3	0.10	-15.4
4	307.7	0.11	-15.4
5	305.4	0.08	-15.6
6	308.4	0.09	-15.5
7	306.5	0.10	-16.5
8	306.4	0.08	-16.2
9	306.7	0.07	-15.7
Mean	306.5	0.09	-15.7
STD	0.01	0.01	0.37

Table 33 The raw data of particle size, polydispersity index and zeta potential of F11

No	Particle Size (nm)	PDI	Zeta Potential
1	305.4	0.06	-15.1
2	304.3	0.07	-14.8
3	305.6	0.06	-16.1
4	301.3	0.06	-14.8
5	305.0	0.06	-14.3
6	305.0	0.06	-15.1
7	306.5	0.06	-14.8
8	304.3	0.05	-14.7
9	306.4	0.06	-14.6
Mean	304.8	0.06	-14.9
STD	1.55	0.01	0.50

Table 34 The raw data of particle size, polydispersity index and zeta potential of F12

No	Particle Size (nm)	PDI	Zeta Potential
1	299.4	0.04	-15.3
2	303.6	0.04	-15.2
3	302.1	0.05	-15.6
4	303.9	0.04	-15.2
5	301.0	0.04	-15.1
6	299.4	0.04	-14.9
7	300.1	0.04	-15.2
8	301.0	0.04	-15.1
9	304.7	0.05	-15.3
Mean	301.6	0.04	-15.2
STD	1.99	0.01	0.19

Table 35 The raw data of particle size, polydispersity index and zeta potential of MPE-SA-SLNs before centrifugation

No	Particle Size (nm)	PDI	Zeta Potential
1	536.9	0.44	-19.1
2	541.3	0.40	-19.5
3	540.6	0.45	-19.7
4	532.7	0.43	-18.6
5	547.4	0.48	-18.9
6	511.8	0.48	-19.1
7	553.8	0.48	-18.7
8	503.7	0.48	-18.3
9	533.5	0.45	-18.2
Mean	533.5	0.45	-18.9
STD	16.15	0.02	0.50

Table 36 The raw data of particle size, polydispersity index and zeta potential of MPE-PA-SLNs before centrifugation

No	Particle size (nm)	PDI	Zeta potential
1	439.6	0.35	-18.8
2	452.1	0.35	-18.5
3	445.0	0.33	-18.8
4	447.3	0.35	-18.4
5	446.9	0.35	-18.3
6	451.3	0.35	-18.5
7	434.0	0.34	-18.8
8	438.9	0.34	-18.6
9	436.5	0.36	-18.8
Mean	443.5	0.35	-18.6
STD	6.50	0.01	0.19

Table 37 The raw data of particle size and polydispersity index of MPE-SA-SLNs after centrifugation at 18,000 rpm for 15 minutes

No	Particle size (nm)	PDI	Zeta Potential
1	604.2	0.64	-18.6
2	608.3	0.63	-18.9
3	615.4	0.60	-19.1
4	611.7	0.63	-19.1
5	625.7	0.63	-19.5
6	606.5	0.64	-19.7
7	611.7	0.62	-18.7
8	621.5	0.64	-18.3
9	609.7	0.64	-18.2
Mean	612.7	0.63	-18.9
STD	7.02	0.01	0.50

Table 38 The raw data of particle size and polydispersity index of MPE-PA-SLNs after centrifugation at 18,000 rpm for 15 minutes

No	Particle size (nm)	PDI	Zeta potential
1	579.4	0.49	-18.8
2	575.9	0.44	-18.6
3	567.6	0.48	-18.8
4	570.1	0.45	-18.4
5	560.5	0.45	-18.3
6	561.1	0.42	-18.5
7	570.5	0.40	-18.8
8	560.9	0.42	-18.5
9	567.4	0.47	-18.8
Mean	568.1	0.44	-18.6
STD	6.68	0.03	0.19

Table 39 Raw data of entrapment efficiency of MPE-SLNs

Formulation	% α-mangostin in SLNs		% α-mangostin in supernatant	
	Batch	Mean±SD	Batch	Mean±SD
MPE-PA-SLNs	83.96	84.17±0.21	13.53	13.87±0.30
	84.39		14.11	
	84.17		13.99	
MPE-SA-SLNs	84.35	83.23±1.11	14.55	15.01±0.90
	82.12		15.79	
	83.21		14.69	

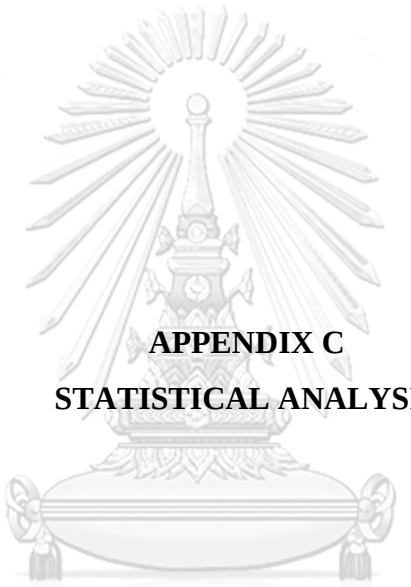

APPENDIX C
STATISTICAL ANALYSIS

Table 40 Analysis of variance result of particle size of blank SLNs

ANOVA					
ParticleSize					
	Sum of Squares	df	Mean Square	F	Sig.
Between Groups	1.176E7	11	1069293.183	33.241	.000
Within Groups	3088120.042	96	32167.917		
Total	1.485E7	107			

ParticleSize

Tukey HSD[a]

		Subset for alpha = 0.05			
Formulations	N	1	2	3	4
F12	9	301.6889			
F11	9	304.8741			
F10	9	306.5000			
F6	9	336.1000			
F5	9	341.5333			
F4	9	382.6111			
F7	9	553.4556	553.4556		
F1	9	584.3333	584.3333		
F8	9		765.3222	765.3222	
F2	9		818.9778	818.9778	
F9	9			985.7111	
F3	9				1397.3333
Sig.		.051	.088	.291	1.000

Means for groups in homogeneous subsets are displayed.

a. Uses Harmonic Mean Sample Size = 9.000.

Table 41 Analysis of variance result of polydispersity index of blank SLNs

ANOVA					
PDI					
	Sum of Squares	df	Mean Square	F	Sig.
Between Groups	11.846	11	1.077	1.091E3	.000
Within Groups	.095	96	.001		
Total	11.941	107			

PDI

Tukey HSD[a]

		Subset for alpha = 0.05							
Formulations	N	1	2	3	4	5	6	7	8
F12	9	.047296							
F6	9	.054296							
F11	9	.062444							
F5	9	.076444							
F10	9	.091185							
F4	9		.152778						
F7	9			.487556					
F1	9				.537444				
F8	9					.594667			
F2	9						.697556		
F9	9							.855000	
F3	9								.982556
Sig.		.136	1.000	1.000	1.000	1.000	1.000	1.000	1.000

Means for groups in homogeneous subsets are displayed.

a. Uses Harmonic Mean Sample Size = 9.000.

Table 42 Analysis of variance result of zeta potential of blank SLNs

ANOVA

Zeta					
	Sum of Squares	df	Mean Square	F	Sig.
Between Groups	4908.544	11	446.231	385.775	.000
Within Groups	111.044	96	1.157		
Total	5019.588	107			

Zeta

Tukey HSD[a]

		Subset for alpha = 0.05				
Formulations	N	1	2	3	4	5
F8	9	-31.011111				
F7	9	-30.188889	-30.188889			
F9	9	-29.333333	-29.333333	-29.333333		
F1	9		-28.555556	-28.555556		
F3	9			-27.988889		
F2	9			-27.922222		
F6	9				-16.655556	
F5	9				-16.555556	-16.555556
F4	9				-15.761111	-15.761111
F10	9				-15.755556	-15.755556
F12	9				-15.211111	-15.211111
F11	9					-14.922222
Sig.		.056	.071	.204	.177	.071

Means for groups in homogeneous subsets are displayed.

a. Uses Harmonic Mean Sample Size = 9.000.

Table 43 Analysis of variance result of particle size of MPE-SLNs

ANOVA

ps					
	Sum of Squares	df	Mean Square	F	Sig.
Between Groups	8947.206	1	8947.206	190.289	.000
Within Groups	752.304	16	47.019		
Total	9699.510	17			

Table 44 Analysis of variance result of polydispersity index of MPE-SLNs

ANOVA

pdi

	Sum of Squares	df	Mean Square	F	Sig.
Between Groups	.154	1	.154	272.111	.000
Within Groups	.009	16	.001		
Total	.163	17			

Table 45 Analysis of variance result of zeta potential of MPE-SLNs

ANOVA

zetapotential

	Sum of Squares	df	Mean Square	F	Sig.
Between Groups	.376	1	.376	2.537	.131
Within Groups	2.369	16	.148		
Total	2.744	17			

Table 46 Analysis of variance result of α-mangostin content of MPE-SLNs

ANOVA

alphamangostincontent

	Sum of Squares	df	Mean Square	F	Sig.
Between Groups	37612.084	1	37612.084	.988	.376
Within Groups	152239.218	4	38059.804		
Total	189851.301	5			

Table 47 Analysis of variance result of particle size MPE-SLNs before and after centrifugation

ANOVA					
Particlesize					
	Sum of Squares	df	Mean Square	F	Sig.
Between Groups	138920.568	3	46306.856	466.179	.000
Within Groups	3178.648	32	99.333		
Total	142099.216	35			

Particlesize					
Tukey HSD					
		Subset for alpha = 0.05			
Formulations	N	1	2	3	4
Before centrifugation MPE-PA-PVA1	9	4.435111E2			
Before centrifugation MPE-SA-PVA1	9		5.335250E2		
After centrifugation MPE-PA-PVA1	9			5.681556E2	
After Centrifugation MPE-SA-PVA1	9				6.127456E2
Sig.		1.000	1.000	1.000	1.000
Means for groups in homogeneous subsets are displayed.					

Table 48 Analysis of variance result of polydispersity index MPE-SLNs before and after centrifugation

ANOVA					
Particlesize					
	Sum of Squares	df	Mean Square	F	Sig.
Between Groups	.375	3	.125	241.056	.000
Within Groups	.017	32	.001		
Total	.392	35			

Particlesize				
Tukey HSD				
		Subset for alpha = 0.05		
Formulations	N	1	2	3
Before centrifugation MPE-PA-PVA1	9	.351111		
After centrifugation MPE-PA-PVA1	9		.449444	
Before centrifugation MPE-SA-PVA1	9		.459000	
After Centrifugation MPE-SA-PVA1	9			.634489
Sig.		1.000	.810	1.000
Means for groups in homogeneous subsets are displayed.				

Table 49 Analysis of variance result of entrapment efficiency of MPE-PA-SLNs and MPE-SA-SLNs

ANOVA Table

			Sum of Squares	df	Mean Square	F	Sig.
EE * Formulations	Between Groups	(Combined)	1.344	1	1.344	2.085	.222
	Within Groups		2.579	4	.645		
	Total		3.924	5			

Table 50 Analysis of variance result of SPF value of cream formulations

Tests of Between-Subjects Effects

Dependent Variable:SPF

Source	Type III Sum of Squares	df	Mean Square	F	Sig.
Corrected Model	479.315[a]	11	43.574	60.267	.000
Intercept	665.726	1	665.726	920.758	.000
formulation	479.018	5	95.804	132.505	.000
Time	.136	1	.136	.188	.669
formulation * Time	.161	5	.032	.045	.999
Error	17.352	24	.723		
Total	1162.393	36			
Corrected Total	496.667	35			

a. R Squared = .965 (Adjusted R Squared = .949)

SPF

	formulation	N	Subset 1	Subset 2	Subset 3
Tukey HSD[a]	cream base	6	1.0250000E0		
	Cream SA-SLNs	6	1.0566667E0		
	cream PA-SLNs	6	1.1400000E0		
	cream MPE	6		4.1850000E0	
	Cream-MPE-SA-SLNs	6			8.6400000E0
	Cream-MPE-PA-SLNs	6			9.7550000E0
	Sig.		1.000	1.000	.244

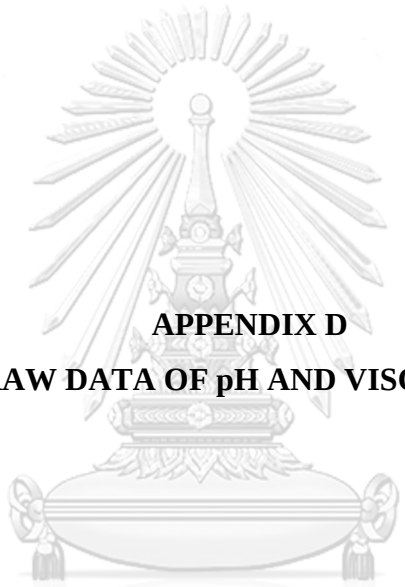

APPENDIX D
RAW DATA OF pH AND VISCOSITY

Table 51 Raw data of pH of blank cream CI during 6 heating-cooling cycles

pH of blank cream C1							
Cycles	Initial	Cycle 1	Cycle 2	Cycle 3	Cycle 4	Cycle 5	Cycle 6
n=1	6.32	6.30	6.33	6.30	6.27	6.26	6.27
n=2	6.35	6.30	6.30	6.30	6.26	6.25	6.25
n=3	6.33	6.31	6.32	6.28	6.27	6.26	6.24
Mean	6.33	6.30	6.31	6.29	6.26	6.25	6.25
STD	0.01	0.01	0.01	0.01	0.01	0.01	0.01

Table 52 Raw data of viscosity of blank cream CI during 6 heating-cooling cycles

Viscosity of blank cream C1 (cP)							
Cycles	Initial	Cycle 1	Cycle 2	Cycle 3	Cycle 4	Cycle 5	Cycle 6
n=1	7077.60	7195.56	7038.28	6881.00	6763.04	6645.08	6487.80
n=2	7234.88	7234.88	7038.28	6841.68	6723.72	6605.76	6448.48
n=3	7195.56	7156.24	6920.32	6802.36	6684.40	6527.12	6448.48
Mean	7169.34	7195.56	6998.96	6841.68	6723.72	6592.65	6461.58
STD	81.85	39.32	68.10	39.32	39.32	60.06	22.70

Table 53 Raw data of pH of blank cream C2 during 6 heating-cooling cycles

pH of blank cream C2							
Cycles	Initial	Cycle 1	Cycle 2	Cycle 3	Cycle 4	Cycle 5	Cycle 6
n=1	6.18	6.19	6.19	6.18	6.15	6.16	6.16
n=2	6.17	6.16	6.16	6.15	6.17	6.14	6.15
n=3	6.19	6.17	6.18	6.16	6.16	6.15	6.13
Mean	6.18	6.17	6.17	6.16	6.16	6.15	6.14
STD	0.01	0.02	0.02	0.02	0.01	0.01	0.02

Table 54 Raw data of viscosity of blank cream C2 during 6 heating-cooling cycles

Viscosity of blank cream C2 (cP)							
Cycles	Initial	Cycle 1	Cycle 2	Cycle 3	Cycle 4	Cycle 5	Cycle 6
n=1	27820.60	27745.36	27728.40	27609.44	27588.08	27470.12	27440.48
n=2	27838.56	27706.04	27750.08	27648.76	27660.76	27452.16	27450.80
n=3	27877.88	27745.36	27698.04	27599.72	27601.44	27522.84	27500.48
Mean	27845.68	27732.25	27725.50	27619.30	27616.76	27481.71	27463.92
STD	29.29	22.70	26.14	25.96	38.68	36.73	32.07

Table 55 Raw data of pH of cream containing MPE-SA-SLNs during stability test

pH of cream containing MPE-SA-SLNs				
Time	Initial	First month	Second month	Third month
n=1	5.95	5.93	5.92	5.92
n=2	5.93	5.92	5.93	5.91
n=3	5.94	5.94	5.92	5.93
Mean	5.94	5.93	5.923	5.92
STD	0.01	0.01	0.01	0.01

Table 56 Raw data of pH of cream containing MPE-PA-SLNs during stability test

pH of cream containing MPE-PA-SLNs				
Time	Initial	First month	Second month	Third month
n=1	5.96	5.96	5.93	5.93
n=2	5.96	5.95	5.94	5.93
n=3	5.94	5.93	5.94	5.91
Mean	5.95	5.94	5.93	5.92
STD	0.01	0.01	0.01	0.01

Table 57 Raw data of viscosity of cream containing MPE-SA-SLNs

Viscosity of cream containing MPE-SA-SLNs (cP)				
Time	Initial	First month	Second month	Third month
n=1	35388.00	35270.04	35152.08	35191.40
n=2	34601.60	35230.72	35230.72	35152.08
n=3	35348.68	35270.04	35230.72	35191.40
Mean	35112.76	35256.93	35204.50	35178.29
STD	443.11	22.70	45.40	22.70

Table 58 Raw data of viscosity of cream containing MPE-PA-SLNs

Viscosity of cream containing MPE-PA-SLNs (cP)				
Time	Initial	First month	Second month	Third month
n=1	34562.28	34522.96	34444.32	34522.96
n=2	34483.64	34444.32	34483.64	34444.32
n=3	34562.28	34483.64	34444.32	34444.32
Mean	34536.06	34483.64	34457.42	34470.53
STD	45.40	39.32	22.70	45.40

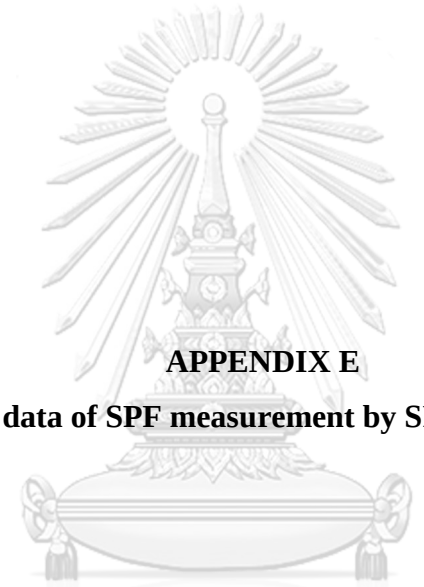

APPENDIX E

Raw data of SPF measurement by SPF Analyzer

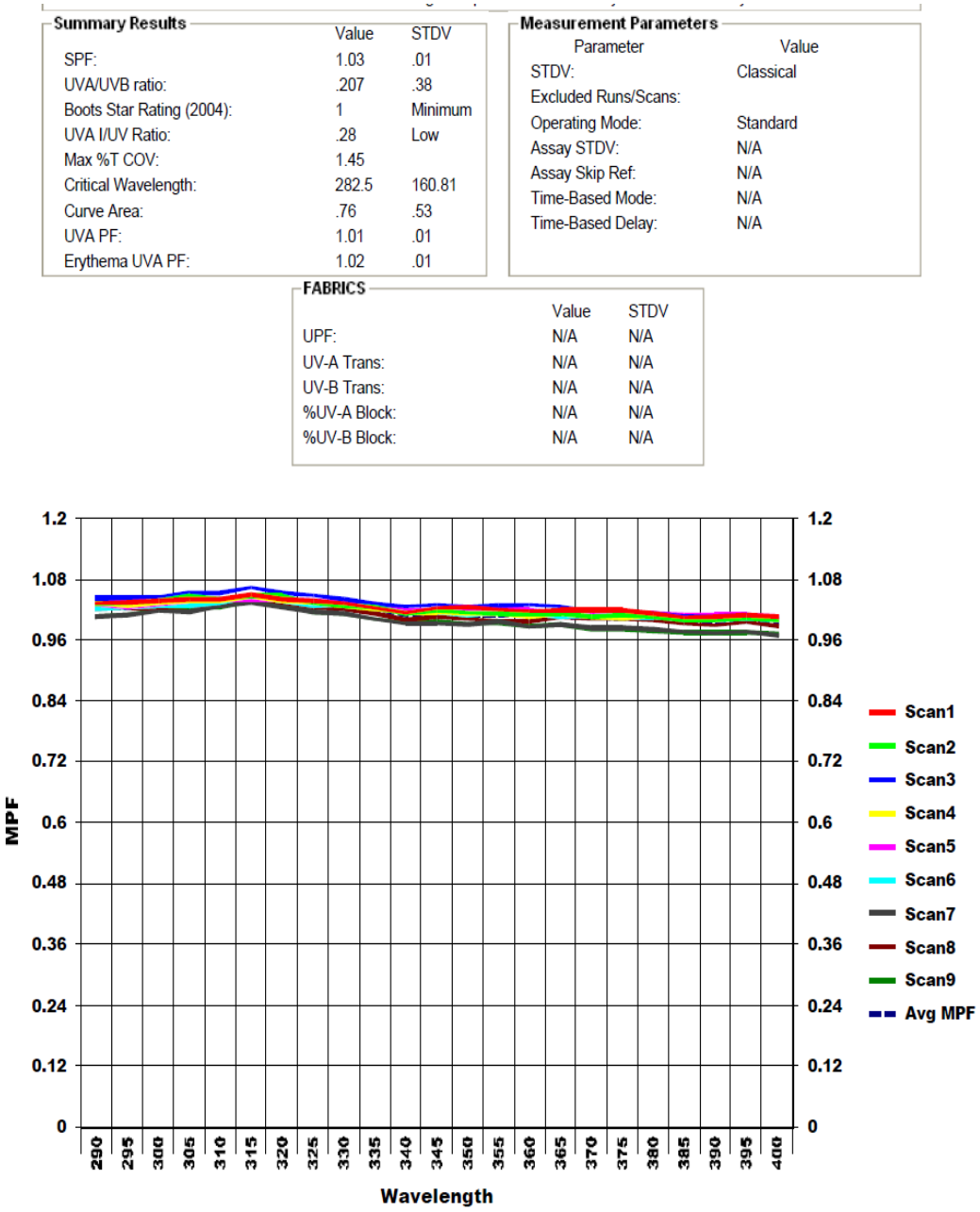

Figure 43 SPF measurement of cream base (C2) at initial time

Summary Results

	Value	STDV
SPF:	1.02	.01
UVA/UVB ratio:	.257	.11
Boots Star Rating (2004):	1	Minimum
UVA I/UV Ratio:	.28	Low
Max %T COV:	1.45	
Critical Wavelength:	282.5	160.81
Curve Area:	.76	.53
UVA PF:	1.01	.01
Erythema UVA PF:	1.02	.01

Measurement Parameters

Parameter	Value
STDV:	Classical
Excluded Runs/Scans:	
Operating Mode:	Standard
Assay STDV:	N/A
Assay Skip Ref:	N/A
Time-Based Mode:	N/A
Time-Based Delay:	N/A

FABRICS

	Value	STDV
UPF:	N/A	N/A
UV-A Trans:	N/A	N/A
UV-B Trans:	N/A	N/A
%UV-A Block:	N/A	N/A
%UV-B Block:	N/A	N/A

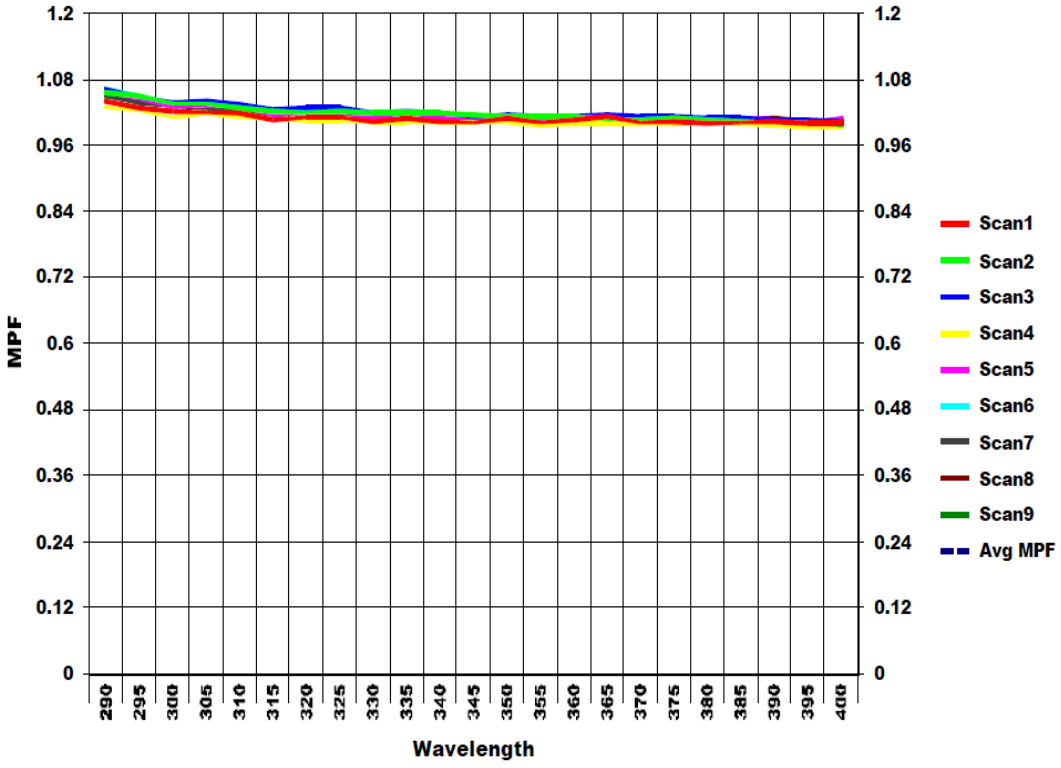

Figure 44 SPF measurement of cream base (C2) after 3 month storage at 4^{o}C

Summary Results

	Value	STDV
SPF:	4.24	.67
UVA/UVB ratio:	.528	.01
Boots Star Rating (2004):	2	Moderate
UVA I/UV Ratio:	.62	Mediu
Max %T COV:	14.31	
Critical Wavelength:	376.6	.22
Curve Area:	50.72	4.64
UVA PF:	2.64	.27
Erythema UVA PF:	3.31	.34

Measurement Parameters

Parameter	Value
STDV:	Classical
Excluded Runs/Scans:	
Operating Mode:	Standard
Assay STDV:	N/A
Assay Skip Ref:	N/A
Time-Based Mode:	N/A
Time-Based Delay:	N/A

FABRICS

	Value	STDV
UPF:	N/A	N/A
UV-A Trans:	N/A	N/A
UV-B Trans:	N/A	N/A
%UV-A Block:	N/A	N/A
%UV-B Block:	N/A	N/A

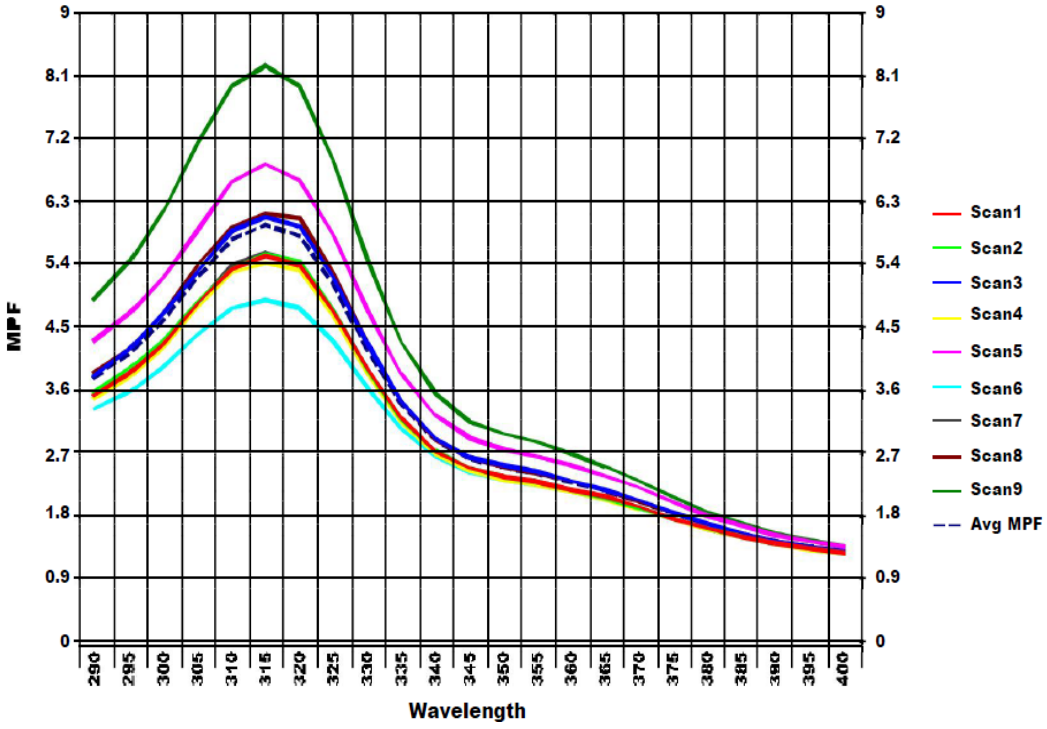

Figure 45 SPF measurement of MPE cream at initial time

Summary Results

	Value	STDV
SPF:	4.13	.44
UVA/UVB ratio:	.528	.01
Boots Star Rating (2004):	2	Moderate
UVA I/UV Ratio:	.64	Mediur
Max %T COV:	11.62	
Critical Wavelength:	377.1	.18
Curve Area:	46.35	3.68
UVA PF:	2.38	.18
Erythema UVA PF:	2.98	.24

Measurement Parameters

Parameter	Value
STDV:	Classical
Excluded Runs/Scans:	
Operating Mode:	Standard
Assay STDV:	N/A
Assay Skip Ref:	N/A
Time-Based Mode:	N/A
Time-Based Delay:	N/A

FABRICS

	Value	STDV
UPF:	N/A	N/A
UV-A Trans:	N/A	N/A
UV-B Trans:	N/A	N/A
%UV-A Block:	N/A	N/A
%UV-B Block:	N/A	N/A

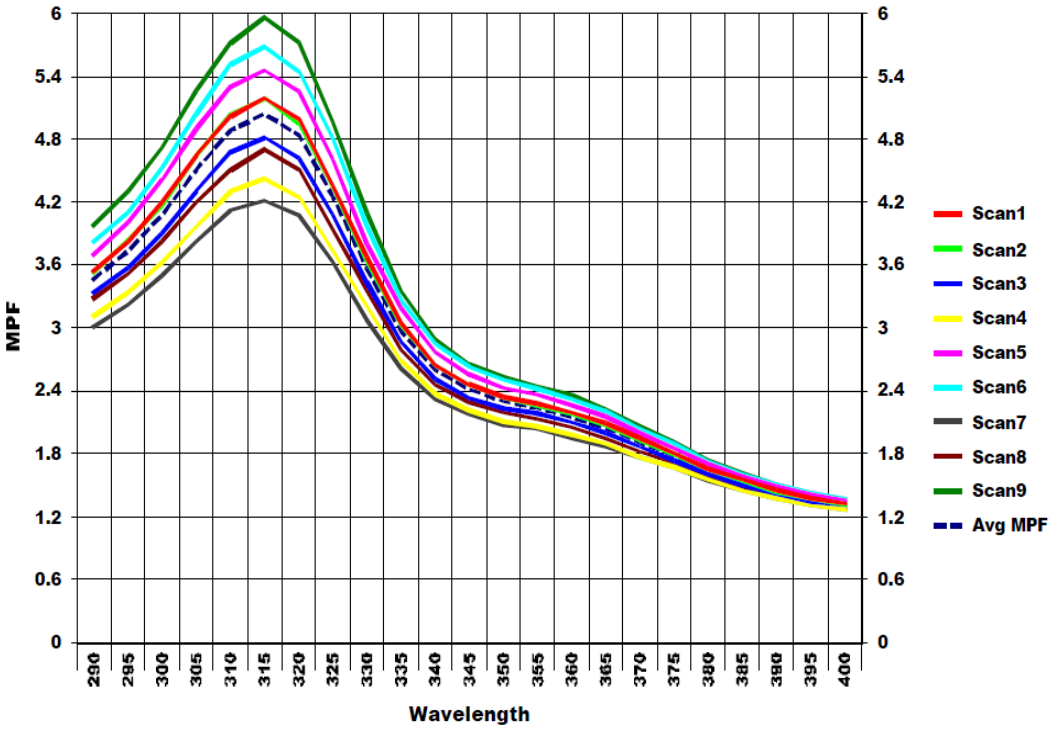

Figure 46 SPF measurement of MPE cream after 3 month storage at 4^{o}C

Summary Results

	Value	STDV
SPF:	1.06	.01
UVA/UVB ratio:	.414	.04
Boots Star Rating (2004):	2	Moderate
UVA I/UV Ratio:	.59	Mediur
Max %T COV:	1.1	
Critical Wavelength:	376.8	3.43
Curve Area:	1.76	.3
UVA PF:	1.03	.01
Erythema UVA PF:	1.04	.01

Measurement Parameters

Parameter	Value
STDV:	Classical
Excluded Runs/Scans:	
Operating Mode:	Standard
Assay STDV:	N/A
Assay Skip Ref:	N/A
Time-Based Mode:	N/A
Time-Based Delay:	N/A

FABRICS

	Value	STDV
UPF:	N/A	N/A
UV-A Trans:	N/A	N/A
UV-B Trans:	N/A	N/A
%UV-A Block:	N/A	N/A
%UV-B Block:	N/A	N/A

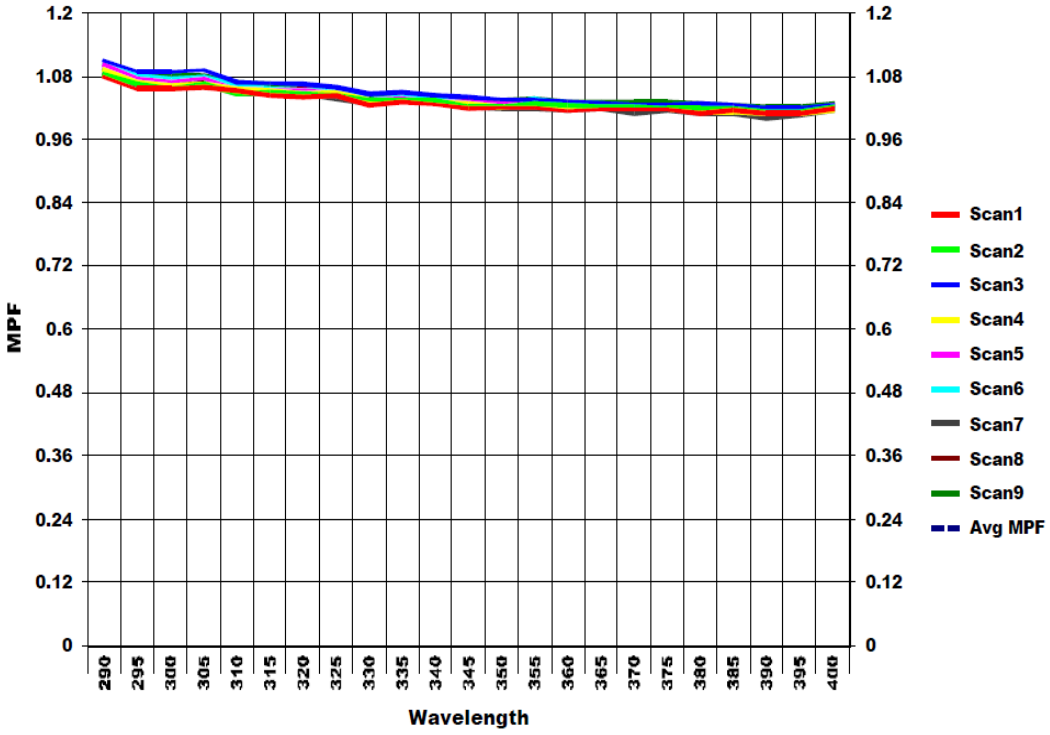

Figure 47 SPF measurement of cream containing blank SA-SLNs at initial time

Summary Results

	Value	STDV
SPF:	1.08	.01
UVA/UVB ratio:	.357	.05
Boots Star Rating (2004):	2	Moderate
UVA I/UV Ratio:	.4	Mediur
Max %T COV:	1.18	
Critical Wavelength:	376.8	3.43
Curve Area:	1.96	.39
UVA PF:	1.03	.01
Erythema UVA PF:	1.06	.01

Measurement Parameters

Parameter	Value
STDV:	Classical
Excluded Runs/Scans:	
Operating Mode:	Standard
Assay STDV:	N/A
Assay Skip Ref:	N/A
Time-Based Mode:	N/A
Time-Based Delay:	N/A

FABRICS

	Value	STDV
UPF:	N/A	N/A
UV-A Trans:	N/A	N/A
UV-B Trans:	N/A	N/A
%UV-A Block:	N/A	N/A
%UV-B Block:	N/A	N/A

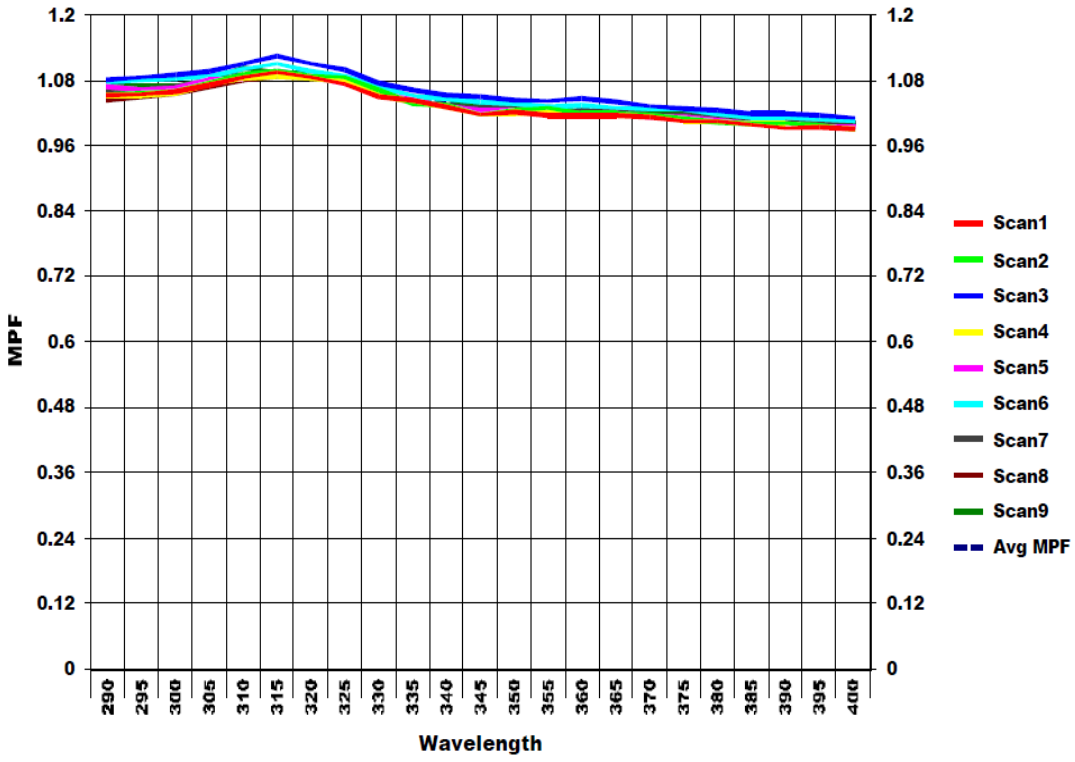

Figure 48 SPF measurement of cream containing blank SA-SLNs after 3 month storage at 4^{o}C

Summary Results

	Value	STDV
SPF:	1.15	.01
UVA/UVB ratio:	.741	.02
Boots Star Rating (2004):	3	Good
UVA I/UV Ratio:	.86	High
Max %T COV:	1.64	
Critical Wavelength:	387.5	0
Curve Area:	5.72	.48
UVA PF:	1.12	.01
Erythema UVA PF:	1.13	.01

Measurement Parameters

Parameter	Value
STDV:	Classical
Excluded Runs/Scans:	
Operating Mode:	Standard
Assay STDV:	N/A
Assay Skip Ref:	N/A
Time-Based Mode:	N/A
Time-Based Delay:	N/A

FABRICS

	Value	STDV
UPF:	N/A	N/A
UV-A Trans:	N/A	N/A
UV-B Trans:	N/A	N/A
%UV-A Block:	N/A	N/A
%UV-B Block:	N/A	N/A

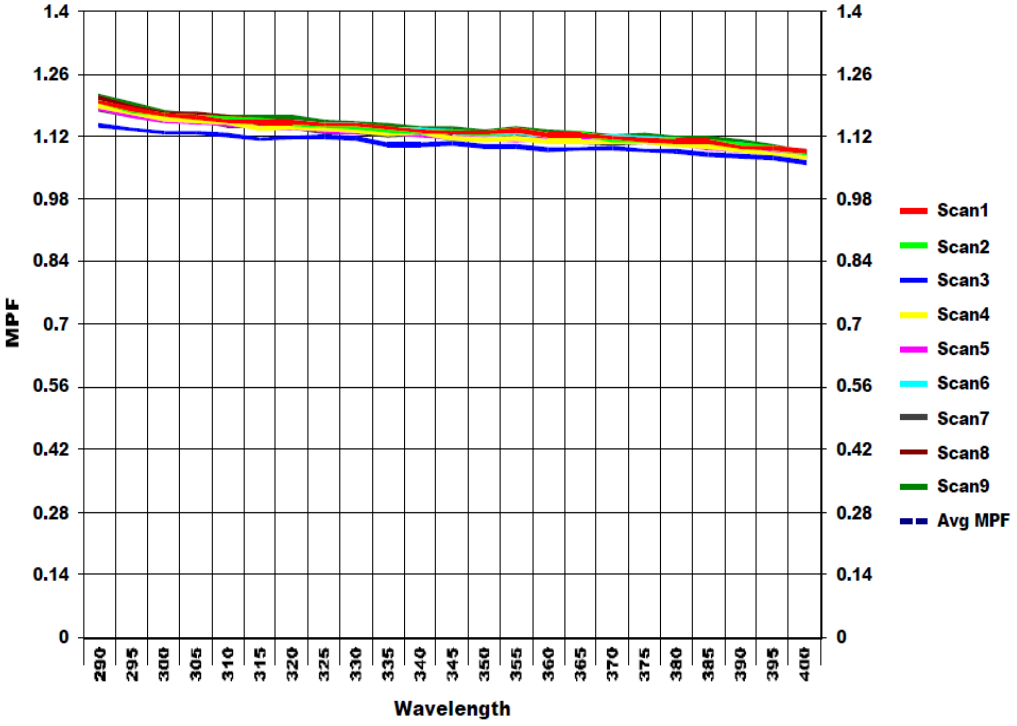

Figure 49 SPF measurement of cream containing blank PA-SLNs at initial time

Summary Results

	Value	STDV
SPF:	1.13	.01
UVA/UVB ratio:	.637	.02
Boots Star Rating (2004):	3	Good
UVA I/UV Ratio:	.79	High
Max %T COV:	1.53	
Critical Wavelength:	376.8	.18
Curve Area:	4.68	.41
UVA PF:	1.09	.01
Erythema UVA PF:	1.11	.01

Measurement Parameters

Parameter	Value
STDV:	Classical
Excluded Runs/Scans:	
Operating Mode:	Standard
Assay STDV:	N/A
Assay Skip Ref:	N/A
Time-Based Mode:	N/A
Time-Based Delay:	N/A

FABRICS

	Value	STDV
UPF:	N/A	N/A
UV-A Trans:	N/A	N/A
UV-B Trans:	N/A	N/A
%UV-A Block:	N/A	N/A
%UV-B Block:	N/A	N/A

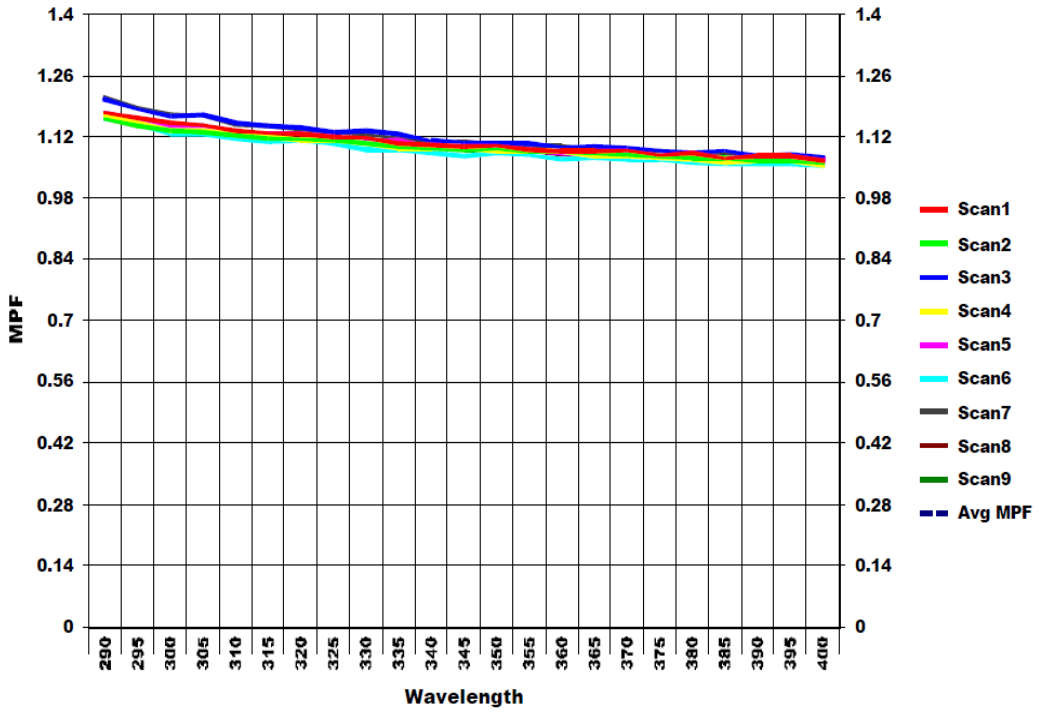

Figure 50 SPF measurement of cream containing blank PA-SLNs after 3 month storage at 4^{o}C

Summary Results

	Value	STDV
SPF:	8.75	.87
UVA/UVB ratio:	.572	.02
Boots Star Rating (2004):	2	Moderate
UVA I/UV Ratio:	.67	Mediur
Max %T COV:	10.44	
Critical Wavelength:	377.6	.59
Curve Area:	74.78	3.74
UVA PF:	4.45	.35
Erythema UVA PF:	5.46	.41

Measurement Parameters

Parameter	Value
STDV:	Classical
Excluded Runs/Scans:	
Operating Mode:	Standard
Assay STDV:	N/A
Assay Skip Ref:	N/A
Time-Based Mode:	N/A
Time-Based Delay:	N/A

FABRICS

	Value	STDV
UPF:	N/A	N/A
UV-A Trans:	N/A	N/A
UV-B Trans:	N/A	N/A
%UV-A Block:	N/A	N/A
%UV-B Block:	N/A	N/A

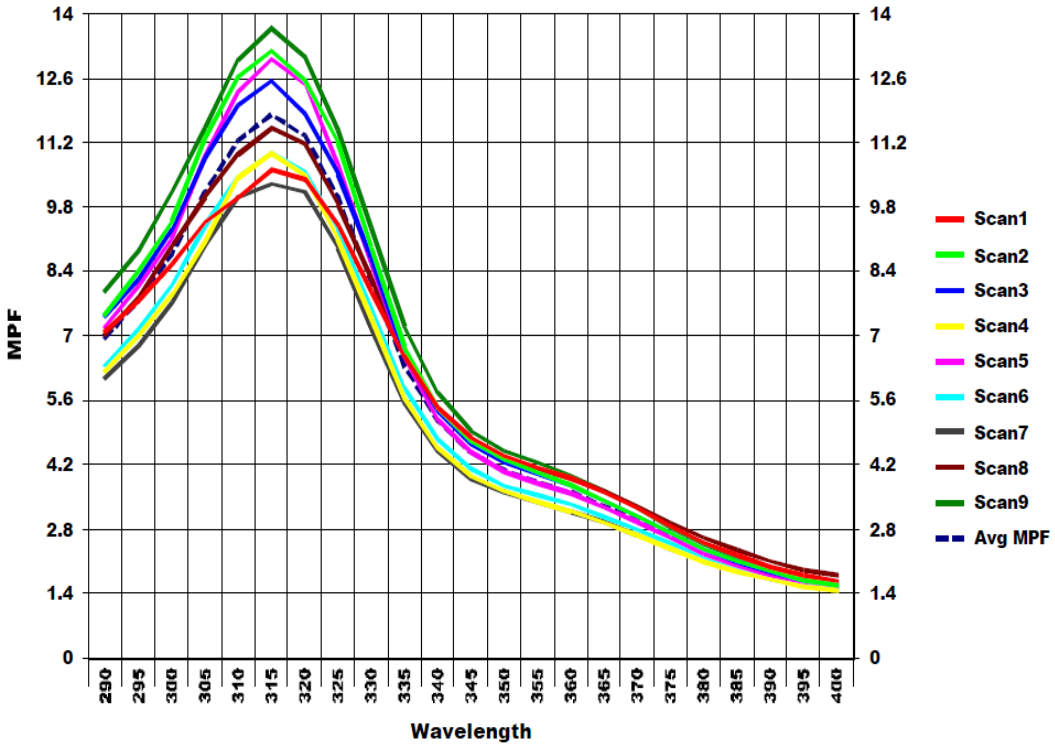

Figure 51 SPF measurement of cream containing MPE-SA-SLNs at initial time

Summary Results

	Value	STDV
SPF:	8.53	1.19
UVA/UVB ratio:	.565	.02
Boots Star Rating (2004):	2	Moderate
UVA I/UV Ratio:	.66	Mediur
Max %T COV:	15.98	
Critical Wavelength:	377.4	.47
Curve Area:	73.26	4.98
UVA PF:	4.33	.46
Erythema UVA PF:	5.31	.52

Measurement Parameters

Parameter	Value
STDV:	Classical
Excluded Runs/Scans:	
Operating Mode:	Standard
Assay STDV:	N/A
Assay Skip Ref:	N/A
Time-Based Mode:	N/A
Time-Based Delay:	N/A

FABRICS

	Value	STDV
UPF:	N/A	N/A
UV-A Trans:	N/A	N/A
UV-B Trans:	N/A	N/A
%UV-A Block:	N/A	N/A
%UV-B Block:	N/A	N/A

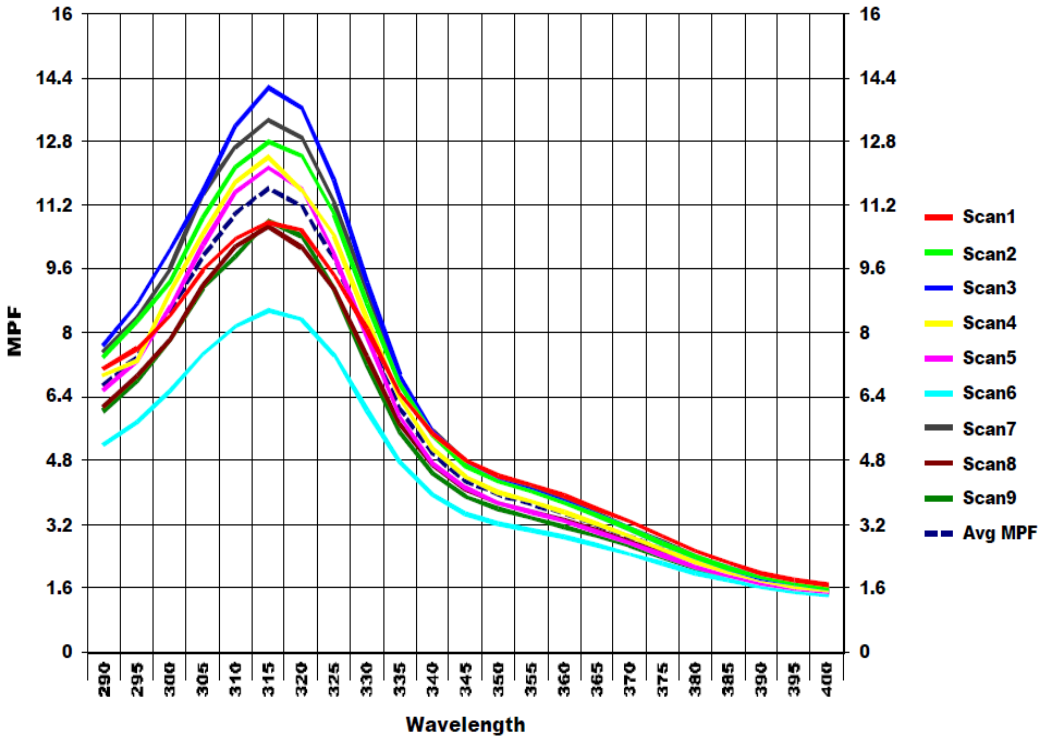

Figure 52 SPF measurement of cream containing MPE-SA-SLNs after 3 month storage at 4^{o}C

Summary Results

	Value	STDV
SPF:	9.94	1.42
UVA/UVB ratio:	.591	.02
Boots Star Rating (2004):	2	Moderate
UVA I/UV Ratio:	.68	Mediur
Max %T COV:	15.18	
Critical Wavelength:	377.9	.57
Curve Area:	80.53	4.87
UVA PF:	5.08	.56
Erythema UVA PF:	6.18	.62

Measurement Parameters

Parameter	Value
STDV:	Classical
Excluded Runs/Scans:	
Operating Mode:	Standard
Assay STDV:	N/A
Assay Skip Ref:	N/A
Time-Based Mode:	N/A
Time-Based Delay:	N/A

FABRICS

	Value	STDV
UPF:	N/A	N/A
UV-A Trans:	N/A	N/A
UV-B Trans:	N/A	N/A
%UV-A Block:	N/A	N/A
%UV-B Block:	N/A	N/A

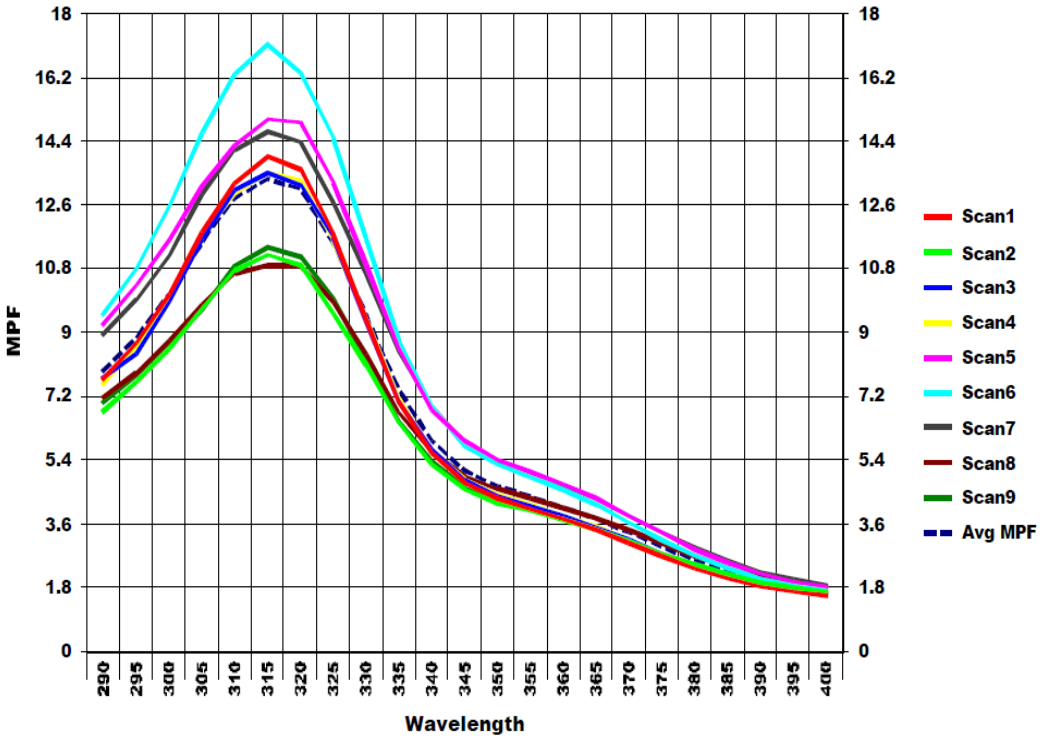

Figure 53 SPF measurement of cream containing MPE-PA-SLNs at initial time

Summary Results

	Value	STDV
SPF:	9.57	1.96
UVA/UVB ratio:	.556	.01
Boots Star Rating (2004):	2	Moderate
UVA I/UV Ratio:	.65	Mediur
Max %T COV:	23	
Critical Wavelength:	377.2	.4
Curve Area:	76.88	6.56
UVA PF:	4.74	.74
Erythema UVA PF:	5.69	.74

Measurement Parameters

Parameter	Value
STDV:	Classical
Excluded Runs/Scans:	
Operating Mode:	Standard
Assay STDV:	N/A
Assay Skip Ref:	N/A
Time-Based Mode:	N/A
Time-Based Delay:	N/A

FABRICS

	Value	STDV
UPF:	N/A	N/A
UV-A Trans:	N/A	N/A
UV-B Trans:	N/A	N/A
%UV-A Block:	N/A	N/A
%UV-B Block:	N/A	N/A

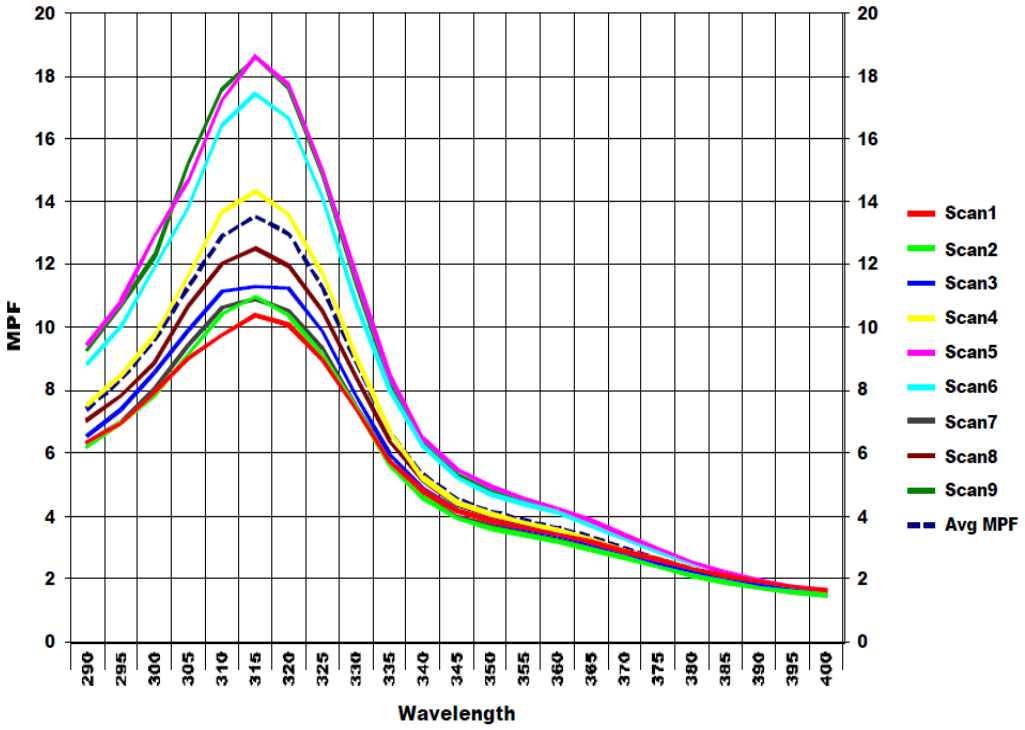

Figure 54 SPF measurement of cream containing MPE-PA-SLNs after 3 month storage at 4^{o}C

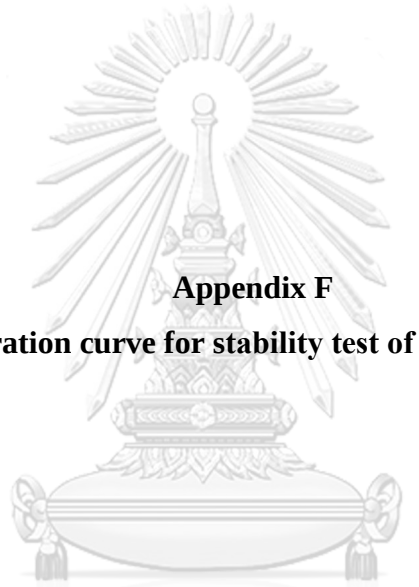

Appendix F

Calibration curve for stability test of α-mangostin

Table 59 Calibration curve for stability test of α-mangostin at initial time

Concentration of α-mangostin (µg/ml)	Peak area
10.09	902228
20.18	1768241
30.27	2682012
40.36	3579776
50.45	4515968
60.54	5391937

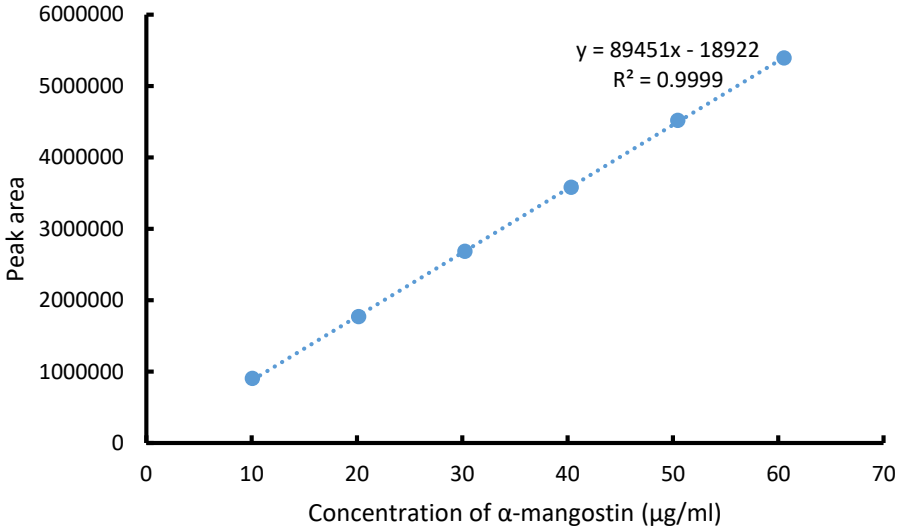

Figure 55 Calibration Curve for stability test at initial time

Table 60 Calibration curve for stability test of α-mangostin at the first month

Concentration of α-mangostin (µg/ml)	Peak area
10.09	902208
20.18	1768624
30.27	2682018
40.36	3579779
50.45	4515967
60.54	5391872

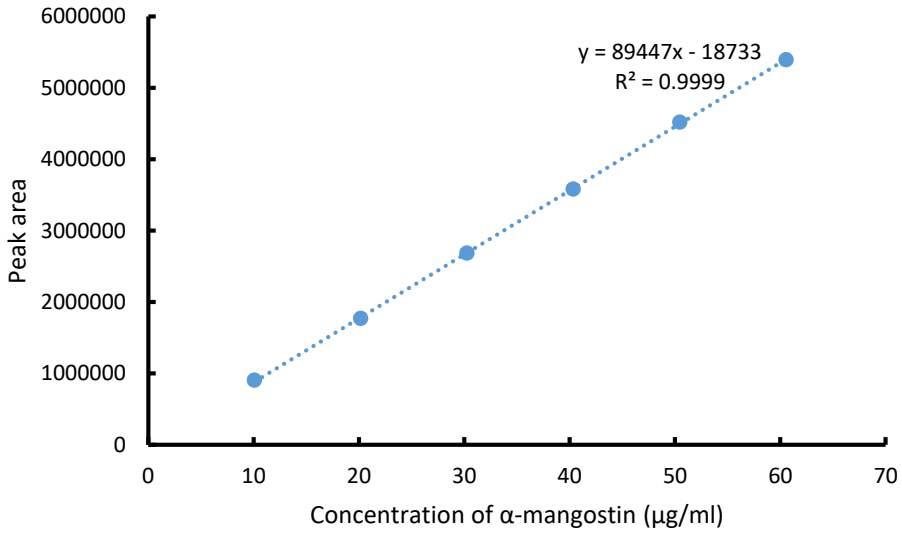

Figure 56 Calibration curve for stability test of α-mangostin at the first month

Table 61 Calibration curve for stability test of α-mangostin at the second month

Concentration of α-mangostin (µg/ml)	Peak area
10.08	898533
20.16	1781719
30.24	2681982
40.32	3580108
50.40	4515235
60.48	5389682

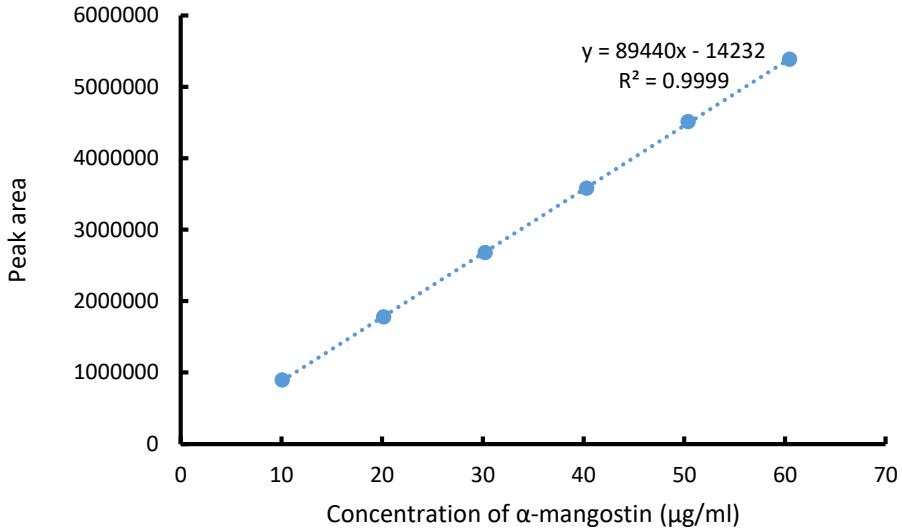

Figure 57 Calibration curve for stability test of α-mangostin at the second month

Table 62 Calibration curve for stability test of α-mangostin at the third month

Concentration of α-mangostin (µg/ml)	Peak area
10.06	896655
20.12	1768510
30.18	2664484
40.24	3579989
50.30	4480678
60.36	5384100

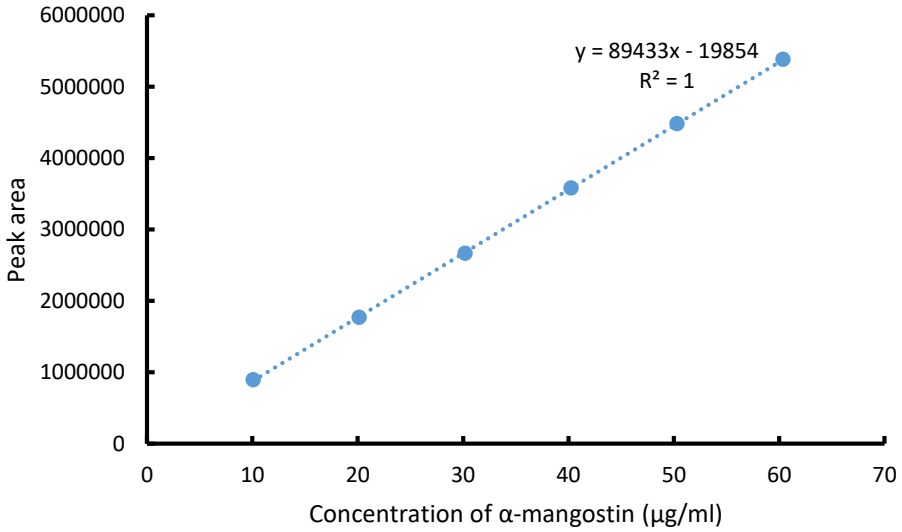

Figure 58 Calibration curve for stability test of α-mangostin at the third month

Appendix G

Raw data of α-mangostin content for stability test

Table 63 Raw data of α-mangostin content of cream containing MPE-PA-SLNs during stability test

Time	Peak area	Concentration (μg/ml)	Amount (μg extract/2 mg cream)	% remaining of α-mangostin
Initial time	2357626	26.56	59.96	100.00
	2358045	26.57	59.97	100.00
	2355160	26.54	59.90	100.00
1st month	2350861	26.49	59.79	99.74
	2349740	26.47	59.76	99.69
	2348747	26.46	59.74	99.65
2nd month	2344102	26.36	59.51	99.27
	2342206	26.34	59.46	99.19
	2341262	26.33	59.44	99.15
3rd month	2329776	26.27	59.29	98.91
	2328102	26.25	59.25	98.84
	2329853	26.27	59.30	98.91

Table 64 Raw data of α-mangostin content of cream containing MPE-SA-SLNs during stability test

Time	Peak area	Concentration (μg/ml)	Amount (μg extract/2 mg cream)	% remaining of α-mangostin
Initial time	2356951	26.56	59.94	100.00
	2356334	26.55	59.93	100.00
	2356634	26.55	59.94	100.00
1st month	2344176	26.41	59.62	99.47
	2343864	26.41	59.61	99.45
	2344551	26.42	59.63	99.48
2nd month	2337488	26.29	59.34	99.00
	2338438	26.30	59.37	99.04
	2337814	26.29	59.35	99.02
3rd month	2324824	26.21	59.17	98.71
	2325054	26.21	59.18	98.72
	2323078	26.19	59.13	98.64

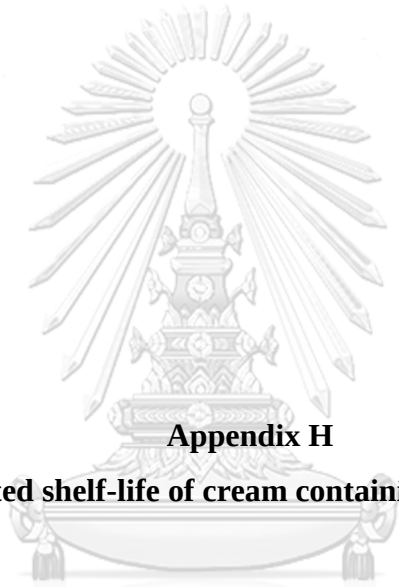

Appendix H

Estimated shelf-life of cream containing MPE-SLNs

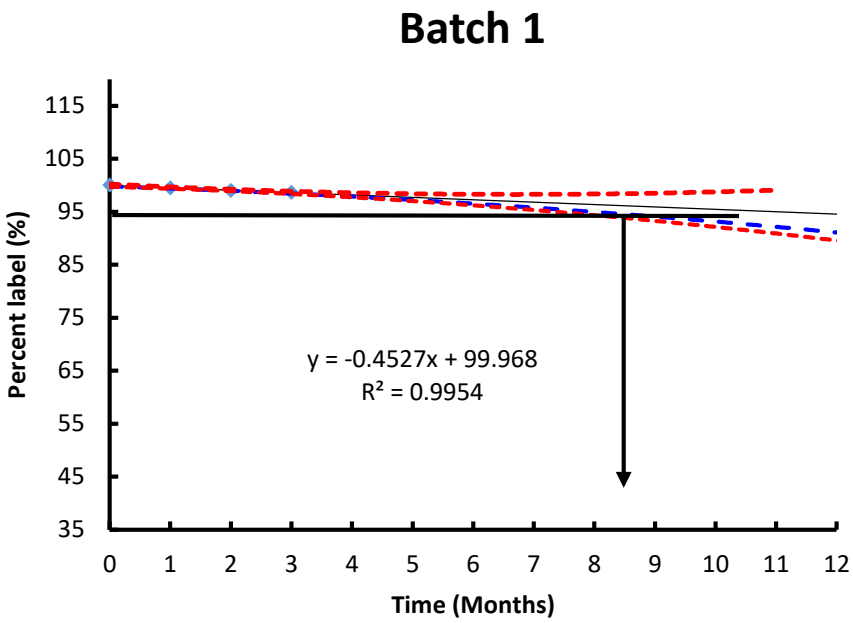

Figure 59 The estimated shelf-life of cream containing MPE-PA-SLNs (1st batch)

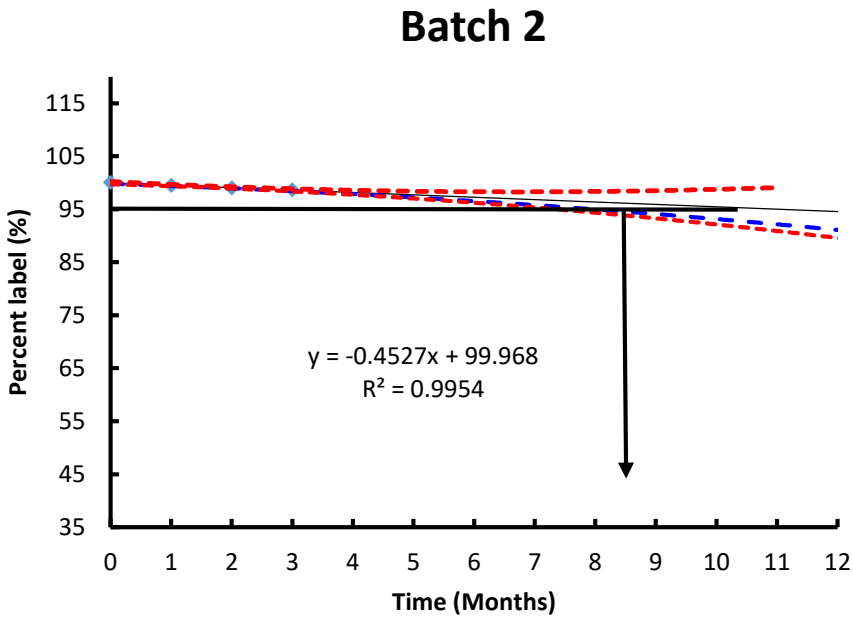

Figure 60 The estimated shelf-life of cream containing MPE-PA-SLNs (2nd batch)

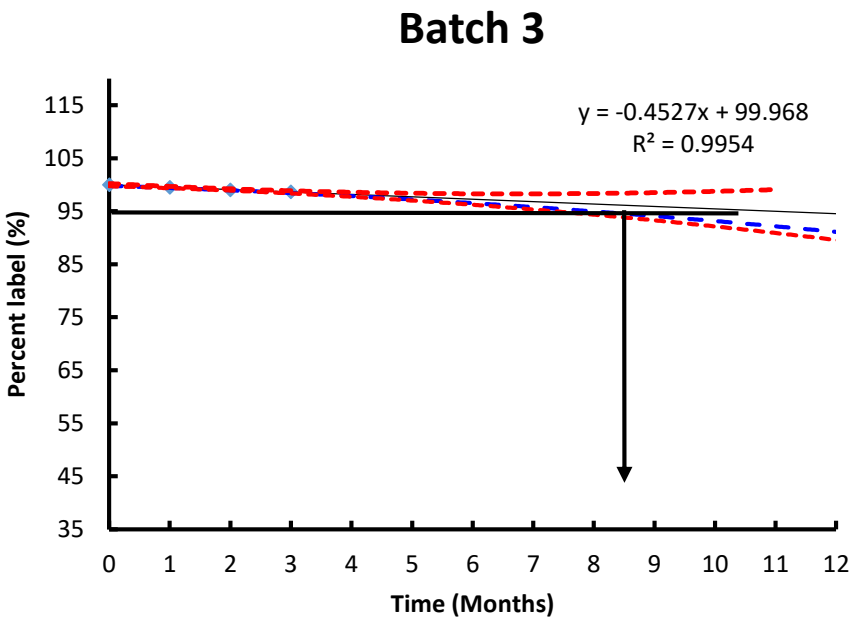

Figure 61 The estimated shelf-life of cream containing MPE-PA-SLNs (3rd batch)

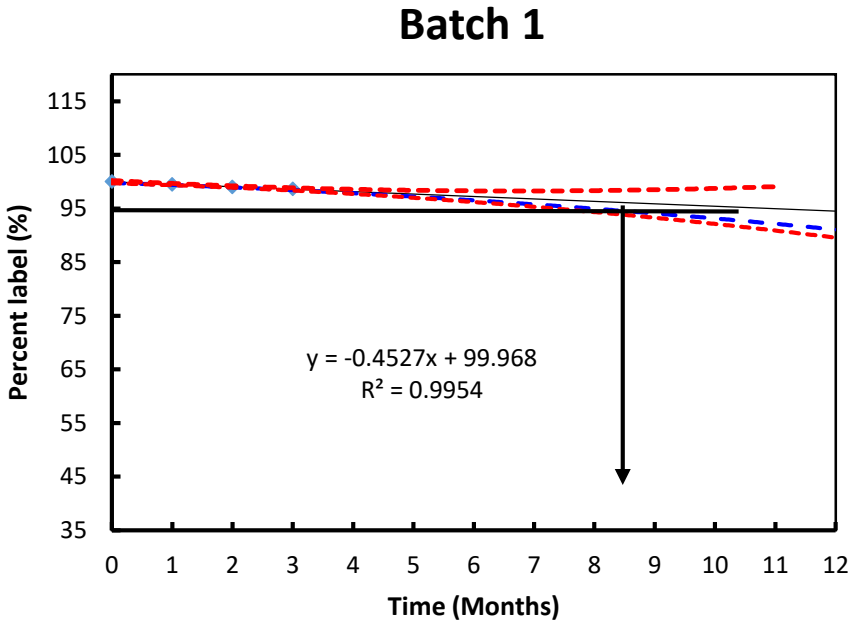

Figure 62 The estimated shelf-life of cream containing MPE-SA-SLNs (1st batch)

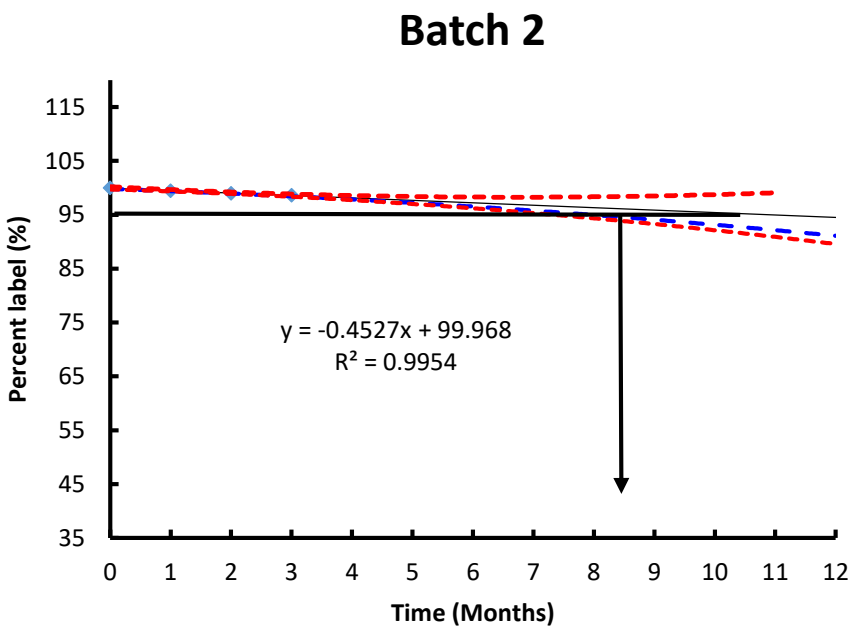

Figure 63 The estimated shelf-life of cream containing MPE-SA-SLNs (2nd batch)

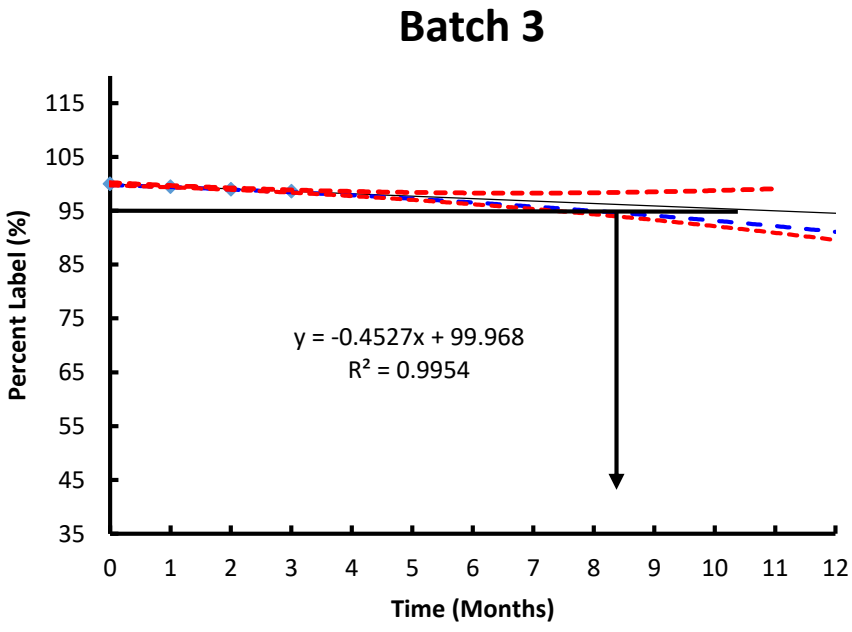

Figure 64 The estimated shelf-life of cream containing MPE-SA-SLNs (3rd batch)

VITA

Miss Siti Nur Diniyanti was born on November 02, 1993 in Aceh Tamiang, Indonesia. She received her Bachelor Degree in Pharmacy from Faculty of Pharmacy, the University of North Sumatra in 2015. She continued the enrollment to the Master degree program in Pharmaceutical Technology at Chulalongkorn University in 2016.